STANFORD UNIVERSITY

CENTER FOR SYSTEMS RESEARCH

IMPROVED NAVIGATION BY COMBINING VOR/DME INFORMATION WITH AIR OR INERTIAL DATA

BY

John C. Bobick
Arthur E. Bryson, Jr.
Department of Applied Mechanics,
Department of Aeronautics and Astronautics

May 1972

Guidance and Control Laboratory

SUDAAR No. 442

Research sponsored by
NATIONAL SCIENCE FOUNDATION
(Traineeship for J.C. Bobick)
NATIONAL AERONAUTICS AND SPACE ADMINISTRATION
under Grant NGL 05-020-007
UNITED STATES AIR FORCE, AVIONICS LABORATORY
under Contract F33615-72-C-1297

IMPROVED NAVIGATION BY COMBINING VOR/DME INFORMATION WITH AIR OR INERTIAL DATA*

by

John C. Bobick
Arthur E. Bryson, Jr.

Department of Applied Mechanics,
Department of Aeronautics and Astronautics
STANFORD UNIVERSITY
Stanford, California 94305

Research sponsored by

NATIONAL SCIENCE FOUNDATION
(Traineeship for J.C. Bobick)

NATIONAL AERONAUTICS AND SPACE ADMINISTRATION
under Grant NGL 05-020-007

UNITED STATES AIR FORCE, AVIONICS LABORATORY
under Contract F33615-72-C-1297

SUDAAR No. 442

May 1972

---

* A dissertation submitted by John C. Bobick to the Department of Applied Mechanics and the Committee on Graduate Studies of Stanford University in partial fulfillment of the requirements for the Degree of Doctor of Philosophy.

ABSTRACT

The primary navigation aid for civil aircraft flying in the U.S. airspace, as well as the airspaces of most of the developed countries of the world, is the VOR/DME system. Using VOR and DME measurements, bearing and range relative to a fixed ground station can be determined onboard the aircraft. Even though this is a good navigation system, reductions in air traffic congestion and air controller workloads could be realized if still more accurate onboard navigation were available. Current practice is to use information from a single VOR/DME station. This work is concerned with determining the improvement in navigational accuracy obtainable by combining VOR/DME information (from one or two stations) with air data (airspeed and heading) or with data from an inertial navigation system (INS) by means of a maximum-likelihood filter.

It was found that the addition of air data to the information from one VOR/DME station reduces the RMS position error by a factor of about 2, whereas the addition of inertial data from a low-quality INS reduces the RMS position error by a factor of about 3. The use of information from two VOR/DME stations with air or inertial data yields large factors of improvement in RMS position accuracy over the use of a single VOR/DME station, roughly 15 to 20 for the air-data case and 25 to 35 for the inertial-data case. As far as position accuracy is concerned, at most one VOR station need be used. When continuously updating an INS with VOR/DME information, the use of a high-quality INS (0.01 deg/hr gyro drift) instead of a low-quality INS (1.0 deg/hr gyro drift) does not substantially improve position accuracy.

Accurate in-flight alignment of an INS platform can be accomplished in about 30 minutes by using VOR/DME information. The accuracy of in-flight alignment when using two DME's is about the same as for ground alignment, whereas when using one VOR/DME, alignment is less accurate by a factor of 2 or 3. Although the need for initial in-flight alignment of INS's onboard commercial aircraft is questionable, realignment of the system before a transoceanic flight could result in significant improvements in navigational accuracy. This might permit a reduction in separation requirements over the North Atlantic routes. Also,

realignment after a transoceanic flight would result in more accurate position, velocity, and attitude information in the terminal area.

Periodic realignment (every one or two hours) of a high-quality INS during a transcontinental flight results in significant reductions in position and velocity errors over unaided-inertial operation or the use of position display resets. If a realignment is performed just prior to entering the terminal area, accurate position, velocity, and attitude information would be available for approach and landing without reliance upon VOR/DME information.

The performance of the air-data filter was found to be rather insensitive to wide variations in error model statistics. Also, in general, when combining VOR/DME information with air or inertial data, the suboptimal filter resulting when the DME bias errors are neglected performs nearly optimally.

CONTENTS

CONTENTS (Cont)

ILLUSTRATIONS

ILLUSTRATIONS (Cont)

TABLES

LIST OF SYMBOLS

$\underline{a}$	actual acceleration sensed by the accelerometers
a_x, a_y, a_z	easterly, northerly, vertical component of $\underline{a}$
A	$\bar{x}_1^{-2} + \bar{y}_1^{-2}$
$\underline{A}$	ideal output of the accelerometers
A_n	see Eqs. (E.14)
b_D	DME bias
b_{D1}, b_{D2}	DME bias associated with station 1, station 2
b_V	VOR bias
b_{V1}, b_{V2}	VOR bias associated with station 1, station 2
B	$(\bar{x}_1 - x_{12})^2 + (\bar{y}_1 - y_{12})^2$
$\underline{B}_n$	see Eqs. (E.14)
C	see Eqs. (E.12)
C(i,j)	element of C in the i^{th} row and j^{th} column
D	see Eqs. (E.16)
D(i,j)	element of D in the i^{th} row and j^{th} column
D_1, D_2	DME measurement from station 1, station 2
$\bar{D}_1, \bar{D}_2$	nominal value of D_1, D_2
exp	the exponential function
e_D	white noise in DME measurement
e_{D1}, e_{D2}	white noise in the DME measurement from station 1, station 2

e_V	white noise in VOR measurement
e_{V1}, e_{V2}	white noise in the VOR measurement from station 1, station 2
E, E_i	difference between the actual and calculated error covariances
$E[\ ]$	expected value of [ ]
E_{D1}	total error in the DME measurement from station 1
E_{V1}	total error in the VOR measurement from station 1
E_{x_1}, E_{y_1}	error in determining x_1, y_1
$\underline{f}$	known forcing function
$\underline{f}_e, \underline{f}_n$	see Eqs. (D.22)
F	state matrix
$F_{ee}, F_{en}, F_{ne}, F_{nn}$	see Eqs. (D.22)
g	magnitude of $\underline{g}$
$\underline{g}$	gravity vector, including centripetal acceleration
g_o	magnitude of $\underline{g}$ at the surface of the earth
$\underline{g}_m$	gravitational mass attraction vector
g_x, g_y, g_z	easterly, northerly, vertical component of $\underline{g}$
$\mathcal{h}$	nonlinear measurement function
h_1, h_2, h_{12}	vertical component of $\underline{R}_1$, $\underline{R}_2$, $\underline{R}_{12}$
H	high-altitude VOR station category or measurement matrix
H_e, H_n	see Eqs. (D.23)

H_i	measurement matrix
$(H_e)_i, (H_n)_i$	see Eqs. (D.5)
i	subscript or matrix row index
I	identity matrix
j	subscript or matrix column index
J	see Eq. (4.30)
J(i,j)	element of J in the i^{th} row and j^{th} column
k	subscript
K, K_i	matrix of optimal filter gains
K_e, K_n	see Eqs. (D.24)
$(K_e)_i, (K_n)_i$	see Eqs. (D.3)
K^s, K_i^s	suboptimal value of K, K_i
K_e^s, K_n^s	suboptimal value of K_e, K_n
$(K_e^s)_i, (K_n^s)_i$	suboptimal value of $(K_e)_i$, $(K_n)_i$
L	low-altitude VOR station category
m	number of states to be estimated
M	see Eqs. (4.29)
n	subscript
$\underline{n}, \underline{n}_i$	process noise vector
$\underline{n}_e, \underline{n}_n$	see Eqs. (D.22)
$(\underline{n}_e)_i, (\underline{n}_n)_i$	see Eqs. (D.2)

n_{wx}, n_{wy}	white noise process forcing the shaping filter that generates V_{wx}, V_{wy}
$n_{\alpha_x}, n_{\alpha_y}$	white noise process forcing the shaping filter that generates α_x, α_y
$n_{\epsilon_x}, n_{\epsilon_y}, n_{\epsilon_z}$	white noise process forcing the shaping filter that generates ϵ_x, ϵ_y, ϵ_z
N	see Eqs. (4.29)
P	dimension of state vector
P, P_i	error covariance matrix associated with $\hat{\underline{x}}$, $\hat{\underline{x}}_i$
$\bar{P}, \bar{P}_i$	actual error covariance matrix associated with $\hat{\underline{x}}^s$, $\hat{\underline{x}}^s_i$
$P(i,j), P_{ij}$	element of P in the i^{th} row and j^{th} column
P_o	initial error covariance matrix
$P_{ee}, P_{en}, P_{ne}, P_{nn}$	see Eqs. (D.24)
$(P_{ee})_o, (P_{en})_o, (P_{ne})_o, (P_{nn})_o$	initial value of P_{ee}, P_{en}, P_{ne}, P_{nn}
$(P_{ee})_i, (P_{en})_i, (P_{ne})_i, (P_{nn})_i$	see Eqs. (D.4)
P^s, P^s_i	value of P, P_i obtained from suboptimal filter
P^a_o	actual value of P_o
P^s_o	estimated value of P_o
$P^s_{ee}, P^s_{en}, P^s_{ne}, P^s_{nn}$	value of P_{ee}, P_{en}, P_{ne}, P_{nn} obtained from suboptimal filter
$(P^s_{ee})_i, (P^s_{en})_i, (P^s_{ne})_i, (P^s_{nn})_i$	value of $(P_{ee})_i$, $(P_{en})_i$, $(P_{ne})_i$, $(P_{nn})_i$ obtained from suboptimal filter

r_{P_k}	see Eq. (E.8)
Q, Q_i	spectral density of $\underline{n}$, covariance of $\underline{n}_i$
Q'	$Q/\Delta T$
$Q_{ee}, Q_{en}, Q_{ne}, Q_{nn}$	see Eqs. (D.23)
$\left(Q_{ee}\right)_i, \left(Q_{en}\right)_i, \left(Q_{ne}\right)_i, \left(Q_{nn}\right)_i$	see Eqs. (D.3)
Q^a, Q_i^a	actual value of Q, Q_i
Q^s, Q_i^s	estimated value of Q, Q_i
r	magnitude of $\underline{r}$
$\underline{r}$	radius vector from a reference VOR/DME station to an aircraft
R	magnitude of $\underline{R}$ or spectral density of $\underline{v}$
$\underline{R}$	radius vector from the center of the earth to an aircraft
$\overline{R}$	magnitude of $\overline{\underline{R}}$
$\overline{\underline{R}}$	computed value of $\underline{R}$
R'	$R/\Delta T$
R_o	mean radius of the earth
R_1	magnitude of $\underline{R}_1$
$\underline{R}_1, \underline{R}_2$	radius vector to an aircraft from station 1, station 2
$\underline{R}_{12}$	$\underline{R}_1 - \underline{R}_2$
R_i	covariance of $\underline{v}_i$

R_x, R_y, R_z	easterly, northerly, vertical component of $\underline{R}$
R^a, R_i^a	actual value of R, R_i
R^s, R_i^s	estimated value of R, R_i
t	time
t_o	time when filter is initialized
t_i	instants of time, $i = 0, 1, 2, \ldots$
T	terminal VOR station category
$T_{e_D}, T_{e_{D1}}, T_{e_{D2}}$	correlation time of e_D, e_{D1}, e_{D2}
$T_{e_V}, T_{e_{V1}}, T_{e_{V2}}$	correlation time of e_V, e_{V1}, e_{V2}
T_{wx}, T_{wy}	correlation time of V_{wx}, V_{wy}
$T_{\alpha_x}, T_{\alpha_y}$	correlation time of α_x, α_y
$T_{\epsilon_x}, T_{\epsilon_y}, T_{\epsilon_z}$	correlation time of ϵ_x, ϵ_y, ϵ_z
$\underline{v}, \underline{v}_i$	measurement noise vector
V	magnitude of $\underline{V}$
$\underline{V}$	velocity relative to the earth
$\overline{V}$	magnitude of $\underline{\overline{V}}$
$\underline{\overline{V}}$	computed value of $\underline{V}$
V_1, V_2	VOR measurement from station 1, station 2
$\overline{V}_1, \overline{V}_2$	nominal value of V_1, V_2
$\underline{V}_a$	velocity determined from air data
V_{ax}, V_{ay}	easterly, northerly component of $\underline{V}_a$

$\underline{V}_w$	air data error
V_{wx}, V_{wy}	easterly, northerly component of $\underline{V}_w$
V_x, V_y, V_z	easterly, northerly, vertical component of $\underline{V}$
x	easterly component of $\underline{r}$ or east axis
$\underline{x}, \underline{x}_i$	state vector
$\bar{\underline{x}}$	nominal value of $\underline{x}$
$\hat{\underline{x}}, \hat{\underline{x}}_i$	best estimate of $\underline{x}$, $\underline{x}_i$
x_1, x_2, x_{12}	easterly component of $\underline{R}_1$, $\underline{R}_2$, $\underline{R}_{12}$
x_{1m}	value of x_1 determined from a fix using VOR/DME station 1
$\bar{x}_1$	nominal value of x_1
$\underline{x}_e, \underline{x}_n$	see Eq. (D.21)
$\left(x_e\right)_i, \left(x_n\right)_i$	see Eq. (D.1)
$\hat{x}_e, \hat{x}_n$	best estimate of $\underline{x}_e$, $\underline{x}_n$
$\left(\hat{x}_e\right)_i, \left(\hat{x}_n\right)_i$	best estimate of $(\underline{x}_e)_i$, $(\underline{x}_n)_i$
$\hat{\underline{x}}^s, \hat{\underline{x}}^s_i$	suboptimal estimate of $\underline{x}$, $\underline{x}_i$
$\underline{x}^1_k, \underline{x}^2_k$	see Eqs. (E.6)
$\hat{\underline{x}}^s_e, \hat{\underline{x}}^s_n$	suboptimal estimate of $\underline{x}_e$, $\underline{x}_n$
$\left(\hat{\underline{x}}^s_e\right)_i, \left(\hat{\underline{x}}^s_n\right)_i$	suboptimal estimate of $(x_e)_i$, $(x_n)_i$
$^r\underline{x}_k$	state vector immediately after position display reset
$^r\underline{x}^1_k$	see Eqs. (E.6)
X	see Fig. 3.1.

y	northerly component of $\underline{r}$ or north axis
y_1, y_2, y_{12}	northerly component of $\underline{R}_1$, $\underline{R}_2$, $\underline{R}_{12}$
$\bar{y}_1$	nominal value of y_1
y_{1m}	value of y_1 determined from a fix using VOR/DME station 1
Y	see Fig. 3.1
z	vertical axis
$\underline{z}, \underline{z}_i$	measurement vector
$\bar{\underline{z}}$	nominal measurement vector
Z	see Fig. 3.1

Greek Symbols

$\underline{\alpha}$	error in sensed acceleration due to accelerometer errors
α_x, α_y	easterly, northerly component of $\underline{\alpha}$
Γ_i	noise influence matrix
δ_{ij}	Kronecker delta (1 if $i = j$, 0 otherwise)
$\delta(\tau)$	Dirac delta function
$\delta D_1, \delta D_2$	$D_1 - \bar{D}_1$, $D_2 - \bar{D}_2$
δR	magnitude of $\underline{\delta R}$
$\underline{\delta R}$	error in computing $\underline{R}$
$\delta R_x, \delta R_y, \delta R_z$	easterly, northerly, vertical component of $\underline{\delta R}$
δV	magnitude of $\underline{\delta V}$

$\underline{\delta V}$	error in computing $\underline{V}$
$\delta V_1, \delta V_2$	$V_1 - \bar{V}_1$, $V_2 - \bar{V}_2$
$\delta V_x, \delta V_y, \delta V_z$	easterly, northerly, vertical component of $\underline{\delta V}$
$\underline{\delta x}$	$\underline{x} - \underline{\bar{x}}$
$\delta x_1, \delta y_1$	$x_1 - \bar{x}_1$, $y_1 - \bar{y}_1$
$\underline{\delta z}$	$z - \bar{z}$
$\underline{\delta\theta}$	vector angle relating computer and true coordinates
$\delta\theta_x, \delta\theta_y, \delta\theta_z$	easterly, northerly, vertical component of $\underline{\delta\theta}$
ΔT	time between measurement updates
$\underline{\epsilon}$	platform drift due to gyro drift
$\epsilon_x, \epsilon_y, \epsilon_z$	drift of the east, north, vertical gyro
θ	bearing of aircraft relative to north of VOR/DME station
θ_1, θ_2	bearing of aircraft relative to north of station 1, station 2
θ_d	desired bearing signal
θ_u	undesired bearing signal due to reflections
λ	latitude
Λ	longitude
$\underline{\rho}$	angular velocity of true coordinates relative to the earth
$\underline{\rho}_c$	angular velocity of computer coordinates relative to the earth
ρ_x, ρ_y, ρ_z	easterly, northerly, vertical component of $\underline{\rho}$

$\sigma_{b_D}, \sigma_{b_{D1}}, \sigma_{b_{D2}}$	standard deviation of b_D, b_{D1}, b_{D2}
$\sigma_{b_V}, \sigma_{b_{V1}}, \sigma_{b_{V2}}$	standard deviation of b_V, b_{V1}, b_{V2}
$\sigma_{e_D}, \sigma_{e_{D1}}, \sigma_{e_{D2}}$	standard deviation of e_D, e_{D1}, e_{D2}
$\sigma_{e_V}, \sigma_{e_{V1}}, \sigma_{e_{V2}}$	standard deviation of e_V, e_{V1}, e_{V2}
σ_{D1}	see Eq. (4.20)
$\sigma_{R_x}, \sigma_{R_y}$	standard deviation of δR_x, δR_y
$\sigma_{R_x R_y}$	$\left\{E\left[\delta R_x \delta R_y\right]\right\}^{1/2}$
σ_{V1}	see Eq. (4.20)
$\sigma_{V_x}, \sigma_{V_y}$	standard deviation of δV_x, δV_y
σ_{wx}, σ_{wy}	standard deviation of V_{wx}, V_{wy}
$\sigma_{x_1}, \sigma_{y_1}$	standard deviation of x_1, y_1
$\sigma_{x_1 y_1}$	see Eq. (4.14)
$\sigma_{\alpha_x}, \sigma_{\alpha_y}$	standard deviation of α_x, α_y
$\sigma_{\epsilon_x}, \sigma_{\epsilon_y}, \sigma_{\epsilon_z}$	standard deviation of ϵ_x, ϵ_y, ϵ_z
$\sigma_{\psi_x}, \sigma_{\psi_y}, \sigma_{\psi_z}$	standard deviation of ψ_x, ψ_y, ψ_z
τ	time
$\underline{\phi}$	vector angle relating platform and true coordinates
ϕ_x, ϕ_y, ϕ_z	easterly, northerly, vertical component of $\underline{\phi}$
$\left(\phi_x\right)_f, \left(\phi_y\right)_f, \left(\phi_z\right)_f$	value of ϕ_x, ϕ_y, ϕ_z immediately after platform alignment
Φ, Φ_i	transition matrix

$\left(\Phi_{ee}\right)_i, \left(\Phi_{en}\right)_i, \left(\Phi_{ne}\right)_i, \left(\Phi_{nn}\right)_i$	see Eq. (D.2)
Φ^s	see Eq. (C.39)
$\underline{\psi}$	vector angle relating platform and computer coordinates
ψ_x, ψ_y, ψ_z	easterly, northerly, vertical component of $\underline{\psi}$
$\underline{\omega}$	angular velocity of the true coordinates in inertial space
$\underline{\omega}_c$	angular velocity of the computer coordinates in inertial space
$\underline{\omega}_p$	angular velocity of the platform coordinates in inertial space
ω_s	Schuler angular frequency
$\bar{\omega}_s$	computed value of ω_s
$\omega_x, \omega_y, \omega_z$	easterly, northerly, vertical component of $\underline{\omega}$
Ω	magnitude of $\underline{\Omega}$
$\underline{\Omega}$	angular velocity of the earth in inertial space
$\Omega_x, \Omega_y, \Omega_z$	easterly, northerly, vertical component of $\underline{\Omega}$

Mathematical Symbols

$\lvert\ \rvert$	absolute value
$\triangleq$	defined equal to
$\cong$	approximately equal to
$\ll$	much less than

$(\dot{})$	ordinary time derivative of ( )
$(\dot{})_c$	rate of change of ( ) in computer coordinates
$(\dot{})_E$	rate of change of ( ) in earth-fixed coordinates
$(\dot{})_I$	rate of change of ( ) in inertial space
$(\dot{})_p$	rate of change of ( ) in platform coordinates
$(\underline{\ })$	a vector quantity

Subscripts

i, j, k, n	i^{th}, j^{th}, k^{th}, n^{th} stage of a multistage process
-	before incorporating the measurement
+	after incorporating the measurement
i+	after incorporating $\underline{z}_i$

Superscripts

T	matrix transpose
^	estimate
-1	matrix inverse

Abbreviations

deg	degree
DME	distance measuring equipment
ft	feet
FM	frequency modulated
hr	hour

Hz	hertz
INS	inertial navigation system
MHz	megahertz (10^6 Hertz)
NM	nautical mile
RMS	root-mean-square
sec	second
TACAN	tactical air navigation
VOR	very high-frequency omni-range
VOR/DME	co-located VOR and DME
VORTAC	co-located VOR and TACAN

ACKNOWLEDGMENTS

The author is deeply grateful to Professor Arthur E. Bryson, Jr., his advisor, for suggesting the research area and providing encouragement and guidance during the course of this research. His many suggestions, questions, and criticisms were invaluable in developing this thesis. The author also wishes to thank Professors Russell L. Mallett and J. David Powell for their helpful comments and criticisms as readers, and Inga Lof for her conscientious efforts in editing and typing.

Particular gratitude is expressed for the financial support from the National Science Foundation through an NSF Graduate Traineeship, from the National Aeronautics and Space Administration through NASA Grants NGR-05-020-431 and NGL 05-020-007, from the United States Air Force through Contract F33615-72-C-1297, and from Stanford University for computer time.

Special thanks go to my wife, Kathleen, for her encouragement, patience, and support, and to my parents to whom this work is dedicated.

I. INTRODUCTION

1.1 Problem Formulation

This work is concerned with improving the navigational accuracy of aircraft that are equipped to use the VOR/DME system. The VOR (Very high-frequency Omni-Range) enables an aircraft to determine its bearing and the DME (Distance Measuring Equipment) its range relative to a fixed ground station. Current use of the VOR/DME system involves primarily radial navigation, that is, aircraft fly directly to or from the ground stations. Some beginnings have been made in using the VOR/DME system for area navigation [1,2,3], that is, use of the system without being restricted to fly directly to or from ground stations.

Position errors are generally greater for area than for radial navigation. This comes about because the position error resulting from a VOR angular error increases with distance from the station; and an aircraft is farther, on the average, from the VOR stations for area than for radial navigation. Hence, improved navigational accuracy is required to obtain an accuracy for area navigation comparable to that of present-day radial navigation.

The increase in volume of air traffic over the last decade has resulted in air traffic congestion, overburdened air traffic controllers, and lengthy departure and landing delays. These problems can be alleviated by improving the accuracy of aircraft navigation. Improved navigational accuracy would allow decreased separation of aircraft without adversely affecting safety, thus alleviating the congestion problem. Improved navigational accuracy would also reduce the need for radar vectoring and communication, thus lightening the workloads of air traffic controllers. Accurate estimates of flight times, made possible by accurate navigation, would allow airline schedules to be devised so that departure and landing delays would be minimized. But perhaps most importantly, improved navigational accuracy would enhance the use of area navigation. Area navigation would make it possible to fly more direct flight paths, which would result in decreased flight times, route mileages, fuel requirements, pollution, and operating costs. It would also reduce traffic congestion over the VOR/DME stations and permit closely-spaced parallel tracks to accommodate large numbers of aircraft on busy

airways. It also introduces flexibility to fly around bad weather and congested areas. Hence, there is considerable motivation to seek improvements in navigational accuracy.

The availability of a computer to do the triangulation computations required for area navigation suggests the possibility of using the computer to implement a filter to combine VOR/DME information with the information from a dead-reckoning system. Since air data (airspeed and heading) are already available onboard nearly all aircraft and an increasing number of aircraft are equipped with inertial navigation systems, air and inertial data are the foremost choices of dead-reckoning information. Hence, the objective in this work is to study the possibility of improving the accuracy of air navigation by combining VOR/DME information (from one or two stations) with air or inertial data by means of a maximum-likelihood filter.

The use of air data with the information from one VOR/DME station has been discussed by Hemesath [4,5]. However, several extensions of Hemesath's work are made here. First of all, a more realistic error model for the VOR/DME measurements is developed. Hemesath assumed additive exponentially-correlated noise in these measurements, but with such a short correlation time that it was effectively white noise. Although the statistics of the VOR/DME errors are not precisely known, both the VOR and DME measurements seem to contain substantial bias errors (that is, nearly constant errors) as well as some white noise. Modeling these bias errors is important, especially when using the VOR/DME system for area navigation. Secondly, the maximum-likelihood filter is implemented in a more straightforward manner. Thirdly, both radial and area flights are considered rather than only radial flights. Finally, the effects of overflying and switching VOR/DME stations during a flight are studied.

Since more than one VOR/DME station is nearly always in sight at jet altitudes, the simultaneous use of two VOR/DME stations and air data has been investigated. DeGroot and Larsen [6] have considered the use of two VOR's and two DME's (without air data). The possibilities of using 0, 1, or 2 VOR's and 0, 1, or 2 DME's with and without air data are considered in this work.

Several papers appearing in the literature are concerned with combining external position information with inertial data. However, attention has been focused on the use of long-range systems such as LORAN and OMEGA ([7] through [12]). Because the accuracy of the position information derived from the VOR/DME system depends upon the relative location of the aircraft and the VOR/DME station as well as the number of VOR and DME stations used, the possibility of using VOR/DME information requires specific consideration. Although the use of VOR/DME information with an inertial navigator has been mentioned in the literature [5,13,14,53], no comprehensive study of the possibility of combining VOR/DME information and inertial data has been found. The use of VOR/DME information with an inertial navigation system (INS) has thus far been limited to the use of a VOR/DME position fix to reset the position display, no filtering involved [15,16,17].

The inertial systems now onboard aircraft utilize a gyro-stabilized platform on which the accelerometers are mounted. Thus, in order for the INS to be useful, the platform must be initially aligned in some desired orientation. (The locally-level, north-pointing orientation is used in this study.) This alignment is currently done on the ground with the aircraft stationary. The possibility of in-flight alignment of the platform by using VOR/DME information from one or two stations is considered in this study.

Regardless of how the platform is initially aligned, due to calibration and random errors (gyro drift, accelerometer null shifts, etc.), errors in the desired orientation of the platform increase with time. This results in increasing position and velocity errors. In this work, the possibility of improving navigational accuracy by updating the INS with VOR/DME information from one or two stations is investigated.

1.2 Thesis Outline

In Chapter II, brief descriptions of the VOR/DME, inertial, and air data systems are presented, including their principles of operation and sources of error. The various errors associated with these systems are then modeled in Chapter III. A detailed derivation of the INS error equations is presented in Appendix A.

In Chapter IV, a filter to combine the information from two VOR/DME stations with air data is designed. A filter to combine VOR/DME information and inertial data is designed in Chapter V. An estimator to determine the maximum-likelihood position fix from the VOR/DME measurements from two stations is derived in Chapter VI.

The simulation results presented in Chapter VII were obtained from the use of a computer program, a listing of which is contained in Appendix B. The RMS navigation errors for various flight paths using various combinations of VOR/DME information with and without air data are presented. The sensitivity of the air-data filter to variations in error statistics is investigated. The necessary equations for this sensitivity analysis are derived in Appendix C. The performance of a suboptimal air-data filter obtained by neglecting VOR and/or DME bias errors is also investigated. The effect of neglecting states is discussed in Appendix D.

Also in Chapter VII, the results of simulations of in-flight alignment of the INS platform using VOR/DME information are presented. The possibility of improving navigational accuracy by realigning an INS, for example, before or after a transoceanic flight or periodically during a transcontinental flight, is studied. The unaided-inertial, realignment, and position display reset modes of operation are compared. Position display resets are discussed in more detail in Appendix E. The use of a low-quality and a high-quality INS while continuously using VOR/DME data is also investigated. Finally, suboptimal filters, resulting when various states are neglected, are studied.

Based on the simulations performed, the conclusions regarding the possibility of improving navigational accuracy by combining VOR/DME information with air or inertial data are presented in Chapter VIII.

1.3 Contributions

The major contributions of this work are:

(1) An evaluation of the navigational accuracy obtainable by combining the information from two VOR/DME stations with air or inertial data;

(2) An evaluation of the accuracy of in-flight alignment of an INS by using VOR/DME information;

(3) The presentation of results in a form which facilitate comparisons, with regard to navigational accuracy, of the use of one versus two VOR/DME's, the use of an air data versus an inertial navigation system, and the use of a high-quality versus a low-quality INS.

Other contributions include the derivation of a more realistic VOR/DME error model which accounts for bias errors and the investigation of reduced-order suboptimal filters.

II. SYSTEM DESCRIPTIONS

2.1 VOR/DME System

The VOR/DME system is the standard short-range radio navigation aid agreed upon by the International Civil Aviation Organization [18]. It is currently the primary air navigation aid for civil aircraft flying in the airspaces of most of the developed countries of the world. The VOR (Very high-frequency Omni-Range) provides civil aircraft with the bearing, θ, relative to magnetic north at the ground station, whereas the DME (Distance Measuring Equipment) provides the slant range, r, from the ground station, as illustrated in Figure 2.1.

The VOR/DME system in the United States consists mostly of VORTAC stations. Each VORTAC station consists of a co-located TACAN (Tactical Air Navigation) station and a VOR station. The TACAN station provides military aircraft with bearing information and has a DME component which provides both military and civil users with distance information. The VOR portion of the VORTAC provides civil users with bearing information. Besides the VORTAC stations, there are several co-located VOR and DME stations as well as separately located VOR and DME stations. A TACAN station is equivalent to a DME station as far as civil aircraft are concerned. By a VOR/DME station is meant a co-located VOR and DME where the DME may be part of a TACAN station.

Transmitting frequencies are assigned to the various VOR/DME stations in such a way that certain service volumes will be frequency protected, that is, free of interference from adjacent stations. The VOR/DME stations are classified with regard to the size of these cylindrically-shaped, frequency-protected service volumes, as shown in Table 2.1 [19]. A category H station is usually usable to a distance of 200 nautical miles (NM) from the station. Category H facilities also provide L and T service volumes; category L facilities also provide T service volumes. An aircraft flying within the service volume of a particular VOR/DME station is usually assured interference-free navigation signals if it is above the radio horizon and at an elevation angle less than 60 degrees. At elevation angles above 60 degrees, the VOR signals are usually unusable due to excessive interference.

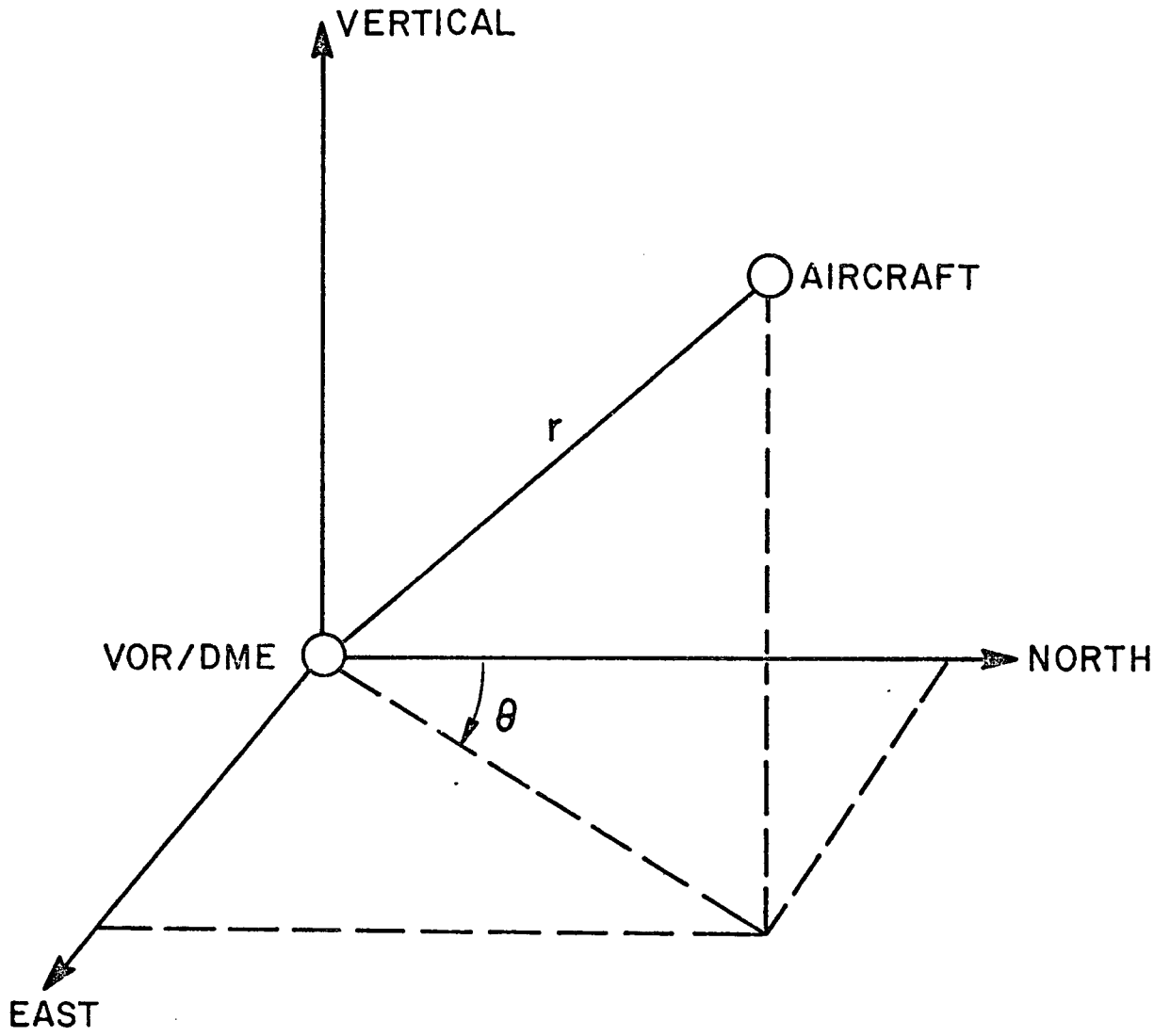

Fig. 2.1. ILLUSTRATION OF VOR/DME INFORMATION.

Table 2.1

FREQUENCY-PROTECTED VOLUMES FOR VOR/DME STATION CATEGORIES

Category	Frequency-Protected Volume
H	130-NM Radius, up to 45,000 Feet 100-NM Radius, above 45,000 Feet
L	40-NM Radius, up to 18,000 Feet
T	25-NM Radius, up to 12,000 Feet

2.1.1 Principle of Operation and Sources of Error for the VOR

VOR ground stations use a radio frequency carrier (108-118 MHz) with which are associated two separate 30 Hz modulations. One signal component is a subcarrier of 9960 Hz of constant amplitude, frequency modulated at 30 Hz. For the conventional VOR,* the 30 Hz component of the FM subcarrier is independent of azimuth and is termed the "reference phase." The other signal component is a 30 Hz amplitude modulation, resulting from a rotating field pattern, the phase of which varies with azimuth. This signal component is called the "variable phase." The reference and variable phase modulations are in phase along the radial corresponding to magnetic north. Thus, the VOR station radiates a fixed pattern in space such that at any point of observation, the reference phase and variable phase differ by an angle equal to the magnetic bearing of the observation point relative to the VOR station. For a detailed technical description, see [20,23].

A major source of error in the VOR system is the misalignment of the station radials, that is, an error resulting because the phase difference between the reference and variable signals is not precisely zero

*Although the conventional VOR is the most widely used type of VOR, there are several other types [20,21,22]. However, the only other type in general use is the Doppler VOR which has been installed at sites where the conventional VOR yields excessive error.

along the radial in the direction of magnetic north. A similar type of error is due to imperfect calibration of the VOR receiver.

Another major source of error in the VOR system is the reflection of the emitted radio signals from fixed obstacles (trees, power lines, buildings, etc.) in their paths [20,24]. These so-called siting errors are demonstrated in Fig. 2.2. The course perturbations caused by siting errors are classified as follows:

(a) Bends: very low-frequency, flyable course perturbations,

(b) Scalloping: low-frequency, non-flyable course perturbations,

(c) Roughness: rapid, irregular, non-flyable course perturbations.

Vertical polarization is another source of error in the VOR system [20,23]. Ideally, the VOR signal is to be horizontally polarized. However, there is a vertically-polarized component which produces bearing indications which are at quadrature with true bearing information. Polarization error can cause the bearing indication at a given observation point to vary with the heading and attitude of the aircraft.

Other sources of error in the VOR system include fluctuations in the 60 Hz power supply of the VOR station, reflections from other aircraft [25], meteorological effects, receiver produced noise, and receiver sensitivity to frequency and strength variations of the 30 Hz signal.

2.1.2 Principle of Operation and Sources of Error for the DME

The airborne DME interrogator emits a signal (960-1215 MHz) consisting of a pair of pulses. Upon receiving the signal, the ground transponder emits a pair of reply pulses which are received by the aircraft. Knowing the speed at which the signal travels and the elapsed time between the transmission of the interrogation signal and the reception of the reply signal, the slant range of the aircraft relative to the ground station is readily determined. In normal operation, the DME gives the slant range at a rate of 15 samples per second. For further details, see [26,27].

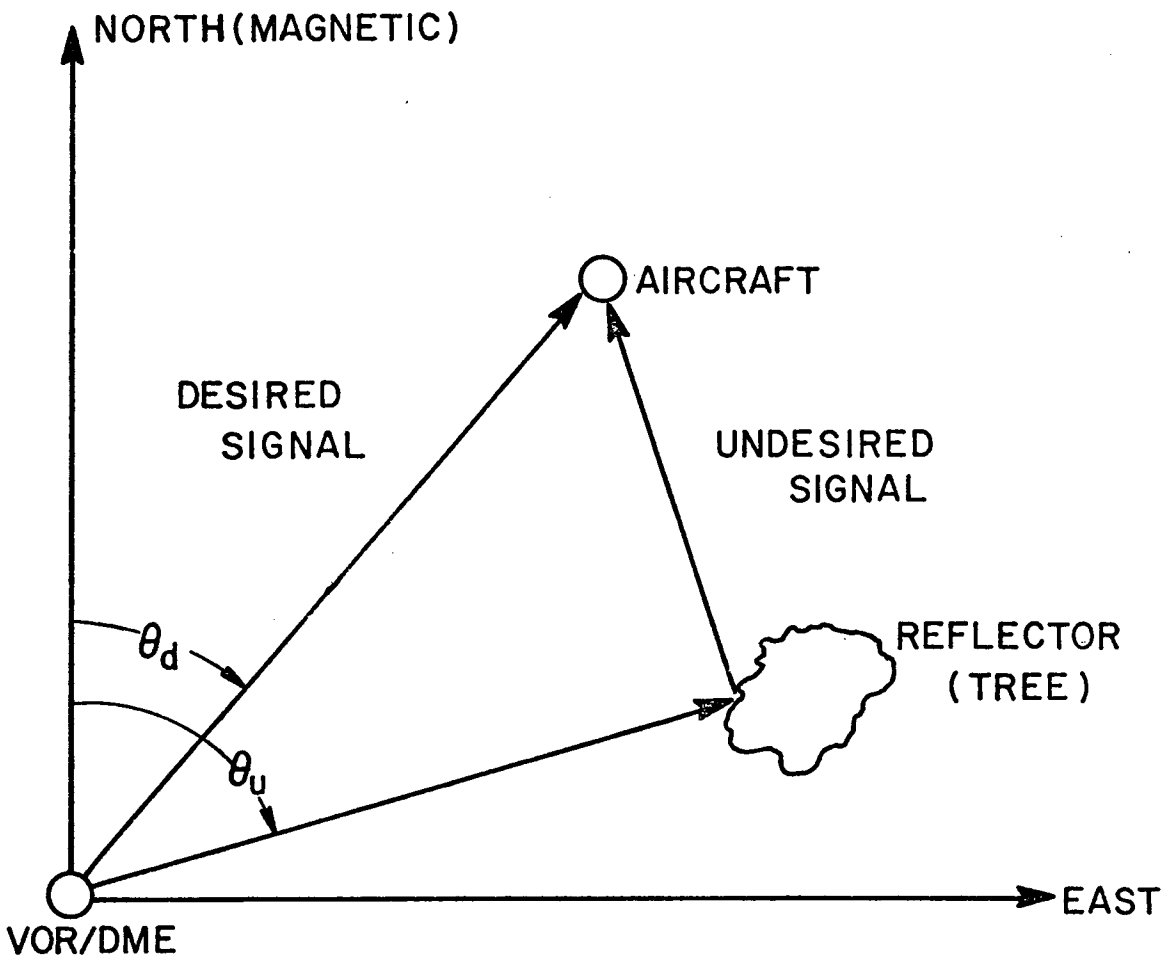

Fig. 2.2. SITING ERROR IN THE VOR SYSTEM.

Errors in the DME system arise from errors in the determination of the total traveling time of the interrogation and reply signals. One such error arises from error in the time delay between the reception of the interrogation signal by the ground transponder and the emission of a reply signal. An error of similar type results from a calibration error in the airborne equipment. Pulse-distorting echoes cause errors in the determination of the arrival time of the interrogation pulse at the ground transponder and of the reply pulse at the airborne receiver. Also, the randomness of the amplitude of successively received interrogation signals, due to the fact that both near and far aircraft are using the same transponder, introduces error into the DME system since the time-of-arrival of a pulse is based on the instant the leading edge reaches a fixed voltage level. Other sources of error in the DME system include transponder replies to other aircraft, pulses randomly emitted by the transponder, and receiver generated noise. For additional information concerning DME errors, see [27].

2.2 Inertial Navigation System

An inertial navigation system (INS) utilizes accelerometers, whose orientation in inertial space is known, to sense the acceleration of a vehicle, and then, integrates the acceleration to determine velocity and position. The INS's currently onboard aircraft have the accelerometers mounted on a gyro-stabilized platform, a structure gimbaled relative to the aircraft in such a way that it will maintain a specified spatial orientation regardless of the motion of the vehicle.

Although there are many types of accelerometers, an accelerometer is basically a proof mass suspended within a case which is attached to the platform. As the vehicle accelerates, the proof mass is displaced relative to the case, the magnitude of the displacement being a measure of the acceleration of the vehicle. The acceleration measured by the accelerometer is the component, along the sensitive axis of the accelerometer, of the vehicle acceleration in inertial space minus the gravity mass attraction. Thus, a knowledge of the gravitational field in the space where an inertial navigator operates is necessary.

Basically, a gyro is a device consisting of a spinning rotor supported by gimbals. In the absence of torques, the spin axis of the rotor will remain fixed in inertial space. However, when a torque is applied perpendicular to the spin axis, the spin axis will rotate in inertial space in such a way that the rate of change of angular momentum with respect to inertial space is equal to the applied torque. Thus, a gyro can be used to establish a reference line in inertial space and the direction of this reference line can be changed by the application of torques.

In this study, it is assumed that three single-degree-of-freedom gyros (see e.g., [28]) with their input axes mutually orthogonal are mounted on the stable platform as are three accelerometers with their sensitive axes along the input axes of the gyros. Furthermore, it is assumed that the platform is always maintained as close as possible to level with the earth with the sensitive axes of the accelerometers pointing east, north, and up. This is accomplished by feeding the gyro output signals (which are a measure of the rotation of the platform in inertial space) to servo loops which drive the platform gimbals to maintain the platform in its desired orientation. The gyros are torqued to compensate for earth rotation and other known (but undesired) torques acting upon the gyros, thus preventing undesired platform rotations.

The errors in the navigational information from an INS are due mainly to errors in the accelerometers and gyros. The principle accelerometer errors are null-shift, scale-factor, and axes-misalignment errors. Null shifts result in a nonzero accelerometer output for a zero acceleration input. Scale-factor error is a result of an inaccuracy in the proportionality constant relating proof mass displacement to actual acceleration. Axes-misalignment errors are due to errors in mounting the accelerometers so that their sensitive axes lie precisely along the desired directions on the platform, thus resulting in the accelerometers reading a component of acceleration orthogonal to their intended sensitive directions.

The major gyro errors are uncompensated drift, torquer scale-factor error, and axes misalignment. Uncompensated gyro drift, due to undesired

mechanical or electrical torques, results in a gyro output that is not due to rotational motion, thus resulting in errors in positioning the platform. Torquer scale-factor error causes an error in the control torque applied to the gyros, which results in an error in platform rotation proportional to the rotation. Misalignment of the input axis of a gyro causes the gyro to sense a component of rotation orthogonal to the intended direction of its input axis, resulting in improper inputs to the platform stabilization servos. For detailed discussions of accelerometers and gyros, and their associated errors, see e.g., [28] through [31].

2.3 Air Data System

Air data, that is, airspeed and heading, are available onboard most aircraft. By measuring the static pressure (the absolute pressure of the still air surrounding the aircraft), the stagnation pressure (the pressure measured in a tube with one open end and one closed end, the open end pointed into the relative wind), and the air temperature, the true airspeed (speed with respect to local air mass) of an aircraft can be determined ([30], Chapter 11). Aircraft heading information can be determined from a simple magnetic compass and/or from a directional gyro ([30], Chapter 10).

When taking air data to be a measure of the velocity of the aircraft relative to the ground, the dominant error is the uncertainty in the velocity of the winds. Although there are certainly sensor errors involved with obtaining air data, they are so small when compared to the error due to winds that it is not worthwhile to treat them separately.

III. ERROR MODELS

3.1 Air Data System

A simple kinematic model of the aircraft is*

$$\dot{\underline{r}} = \underline{V} \quad , \tag{3.1}$$

where $\underline{r}$ is the radius vector from a reference VOR/DME station to the aircraft with the differentiation being performed in the reference frame shown in Fig. 2.1, and $\underline{V}$ is the velocity of the aircraft relative to the ground. Now,

$$\underline{V} = \underline{V}_a + \underline{V}_w \quad , \tag{3.2}$$

where $\underline{V}_a$ is the velocity of the aircraft as determined by the onboard air data and $\underline{V}_w$ is the air data error. Letting x and y, V_{ax} and V_{ay}, and V_{wx} and V_{wy} denote the easterly and northerly components of $\underline{r}$, $\underline{V}_a$, and $\underline{V}_w$, respectively, it is seen from Eqs. (3.1) and (3.2) that

$$\dot{x} = V_{ax} + V_{wx} \quad , \tag{3.3}$$

$$\dot{y} = V_{ay} + V_{wy} \quad . \tag{3.4}$$

The aircraft is assumed to be flying at a known, constant altitude.

The air data errors, V_{wx} and V_{wy}, are caused by winds and by airspeed and heading instrument errors. As mentioned earlier, the winds usually dominate the airspeed and heading errors, so it is not worthwhile to go into detailed models for the airspeed and heading instrument errors.

---

*A dot denotes differentiation with respect to time; an underlined quantity is a vector.

Hence, the air data errors, V_{wx} and V_{wy}, are essentially the easterly and northerly components of the wind velocity.

It seems intuitively reasonable to model the wind velocity components as exponentially-correlated processes. Thus, processes V_{wx} and V_{wy} are sought which approximate the wind velocity components and have correlation functions*

$$E\left[V_{wx}(t+\tau)V_{wx}(t)\right] = \sigma_{wx}^2 \exp\left[-|\tau|/T_{wx}\right] , \tag{3.5}$$

$$E\left[V_{wy}(t+\tau)V_{wy}(t)\right] = \sigma_{wy}^2 \exp\left[-|\tau|/T_{wy}\right] , \tag{3.6}$$

where σ_{wx} and T_{wx}, and σ_{wy} and T_{wy} are the standard deviation and correlation time of V_{wx} and V_{wy}, respectively. Only the slowly-varying, high-magnitude winds are of concern, since high-frequency gusts produce no net displacement of the aircraft. Experimental data regarding wind conditions are difficult to interpret. However, a reasonable value for σ_{wx} and σ_{wy} seems to be about 40 knots [4] while the mean values of V_{wx} and V_{wy} should be assumed to be zero unless other values are known from prior knowledge of the wind conditions along a particular flight path. A reasonable value for the correlation distances of both V_{wx} and V_{wy} is thought to be about 50 nautical miles (NM). Although V_{wx} and V_{wy} are likely to be correlated, they are assumed to be uncorrelated here because of a lack of experimental data regarding their correlation. More accurate estimates of V_{wx} and V_{wy} by a filter would be possible if their correlation were known.

Shaping filters that generate the independent, exponentially-correlated processes V_{wx} and V_{wy} are given by** ([32], Section 11.4)

---

*$E[\cdot]$ is the expected value function.

**Implicit in this model is the assumption that V_{wx} and V_{wy} are gauss-markov processes. This assumption is made so that presently developed filter design techniques will be applicable. There is no reason to believe this assumption is not a reasonable one. All errors in the systems which are considered in this work are assumed to be gauss-markov processes.

$$\dot{V}_{wx} = -\frac{1}{T_{wx}} V_{wx} + \frac{1}{T_{wx}} n_{wx} \quad , \tag{3.7}$$

$$\dot{V}_{wy} = -\frac{1}{T_{wy}} V_{wy} + \frac{1}{T_{wy}} n_{wy} \quad , \tag{3.8}$$

with

$$E\left[V_{wx}\right] \quad \text{and} \quad E\left[V_{wy}\right] \quad \text{given} \ , \tag{3.9}$$

$$\sigma_{wx} = \sigma_{wy} = 40 \text{ knots} \ , \tag{3.10}$$

$$T_{wx} = T_{wy} = \frac{50 \text{ NM}}{V} \quad , \tag{3.11}$$

where n_{wx} and n_{wy} are independent white noise processes with*

$$E\left[n_{wx}\right] = 0 \ , \qquad E\left[n_{wx}(t+\tau)n_{wx}(t)\right] = 2T_{wx}\sigma_{wx}^2\delta(\tau) \quad , \tag{3.12}$$

$$E\left[n_{wy}\right] = 0 \ , \qquad E\left[n_{wy}(t+\tau)n_{wy}(t)\right] = 2T_{wy}\sigma_{wy}^2\delta(\tau) \quad . \tag{3.13}$$

3.2 Inertial Navigation System

In Appendix A, the INS error equations are shown to be

$$\dot{\underline{\delta R}} = \underline{\delta V} - \underline{\rho} \times \underline{\delta R} \quad , \tag{3.14}$$

$$\dot{\underline{\delta V}} = \underline{\alpha} - \omega_s^2 \underline{\delta R} - \underline{\Psi} \times \underline{a} - (2\underline{\Omega} \times \underline{\rho}) \times \underline{\delta V} + 3\frac{\omega_s^2}{R}\delta R \underline{R} \quad , \tag{3.15}$$

$$\dot{\underline{\Psi}} = \underline{\epsilon} - \underline{\omega} \times \underline{\Psi} \quad , \tag{3.16}$$

*$\delta(\tau)$ is the Dirac delta function.

where the time derivatives are taken in true coordinates and

$\underline{R}$ = radius vector from the center of the earth to the vehicle,

R = magnitude of $\underline{R}$,

$\underline{\delta R}$ = error in computing $\underline{R}$, that is, position error,

δR = magnitude of $\underline{\delta R}$,

$\underline{\delta V}$ = error in computing $\underline{V}$,

$\underline{\rho}$ = angular velocity of the true coordinates relative to the earth,

$\underline{\Omega}$ = angular velocity of the earth relative to inertial space,

ω_s^2 = g/R, the square of the Schuler angular frequency,

g = magnitude of the gravity vector (including centripetal acceleration),

$\underline{\alpha}$ = accelerometer error,

$\underline{\psi}$ = vector angle relating the platform and computer coordinates,

$\underline{\epsilon}$ = platform drift rate,

$\underline{\omega} = \underline{\rho} + \underline{\Omega}$, and

$\underline{a}$ = accelerometer output.

For the simulations performed here, $\underline{a}$ is taken to be the nominal accelerometer output along a nominal flight path, that is, from Appendix A,

$$\underline{a} = \dot{\underline{V}} + (2\underline{\Omega} + \underline{\rho}) \times \underline{V} - \underline{g} \quad , \tag{3.17}$$

where the differentiation is taken in true coordinates, $\underline{V}$ is the velocity of the vehicle relative to the earth, and $\underline{g}$ is the gravity vector which includes centripetal acceleration due to the earth's rotation.

For this study, a latitude-longitude mechanization is used, that is, the platform is maintained as closely as possible to locally-level, with respect to the earth, with accelerometer sensitive axes pointing

east (x), north (y), and up (z). The relationship between the platform axes (x,y,z) and the earth-fixed axes (X,Y,Z) for the latitude-longitude mechanization is illustrated in Fig. 3.1 where λ and Λ denote latitude and longitude, respectively. Since the latitude-longitude mechanization breaks down near the poles of the earth, it is assumed that the vehicle does not operate at high latitudes.

Since the vertical channel of the INS is unstable ([33], Section 4.6), for this study it is assumed that accurate altitude information is available from another source. Thus, only the two horizontal channels of the INS are considered. A further assumption is that the earth is spherical and that gravitational equipotential surfaces associated with $\underline{g}$ are spherical. Although the nonspherical character of the earth and its gravitational field must be taken into account during actual operation, for the simulations performed in this work, this assumption is considered reasonable.

Under the above assumptions, it follows that

$$R_x = R_y = 0 , \qquad R_z = R , \qquad \delta R_z \cong \delta R \cong 0 , \tag{3.18}$$

$$g_x = g_y = 0 , \qquad g_z = -g , \qquad g = g_o \frac{R_o^2}{R^2} , \tag{3.19}$$

$$\Omega_x = 0 , \qquad \Omega_y = \Omega \cos \lambda , \qquad \Omega_z = \Omega \sin \lambda , \tag{3.20}$$

$$\rho_x = - \frac{V_y}{R} , \qquad \rho_y = \frac{V_x}{R} , \qquad \rho_z = \frac{V_x}{R} \tan \lambda , \tag{3.21}$$

where g_o is the magnitude of $\underline{g}$ at the surface of the earth ($\cong$ 32.2 ft/sec/sec), R_o is the radius of the earth ($\cong$ 3440 NM), and Ω is the earth rotation rate ($\cong$ 15.04 deg/hr). The subscript x, y, or z denotes the component along the x, y, or z axis of the associated vector quantity.

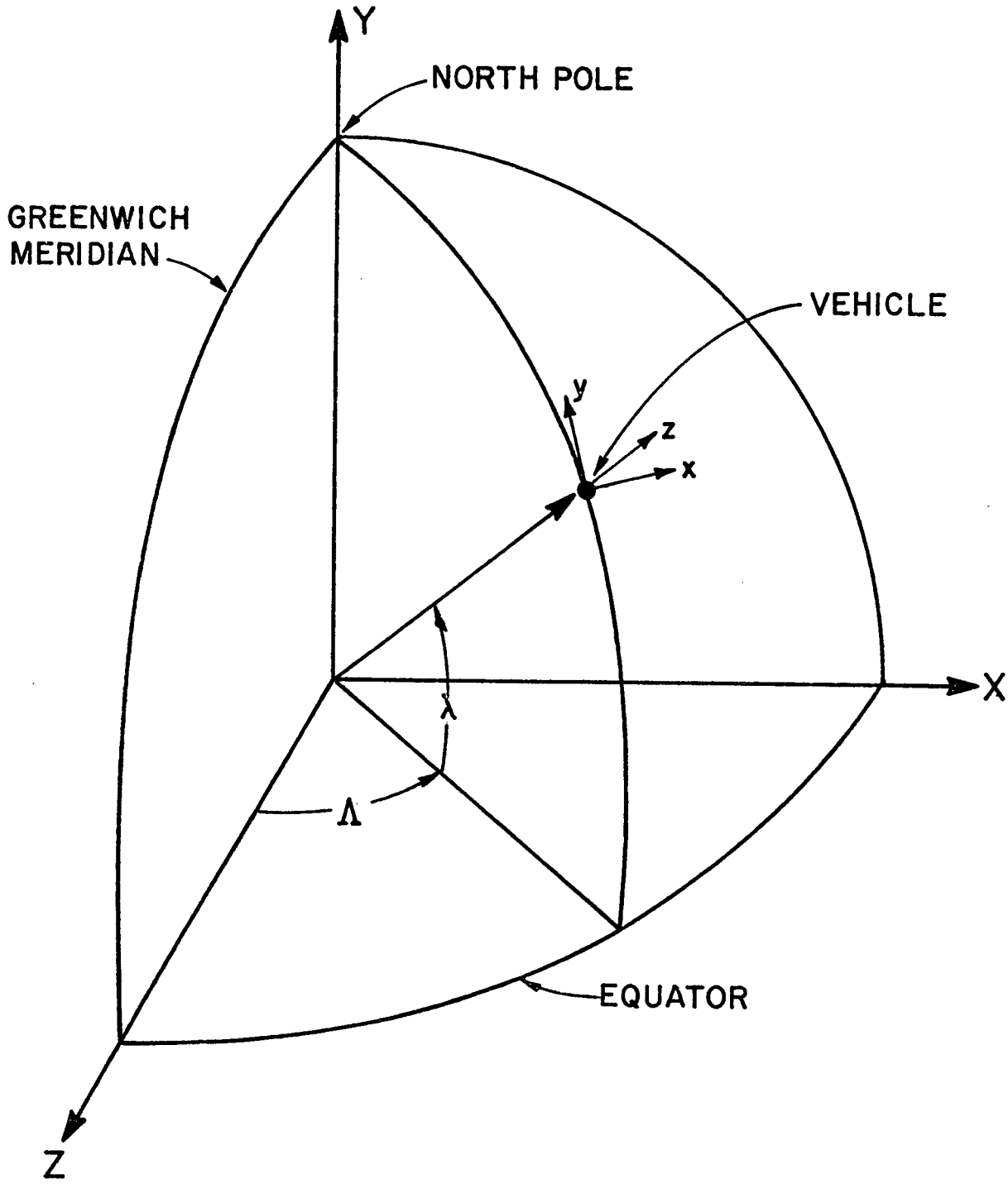

Fig. 3.1. RELATIONSHIP BETWEEN PLATFORM AND EARTH-FIXED AXES FOR LATITUDE-LONGITUDE MECHANIZATION.

Resolving Eqs. (3.14), (3.15), and (3.17) along the x and y axes and Eq. (3.16) along the x, y, and z axes and using Eqs. (3.18) through (3.21) yields:

$$\left.\begin{aligned}
\delta\dot{R}_x &= \delta V_x + \rho_z \delta R_y \,, \\
\delta\dot{R}_y &= \delta V_y - \rho_z \delta R_x \,, \\
\delta\dot{V}_x &= \alpha_x - \omega_s^2 \delta R_x - \psi_y a_z + \psi_z a_y + (2\Omega_z + \rho_z)\, \delta V_y \,, \\
\delta\dot{V}_y &= \alpha_y - \omega_s^2 \delta R_y - \psi_z a_x + \psi_x a_z - (2\Omega_z + \rho_z)\, \delta V_x \,, \\
\dot{\psi}_x &= \epsilon_x - \omega_y \psi_z + \omega_z \psi_y \,, \\
\dot{\psi}_y &= \epsilon_y - \omega_z \psi_x + \omega_x \psi_z \,, \\
\dot{\psi}_z &= \epsilon_z - \omega_x \psi_y + \omega_y \psi_x \,,
\end{aligned}\right\} \qquad (3.22)$$

and

$$\left.\begin{aligned}
a_x &= \dot{V}_x + (2\Omega_y + \rho_y) V_z - (2\Omega_z + \rho_z)\, V_y \,, \\
a_y &= \dot{V}_y + (2\Omega_z + \rho_z) V_x - \rho_x V_z \,, \\
a_z &= \dot{V}_z - (2\Omega_y + \rho_y) V_x + \rho_x V_y + g \,.
\end{aligned}\right\} \qquad (3.23)$$

The platform attitude error, $\underline{\phi}$, that is, the vector angle relating the platform and true axes, is given by

$$\underline{\phi} = \underline{\psi} + \underline{\delta\theta} \,, \qquad (3.24)$$

where $\underline{\delta\theta}$ is the vector angle relating the computer and true axes. For the mechanization used, the components of $\underline{\delta\theta}$ are given by

$$\delta\theta_x = -\frac{\delta R_y}{R}, \qquad \delta\theta_y = \frac{\delta R_x}{R}, \qquad \delta\theta_z = \frac{\delta R_x}{R}\tan\lambda \quad . \tag{3.25}$$

Hence, in view of Eqs. (3.24) and (3.25),

$$\left.\begin{aligned} \phi_x &= \psi_x - \frac{\delta R_y}{R} \quad , \\ \phi_y &= \psi_y + \frac{\delta R_x}{R} \quad , \\ \phi_z &= \psi_z + \frac{\delta R_x}{R}\tan\lambda \quad , \end{aligned}\right\} \tag{3.26}$$

where ϕ_x and ϕ_y are called the platform tilt about the east and north axes, respectively; and ϕ_z is called the platform azimuth error.

Having described in Section 2.2 the sources of error in the accelerometers, the east accelerometer error (α_x) and the north accelerometer error (α_y) will now be modeled. Assuming a high-quality INS operating in cruise conditions, the main source of error in the accelerometers is due to null shifts. This error can be modeled as an exponentially-correlated process [7,8,34]. A reasonable value for the standard deviation of this process is 10^{-4} g [7,8,31] while the mean value is assumed to be zero. The correlation time is very long, a reasonable value being 10 hours [7,8]. Hence, the models used for α_x and α_y are given by

$$\left.\begin{aligned} \dot{\alpha}_x &= -\frac{1}{T_{\alpha_x}}\alpha_x + \frac{1}{T_{\alpha_x}} n_{\alpha_x} \quad , \\ \dot{\alpha}_y &= -\frac{1}{T_{\alpha_y}}\alpha_y + \frac{1}{T_{\alpha_y}} n_{\alpha_y} \quad , \end{aligned}\right\} \tag{3.27}$$

with

$$\left.\begin{aligned} E\left[\alpha_x\right] &= E\left[\alpha_y\right] = 0 \quad , \\ \sigma_{\alpha_x} &= \sigma_{\alpha_y} = 10^{-4}\ g \quad , \\ T_{\alpha_x} &= T_{\alpha_y} = 10 \text{ hours} \quad , \end{aligned}\right\} \tag{3.28}$$

where n_{α_x} and n_{α_y} are independent white noise processes with

$$\left.\begin{aligned} E\left[n_{\alpha_x}\right] &= 0 \ , \qquad E\left[n_{\alpha_x}(t+\tau)n_{\alpha_x}(t)\right] = 2T_{\alpha_x}\sigma^2_{\alpha_x}\delta(\tau) \ , \\ E\left[n_{\alpha_y}\right] &= 0 \ , \qquad E\left[n_{\alpha_y}(t+\tau)n_{\alpha_y}(t)\right] = 2T_{\alpha_y}\sigma^2_{\alpha_y}\delta(\tau) \ . \end{aligned}\right\} \tag{3.29}$$

The quantities σ_{α_x} and T_{α_x}, and σ_{α_y} and T_{α_y} are the standard deviation and correlation time of α_x and α_y, respectively.

The platform drift rate $\underline{\epsilon}$ is due mainly to uncompensated gyro drift. Hence, gyro drift is the only source of gyro error that will be modeled. For our purposes the gyro drift can be modeled reasonably well as an exponentially-correlated process [7,8,31,35,36]. For high-quality gyros, a typical value of the standard deviation of the gyro drift is 0.01 deg/hr [17,31] while the mean value is taken to be zero. Furthermore, a reasonable value of the correlation time is 5 hours [7, 8]. Hence, the models for east gyro drift (ϵ_x), north gyro drift (ϵ_y), and vertical gyro drift (ϵ_z) are given by

$$\left.\begin{aligned} \dot{\epsilon}_x &= -\frac{1}{T_{\epsilon_x}}\epsilon_x + \frac{1}{T_{\epsilon_x}}n_{\epsilon_x} \quad , \\ \dot{\epsilon}_y &= -\frac{1}{T_{\epsilon_y}}\epsilon_y + \frac{1}{T_{\epsilon_y}}n_{\epsilon_y} \quad , \\ \dot{\epsilon}_z &= -\frac{1}{T_{\epsilon_z}}\epsilon_z + \frac{1}{T_{\epsilon_z}}n_{\epsilon_z} \quad , \end{aligned}\right\} \tag{3.30}$$

with

$$\left.\begin{aligned} E\left[\epsilon_x\right] = E\left[\epsilon_y\right] = E\left[\epsilon_z\right] = 0 \quad , \\ \sigma_{\epsilon_x} = \sigma_{\epsilon_y} = \sigma_{\epsilon_z} = 0.01 \text{ deg/hr} \quad , \\ T_{\epsilon_x} = T_{\epsilon_y} = T_{\epsilon_z} = 5 \text{ hours} \quad , \end{aligned}\right\} \tag{3.31}$$

where n_{ϵ_x}, n_{ϵ_y}, n_{ϵ_z} are independent white noise processes with

$$\left.\begin{aligned} E\left[n_{\epsilon_x}\right] = 0 \ , \quad E\left[n_{\epsilon_x}(t+\tau)n_{\epsilon_x}(t)\right] = 2T_{\epsilon_x}\sigma^2_{\epsilon_x}\delta(\tau) \ , \\ E\left[n_{\epsilon_y}\right] = 0 \ , \quad E\left[n_{\epsilon_y}(t+\tau)n_{\epsilon_y}(t)\right] = 2T_{\epsilon_y}\sigma^2_{\epsilon_y}\delta(\tau) \ , \\ E\left[n_{\epsilon_z}\right] = 0 \ , \quad E\left[n_{\epsilon_z}(t+\tau)n_{\epsilon_z}(t)\right] = 2T_{\epsilon_z}\sigma^2_{\epsilon_z}\delta(\tau) \ . \end{aligned}\right\} \tag{3.32}$$

The quantities σ_{ϵ_x} and T_{ϵ_x}, σ_{ϵ_y} and T_{ϵ_y}, and σ_{ϵ_z} and T_{ϵ_z} are the standard deviation and correlation time of ϵ_x, ϵ_y, and ϵ_z, respectively.

3.3 VOR System

Having described the sources of error in the VOR system in Section 2.1.1, attention will now be turned to the mathematical modeling of these errors. First of all, consider the errors due to the misalignment of station radials and imperfect calibration of the VOR receiver. The mean values of both of these errors are approximately zero while the standard deviations are about 0.8 degree and 0.6 degree for the former and the latter, respectively [37]. During the time that a given aircraft is using a particular station, these errors are essentially constant.

Hence, they can be modeled as random, but constant, biases. Denoting the sum of these two errors by b_V, a shaping filter which generates b_V is given by

$$\dot{b}_V = 0 \quad . \tag{3.33}$$

Furthermore, since the two errors are independent, the mean value of b_V and the standard deviation of b_V, σ_{b_V}, are

$$E\left[b_V\right] = 0 \ , \qquad \sigma_{b_V} = 1.0 \text{ degree} \ . \tag{3.34}$$

Let e_V denote the error in the VOR system due to all sources except radial misalignment and receiver calibration. The mean value of e_V is essentially zero while a reasonable value for the standard deviation of e_V, σ_{e_V}, is 1.0 degree [4,38]. Since VOR receivers are designed to filter out error components with frequencies comparable to those of roughness, the correlation time of e_V, T_{e_V}, is approximately equal to the inverse of the maximum scalloping frequency. Noting that the spatial pattern established by the VOR is essentially fixed and that it is the motion of the aircraft which causes e_V to vary with time, it follows that the value of T_{e_V} depends on the speed of the aircraft. Hence, a correlation distance is sought. Typical values of the maximum scalloping frequency per knot which were found in the literature [4,6,38] range from 1.25×10^{-4} to 4.2×10^{-4} Hz/knot. Thus, a realistic value of the maximum scalloping frequency per knot is 2.8×10^{-4} Hz/knot. This corresponds to a correlation distance of about 1.0 NM. Hence, at jet airliner cruising speeds, T_{e_V} will have a value on the order of 10 seconds (e.g., $T_{e_V} = 7.2$ seconds at 500 knots). Since this correlation time is very short compared to the correlation times associated with the air data and inertial systems, e_V will be modeled as white noise:

$$E\left[e_V\right] = 0 \ , \qquad E\left[e_V(t+\tau)e_V(t)\right] = 2\sigma_{e_V}^2 T_{e_V} \delta(\tau) \ , \tag{3.35}$$

where

$$\sigma_{e_V} = 1.0 \text{ degree} , \qquad T_{e_V} = \frac{1.0 \text{ NM}}{V} . \tag{3.36}$$

The choice of the values of the parameters in the above model is based on the assumptions that quality receivers are used, that is, the type used on jet airliners, and that the VOR stations are located at good sites (or that Doppler VOR is being used at a poor site) so that siting errors are minimized. Also, it is implicitly assumed that the errors are independent of the flight path. The literature indicates that these assumptions are reasonable [38].

3.4 DME System

The errors in the DME system, which were described in Section 2.1.2, will now be modeled. First of all, consider the error in the time delay between the reception of an interrogation signal by the ground transponder and the emission of a reply signal and the error due to imperfect calibration of the receiver. Although both of these errors may vary slowly because of component drift, temperature changes, or power supply variations, they are essentially constant during the time a particular aircraft is using a particular DME station. Furthermore, these two errors are independent, each having a mean value of zero and an RMS value of about 0.1 NM [26,37,38]. Hence, their sum, b_D, can be modeled as a random bias, that is,

$$\dot{b}_D = 0 , \tag{3.37}$$

with

$$E\left[b_D\right] = 0 , \qquad \sigma_{b_D} = 0.14 \text{ NM} , \tag{3.38}$$

where σ_{b_D} is the standard deviation of b_D.

Let the error in the DME system due to all sources except the two sources of b_D be denoted by e_D. The mean value of e_D is taken to be zero and 0.1 NM is taken as a reasonable value for its standard deviation, σ_{e_D} [4,38]. The correlation distance of e_D is taken to be 0.5 NM. Since the corresponding correlation time at jet cruising speeds is short compared to the characteristic times associated with the air data system or INS, e_D can be modeled as white noise, that is,

$$E\left[e_D\right] = 0 \ , \qquad E\left[e_D(t+\tau)e_D(t)\right] = 2\sigma^2_{e_D} T_{e_D} \delta(\tau) \ , \tag{3.39}$$

with

$$\sigma_{e_D} = 0.1 \text{ NM} \ , \qquad T_{e_D} = \frac{0.5 \text{ NM}}{V} \ , \tag{3.40}$$

where T_{e_D} is the correlation time of e_D.

The above models assume quality airborne DME receivers. For such equipment, the DME error is independent of the range from a station [26,38].

3.5 Summary

The air data, INS, VOR, and DME error models are summarized in Table 3.1. The correlation times shown are for an aircraft flying at a speed of 500 knots. The mean values and RMS (Root-Mean-Square) values are thought to be reasonable values for a "typical" VOR/DME station, assuming the use of quality receivers, that is, the type used on jet airliners. The values of the INS error parameters shown in Table 3.1 are for a high-quality system. For a low-quality INS, the RMS value of the gyro drifts is taken to be 1.0 deg/hr.

Table 3.1

SUMMARY OF AIR DATA, INS, VOR, AND DME ERROR MODELS

System	Error	Mean Value	RMS Value	Correlation Time	Model
Air Data	V_{wx}	Given	40 knots	360 sec	Exponentially Correlated Process
	V_{wy}	Given	40 knots	360 sec	Exponentially Correlated Process
INS	$\epsilon_x, \epsilon_y, \epsilon_z$	0	0.01 deg/hr	5 hours	Exponentially Correlated Process
	α_x, α_y	0	10^{-4} g	10 hours	Exponentially Correlated Process
VOR	b_V	0	1.0 deg	hours	Random Bias
	e_V	0	1.0 deg	7.2 sec	White Noise
DME	b_D	0	0.14 NM	hours	Random Bias
	e_D	0	0.1 NM	3.6 sec	White Noise

IV. FILTER FOR COMBINING VOR/DME INFORMATION AND AIR DATA

In this chapter, a filter is designed which combines the information from two VOR/DME stations with air data. This filter can be used with 0, 1, or 2 VOR's and 0, 1, or 2 DME's.

4.1 System Model

The VOR/DME station configuration is shown in Fig. 4.1. The vector $\underline{R}_{12}$ is defined by

$$\underline{R}_{12} \triangleq \underline{R}_1 - \underline{R}_2 \quad . \tag{4.1}$$

The easterly, northerly, and vertical components of $\underline{R}_1$, $\underline{R}_2$, and $\underline{R}_{12}$ are denoted by (x_1, y_1, h_1), (x_2, y_2, h_2), and (x_{12}, y_{12}, h_{12}), respectively. Furthermore, the VOR and DME measurements from station 1 and station 2 are denoted by V_1 and D_1, and V_2 and D_2, respectively. Using these definitions and the error models derived in Chapter III, the system model is:

State equations:

$$\dot{\underline{x}} = F\underline{x} + \underline{f} + \underline{n} \quad ,$$

that is, (4.2)

$$\begin{bmatrix} \dot{x}_1 \\ \dot{y}_1 \\ \dot{V}_{wx} \\ \dot{V}_{wy} \\ \dot{b}_{V1} \\ \dot{b}_{D1} \\ \dot{b}_{V2} \\ \dot{b}_{D2} \end{bmatrix} = \left[\begin{array}{cccc:c} 0 & 0 & 1 & 0 & \\ 0 & 0 & 0 & 1 & \\ 0 & 0 & -\left(\frac{1}{T_{wx}}\right) & 0 & 0 \\ 0 & 0 & 0 & -\left(\frac{1}{T_{wy}}\right) & (4 \times 4) \\ \hdashline & & & & \\ & & 0 & & \\ & & (4 \times 8) & & \end{array}\right] \begin{bmatrix} x_1 \\ y_1 \\ V_{wx} \\ V_{wy} \\ b_{V1} \\ b_{D1} \\ b_{V2} \\ b_{D2} \end{bmatrix} + \begin{bmatrix} V_{ax} \\ V_{ay} \\ 0 \\ 0 \\ 0 \\ 0 \\ 0 \\ 0 \end{bmatrix} + \begin{bmatrix} 0 \\ 0 \\ \frac{n_{wx}}{T_{wx}} \\ \frac{n_{wy}}{T_{wy}} \\ 0 \\ 0 \\ 0 \\ 0 \end{bmatrix} ,$$

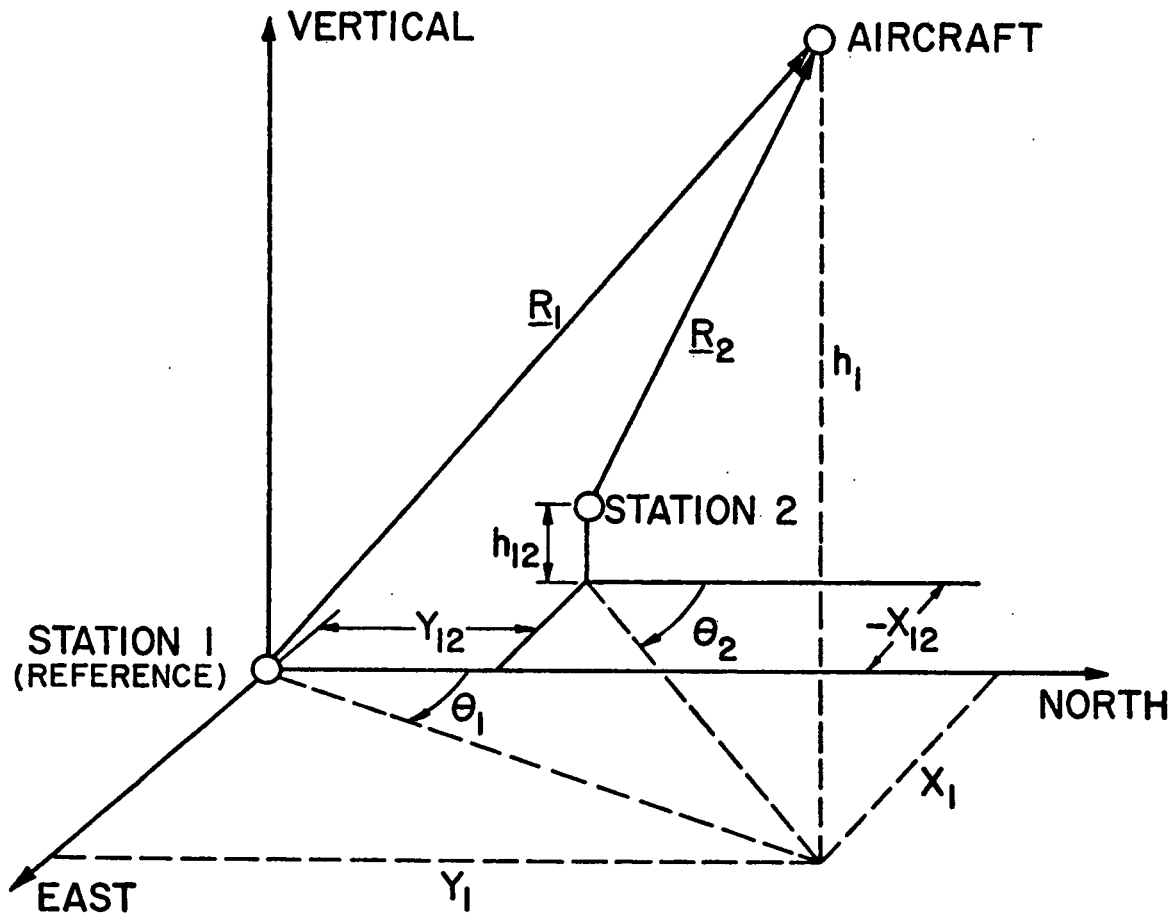

Fig. 4.1. VOR/DME STATION CONFIGURATION.

where the subscripts 1 and 2 indicate the station with which a quantity is associated.

Measurement equations:

$$\underline{z} = \underline{h}(\underline{x}) + \underline{v} \quad ,$$

that is, (4.3)

$$\begin{bmatrix} V_1 \\ D_1 \\ V_2 \\ D_2 \end{bmatrix} = \begin{bmatrix} \arctan\,(x_1/y_1) + b_{V1} \\ \left[x_1^2 + y_1^2 + h_1^2\right]^{1/2} + b_{D1} \\ \arctan\left[(x_1 - x_{12})/(y_1 - y_{12})\right] + b_{V2} \\ \left[(x_1 - x_{12})^2 + (y_1 - y_{12})^2 + (h_1 - h_{12})^2\right]^{1/2} + b_{D2} \end{bmatrix} + \begin{bmatrix} e_{V1} \\ e_{D1} \\ e_{V2} \\ e_{D2} \end{bmatrix} .$$

Note that since a kinematic model is being used, the air data components V_{ax} and V_{ay} are treated as forcing functions, not as measurements.

4.2 Linearization

Since the measurement equations (4.3) are nonlinear, a linearization procedure must be utilized if linear filtering theory is to be applicable. In actual operation, linearization would be performed about the current estimate of the flight path. For the error analysis here, linearization is performed about a predetermined nominal path. Denoting the nominal values of $\underline{x}$ and $\underline{z}$ by $\bar{\underline{x}}$ and $\bar{\underline{z}}$, respectively, it follows that

$$\underline{x} = \bar{\underline{x}} + \delta\underline{x} \quad ,$$

$$\underline{z} = \bar{\underline{z}} + \delta\underline{z} \quad , \qquad (4.4)$$

where $\underline{\delta x}$ and $\underline{\delta z}$ are small perturbations of $\underline{x}$ and $\underline{z}$ about the nominal values. If Eqs. (4.2) and (4.3) are expanded in a Taylor series about the nominal values and only first order terms are retained, the following set of linearized perturbation equations results:

$$\begin{aligned} \underline{\delta \dot{x}} &= F\underline{\delta x} + \underline{n} \quad , \\ \underline{\delta z} &= H\underline{\delta x} + \underline{v} \quad , \end{aligned} \tag{4.5}$$

where H is the derivative of $\underline{\ell}(\underline{x}, t)$ with respect to $\underline{x}$, evaluated at $\bar{\underline{x}}$, that is,

$$H = \left.\frac{\partial \underline{\ell}}{\partial \underline{x}}\right|_{\underline{x}=\bar{\underline{x}}} = \begin{bmatrix} \dfrac{\bar{y}_1}{A} & , & \dfrac{-\bar{x}_1}{A} & , & 0,0,1,0,0,0 \\ \dfrac{\bar{x}_1}{\left[A + h_1^2\right]^{1/2}} & , & \dfrac{\bar{y}_1}{\left[A + h_1^2\right]^{1/2}} & , & 0,0,0,1,0,0 \\ \dfrac{\bar{y}_1 - y_{12}}{B} & , & \dfrac{x_{12} - \bar{x}_1}{B} & , & 0,0,0,0,1,0 \\ \dfrac{\bar{x}_1 - x_{12}}{\left[B + (h_1 - h_{12})^2\right]^{1/2}} & , & \dfrac{\bar{y}_1 - y_{12}}{\left[B + (h_1 - h_{12})^2\right]^{1/2}} & , & 0,0,0,0,0,1 \end{bmatrix} , \tag{4.6}$$

where

$$A = \bar{x}_1^2 + \bar{y}_1^2 , \qquad B = (\bar{x}_1 - x_{12})^2 + (\bar{y}_1 - y_{12})^2 . \tag{4.7}$$

Let t_o denote the time that the filter is initialized. Then, in view of the modeling done in Chapter III, it follows that

$$E[\underline{n}(t)] = E[\underline{v}(t)] = E\left[\underline{n}(t)\underline{v}^T(\tau)\right] = 0 \quad , \tag{4.8}$$

$$E\left[\underline{\delta x}(t_o)\right] = E\left[\underline{\delta x}(t_o)\underline{n}^T(t)\right] = E\left[\underline{\delta x}(t_o)\underline{v}^T(t)\right] = 0 \quad , \tag{4.9}$$

$$E\left[\underline{n}(t+\tau)\underline{n}^T(t)\right] = Q\delta(\tau)$$

$$= \text{diag}\left\{0, 0, 2\sigma_{wx}^2/T_{wx}, 2\sigma_{wy}^2/T_{wy}, 0, 0, 0, 0\right\}\delta(\tau) \quad , \tag{4.10}$$

$$E\left[\underline{v}(t+\tau)\underline{v}^T(t)\right] = R\delta(\tau)$$

$$= \text{diag}\left\{2T_{e_{V1}}\sigma_{e_{V1}}^2, 2T_{e_{D1}}\sigma_{e_{D1}}^2, \right.$$

$$\left. 2T_{e_{V2}}\sigma_{e_{V2}}^2, 2T_{e_{D2}}\sigma_{e_{D2}}^2\right\}\delta(\tau) \quad . \tag{4.11}$$

The error covariance matrix, P, at t_o is given by

$$P(t_o) = E\left[\underline{\delta x}(t_o)\underline{\delta x}^T(t_o)\right] \quad , \tag{4.12}$$

where all the elements of $P(t_o)$ are zero except for those on the main diagonal, $P_{12}(t_o)$ [the element in the first row and second column of $P(t_o)$], and $P_{21}(t_o)$. In particular,

$$\text{diag } P(t_o) = \left\{\sigma_{x_1}^2(t_o), \sigma_{y_1}^2(t_o), \sigma_{wx}^2, \sigma_{wy}^2, \sigma_{b_{V1}}^2, \sigma_{b_{D1}}^2, \sigma_{b_{V2}}^2, \sigma_{b_{D2}}^2\right\} , \tag{4.13}$$

$$\sigma_{x_1y_1}^2 = P_{12}(t_o) = P_{21}(t_o) = E\left[\delta x_1(t_o)\delta y_1(t_o)\right] \quad . \tag{4.14}$$

Note that the values of all quantities appearing in Eqs. (4.10) through (4.14), except $\sigma_{x_1}(t_o)$, $\sigma_{y_1}(t_o)$, and $\sigma_{x_1y_1}(t_o)$, can be readily determined from the previous discussions (see Chapter III).

4.3 Initial Position Errors

From Fig. 4.1, it is easily seen that

$$x_1 = \left[R_1^2 - h_1^2\right]^{1/2} \sin(\theta_1) \quad ,$$

$$y_1 = \left[R_1^2 - h_1^2\right]^{1/2} \cos(\theta_1) \quad , \tag{4.15}$$

where R_1 is the magnitude of $\underline{R}_1$. Denoting the total errors in the VOR and DME measurements from station 1 by E_{V1} and E_{D1}, respectively, the values of x_1 and y_1 determined from this VOR/DME measurement are

$$x_{1m} = \left[(R_1 + E_{D1})^2 - h_1^2\right]^{1/2} \sin(\theta_1 + E_{V1}) \quad ,$$

$$y_{1m} = \left[(R_1 + E_{D1})^2 - h_1^2\right]^{1/2} \cos(\theta_1 + E_{V1}) \quad . \tag{4.16}$$

Subtraction of Eqs. (4.15) from Eqs. (4.16) yields:

$$E_{x_1} = x_{1m} - x_1 = \left[(R_1 + E_{D1})^2 - h_1^2\right]^{1/2} \sin(\theta_1 + E_{V1}) - \left[R_1^2 - h_1^2\right]^{1/2} \sin(\theta_1) \quad ,$$

$$E_{y_1} = y_{1m} - y_1 = \left[(R_1 + E_{D1})^2 - h_1^2\right]^{1/2} \cos(\theta_1 + E_{V1}) - \left[R_1^2 - h_1^2\right]^{1/2} \cos(\theta_1) \quad . \tag{4.17}$$

For $|E_{D1}| \ll R_1$ and $|E_{V1}| \ll 1$, these relations may be approximated by

$$E_{x_1} = \left(1 - h_1^2/2R_1^2\right)\left[R_1 \cos(\theta_1)E_{V1} + \sin(\theta_1)E_{D1}\right] ,$$

$$E_{y_1} = \left(1 - h_1^2/2R_1^2\right)\left[\cos(\theta_1)E_{D1} - R_1 \sin(\theta_1)E_{V1}\right] . \tag{4.18}$$

From Eqs. (4.18) and the fact that E_{V1} and E_{D1} are uncorrelated, it follows that

$$\sigma_{x_1}^2 = E\left[E_{x_1}^2\right] = \left(1 - h_1^2/2R_1^2\right)^2\left[R_1^2 \cos^2(\theta_1)\sigma_{V1}^2 + \sin^2(\theta_1)\sigma_{D1}^2\right] ,$$

$$\sigma_{y_1}^2 = E\left[E_{y_1}^2\right] = \left(1 - h_1^2/2R_1^2\right)^2\left[R_1^2 \sin^2(\theta_1)\sigma_{V1}^2 + \cos^2(\theta_1)\sigma_{D1}^2\right] , \tag{4.19}$$

$$\sigma_{x_1y_1}^2 = E\left[E_{x_1} E_{y_1}\right] = \left(1 - h_1^2/2R_1^2\right)^2 \sin(2\theta_1)\left(\sigma_{D1}^2 - R_1^2\sigma_{V1}^2\right)/2 ,$$

where

$$\sigma_{V1}^2 = E\left[E_{V1}^2\right] = \sigma_{b_{V1}}^2 + \sigma_{e_{V1}}^2 ,$$

$$\sigma_{D1}^2 = E\left[E_{D1}^2\right] = \sigma_{b_{D1}}^2 + \sigma_{e_{D1}}^2 . \tag{4.20}$$

The initial position variances $\sigma_{x_1}^2(t_o)$ and $\sigma_{y_1}^2(t_o)$, and covariance $\sigma_{x_1y_1}^2(t_o)$, are calculated from Eqs. (4.19) and (4.20) by substituting the values of θ_1 and R_1 at t_o.

4.4 Filter Equations

The Kalman-Bucy filter which gives the maximum-likelihood estimate of the state vector, $\hat{\underline{x}}$, for the continuous-time, discrete-data system described by Eqs. (4.1) through (4.14) is given by [40, 41]:

Between measurements,

$$\dot{\underline{\hat{x}}} = F\underline{\hat{x}} + \underline{f} \quad , \tag{4.21}$$

$$\dot{P} = FP + PF^T + Q \quad . \tag{4.22}$$

At a measurement,

$$\underline{\hat{x}}_+ = \underline{\hat{x}}_- + K[\underline{z} - \mathcal{h}(\underline{\hat{x}}_-)] \quad , \tag{4.23}$$

$$P_+ = (I - KH)P_-(I - KH)^T + KR'K^T \quad , \tag{4.24}$$

$$K = P_-H^T\left(HP_-H^T + R'\right)^{-1} \quad , \tag{4.25}$$

where P is the error covariance matrix, I is the 8×8 identity matrix, and the $-$ and $+$ designate values before and after the measurement, respectively. Since a discrete approximation of the continuous measurement process is used for the purposes of simulation, R' is equal to R divided by the time between measurement updates.

A solution to Eq. (4.22) is of the form (see, e.g., [32], p. 453)

$$P(t) = \Phi(t,t_1)P(t_1)\Phi^T(t,t_1) + \int_{t_1}^{t} \Phi(t,\tau)Q(\tau)\Phi^T(t,\tau)\, d\tau \quad , \tag{4.26}$$

where $\Phi(t,t_1)$ is the transition matrix associated with the system $\dot{x} = Fx$ and satisfies

$$\frac{d}{dt}\Phi(t,t_1) = F(t)\Phi(t,t_1) \quad , \qquad \Phi(t_1,t_1) = I \quad . \tag{4.27}$$

For the system under consideration, the following expression for the transition matrix can be found by solving Eq. (4.27):

$$\Phi(t,t_1) = \left[\begin{array}{cccc|c} 1 & 0 & T_{wx}(1-M) & 0 & \\ 0 & 1 & 0 & T_{wy}(1-N) & \begin{matrix}0\\(4\times 4)\end{matrix} \\ 0 & 0 & M & 0 & \\ 0 & 0 & 0 & N & \\ \hline & & \begin{matrix}0\\(4\times 4)\end{matrix} & & \begin{matrix}I\\(4\times 4)\end{matrix} \end{array}\right] , \qquad (4.28)$$

where

$$M = \exp\left\{-(t - t_1)/T_{wx}\right\} ,$$

$$N = \exp\left\{-(t - t_1)/T_{wy}\right\} , \qquad (4.29)$$

$$I = \text{identity matrix} .$$

Define

$$J \triangleq \int_{t_1}^{t} \Phi(t,\tau)Q(\tau)\Phi^T(t,\tau)\, d\tau . \qquad (4.30)$$

Substituting from Eqs. (4.10), (4.28), and (4.29) into Eq. (4.30) and integrating yields:

$$\left.\begin{aligned} &J(i,j) = 0 \quad \text{for all} \quad i,j = 1,2, \ldots, 8 , \\ &\text{except} \\ &J(1,1) = T_{wx}\sigma_{wx}^2\left[2(t - t_1) - T_{wx}(3 - M)(1 - M)\right] , \\ &J(1,3) = J(3,1) = T_{wx}\sigma_{wx}^2(1 - M)^2 , \\ &J(2,2) = T_{wx}\sigma_{wy}^2\left[2(t - t_1) - T_{wy}(3 - N)(1 - N)\right] , \\ &J(2,4) = J(4,2) = T_{wy}\sigma_{wy}^2(1 - N)^2 , \\ &J(3,3) = \sigma_{wx}^2(1 - M^2) , \\ &J(4,4) = \sigma_{wy}^2(1 - N^2) . \end{aligned}\right\} \qquad (4.31)$$

Thus, from Eqs. (4.28) through (4.31), Eq. (4.26) is seen to constitute a closed-form solution to Eq. (4.22) which involves only the multiplication and addition of matrices.

4.5 Summary

The design of a filter to combine VOR/DME information and air data was based on a kinematic model of the motion of the aircraft projected onto the local horizontal plane at the reference station. It estimates two components of position relative to station 1, the two horizontal components of wind velocity, and the VOR and DME biases associated with each station. The initial position error statistics are those obtained by taking a VOR/DME reading from the reference station. When the aircraft stops using a VOR/DME station and begins to use another, the bias error estimates must be re-initialized. For purposes of error analysis the measurement equations were linearized with respect to a nominal flight path. For real-time application the linearization should be with respect to the current estimate of the flight path.

V. FILTER FOR COMBINING VOR/DME INFORMATION AND INERTIAL DATA

A filter to update an inertial navigation system with the information from two VOR/DME stations is designed in this chapter. This filter can be used with 0, 1, or 2 VOR's and 0, 1, or 2 DME's.

5.1 System Model

In view of the models derived in Section 3.2, the state equations are:

$$\dot{\underline{x}} = F\underline{x} + n \quad ,$$

that is, (5.1)

$$\begin{bmatrix} \dot{\delta R}_x \\ \dot{\delta R}_y \\ \dot{\delta V}_x \\ \dot{\delta V}_y \\ \dot{\psi}_x \\ \dot{\psi}_y \\ \dot{\psi}_z \\ \dot{\epsilon}_x \\ \dot{\epsilon}_y \\ \dot{\epsilon}_z \\ \dot{\alpha}_x \\ \dot{\alpha}_y \\ \dot{b}_{V1} \\ \dot{b}_{D1} \\ \dot{b}_{V2} \\ \dot{b}_{D2} \end{bmatrix} = \left[\begin{array}{cccccccccccc|c} 0 & \rho_z & 1 & 0 & 0 & 0 & 0 & 0 & 0 & 0 & 0 & 0 & \\ -\rho_z & 0 & 0 & 1 & 0 & 0 & 0 & 0 & 0 & 0 & 0 & 0 & \\ -\omega_s^2 & 0 & 0 & (2\Omega_z+\rho_z) & 0 & -a_z & a_y & 0 & 0 & 0 & 1 & 0 & \\ 0 & -\omega_s^2 & -(2\Omega_z+\rho_z) & 0 & a_z & 0 & -a_x & 0 & 0 & 0 & 0 & 1 & \\ 0 & 0 & 0 & 0 & 0 & \omega_z & -\omega_y & 1 & 0 & 0 & 0 & 0 & \\ 0 & 0 & 0 & 0 & -\omega_z & 0 & \omega_x & 0 & 1 & 0 & 0 & 0 & \\ 0 & 0 & 0 & 0 & \omega_y & -\omega_x & 0 & 0 & 0 & 1 & 0 & 0 & \\ 0 & 0 & 0 & 0 & 0 & 0 & 0 & -\frac{1}{T_{\epsilon_x}} & 0 & 0 & 0 & 0 & \\ 0 & 0 & 0 & 0 & 0 & 0 & 0 & 0 & -\frac{1}{T_{\epsilon_y}} & 0 & 0 & 0 & \\ 0 & 0 & 0 & 0 & 0 & 0 & 0 & 0 & 0 & -\frac{1}{T_{\epsilon_z}} & 0 & 0 & \\ 0 & 0 & 0 & 0 & 0 & 0 & 0 & 0 & 0 & 0 & -\frac{1}{T_{\alpha_x}} & 0 & \\ 0 & 0 & 0 & 0 & 0 & 0 & 0 & 0 & 0 & 0 & 0 & -\frac{1}{T_{\alpha_y}} & \\ \hline & & & & & & & & & & & & \\ & & & & & 0_{(4\times 16)} & & & & & & & \end{array}\right] \begin{bmatrix} \delta R_x \\ \delta R_y \\ \delta V_x \\ \delta V_y \\ \psi_x \\ \psi_y \\ \psi_z \\ \epsilon_x \\ \epsilon_y \\ \epsilon_z \\ \alpha_x \\ \alpha_y \\ b_{V1} \\ b_{D1} \\ b_{V2} \\ b_{D2} \end{bmatrix} + \begin{bmatrix} 0 \\ 0 \\ 0 \\ 0 \\ 0 \\ 0 \\ 0 \\ \frac{n_{\epsilon_x}}{T_{\epsilon_x}} \\ \frac{n_{\epsilon_y}}{T_{\epsilon_y}} \\ \frac{n_{\epsilon_z}}{T_{\epsilon_z}} \\ \frac{n_{\alpha_x}}{T_{\alpha_x}} \\ \frac{n_{\alpha_y}}{T_{\alpha_y}} \\ 0 \\ 0 \\ 0 \\ 0 \end{bmatrix}$$

(12 × 4)

C 2

Since the state variables of the filter are errors in the inertial and VOR/DME systems, it follows from the linearization performed in Section 4.2 that the measurement equations are

$$\underline{z} = H\underline{x} + \underline{v} \quad ,$$

that is,

(5.2)

$$\begin{bmatrix} \delta V_1 \\ \delta D_1 \\ \delta V_2 \\ \delta D_2 \end{bmatrix} = \left[\begin{array}{cc|c|c} \dfrac{\bar{y}_1}{A} & \dfrac{-\bar{x}_1}{A} & & \\ \dfrac{\bar{x}_1}{\left[A + h_1^2\right]^{1/2}} & \dfrac{\bar{y}_1}{\left[A + h_1^2\right]^{1/2}} & 0 & I \\ \dfrac{\bar{y}_1 - y_{12}}{B} & \dfrac{x_{12} - \bar{x}_1}{B} & (4\times 10) & (4\times 4) \\ \dfrac{\bar{x}_1 - x_{12}}{\left[B + (h_1 - h_{12})^2\right]^{1/2}} & \dfrac{\bar{y}_1 - y_{12}}{\left[B + (h_1 - h_{12})^2\right]^{1/2}} & & \end{array}\right] \begin{bmatrix} \delta R_x \\ \delta R_y \\ \delta V_x \\ \delta V_y \\ \psi_x \\ \psi_y \\ \psi_z \\ \epsilon_x \\ \epsilon_y \\ \epsilon_z \\ \alpha_x \\ \alpha_y \\ b_{V1} \\ b_{D1} \\ b_{V2} \\ b_{D2} \end{bmatrix} + \begin{bmatrix} e_{V1} \\ e_{D1} \\ e_{V2} \\ e_{D2} \end{bmatrix} ,$$

with

$$A = \bar{x}_1^2 + \bar{y}_1^2 \quad , \qquad B = (\bar{x}_1 - x_{12})^2 + (\bar{y}_1 - y_{12})^2 \quad , \tag{5.3}$$

where δV_1 and δD_1, and δV_2 and δD_2 denote the differences between the actual and nominal VOR and DME measurements from stations 1 and 2, respectively.

In the derivation of the measurement equations, it was assumed that true coordinate axes, that is, the set of axes with its origin at the location of the aircraft with the axes pointing east, north, and up, and the reference station coordinate axes (see Fig. 4.1) are parallel when in fact they are not, due to the curvature of the earth's surface. However, since an aircraft can use a VOR/DME station which is at most 200 NM away, the true and coordinate axes are rotated relative to each other through small angles when not at high latitudes. Hence, the differences between the components of $\underline{R}_1$, $\underline{R}_2$, and $\underline{R}_{12}$ in true and station coordinates are small and are therefore neglected. In other words, in the simulations, flight paths consisting of a series of straight-line segments rather than true great circle paths are flown.

Letting t_o denote the time that the filter is initialized, it follows from the models derived in Chapter III that

$$E\left[\underline{n}(t)\right] = E\left[\underline{v}(t)\right] = E\left[\underline{n}(t)\underline{v}^T(\tau)\right] = 0 \quad , \tag{5.4}$$

$$E\left[\underline{x}(t_o)\right] = E\left[\underline{x}(t_o)n^T(t)\right] = E\left[\underline{x}(t_o)\underline{v}^T(t)\right] = 0 \quad , \tag{5.5}$$

$$E\left[\underline{n}(t+\tau)\underline{n}^T(t)\right] = Q\delta(\tau)$$

$$= \left\{0,0,0,0,0,0,0,\frac{2\sigma_{\epsilon_x}^2}{T_{\epsilon_x}},\frac{2\sigma_{\epsilon_y}^2}{T_{\epsilon_y}},\frac{2\sigma_{\epsilon_z}^2}{T_{\epsilon_z}},\frac{2\sigma_{\alpha_x}^2}{T_{\alpha_x}},\frac{2\sigma_{\alpha_y}^2}{T_{\alpha_y}},0,0,0,0\right\}\delta(\tau) , \tag{5.6}$$

$$E\left[\underline{v}(t+\tau)\underline{v}^T(t)\right] = R\delta(\tau) \quad , \tag{5.7}$$

where R is given by Eq. (4.11). The error covariance matrix, P, at time t_o is given by

$$P(t_o) = E\left[\underline{x}(t_o)\underline{x}^T(t_o)\right] \quad , \tag{5.8}$$

where all the elements are zero except those on the main diagonal, and possibly $P_{12}(t_o)$ and $P_{21}(t_o)$. In particular,

$$\text{diag } P(t_o) = \left\{ \sigma^2_{R_x}(t_o), \sigma^2_{R_y}(t_o), \sigma^2_{V_x}(t_o), \sigma^2_{V_y}(t_o), \sigma^2_{\psi_x}(t_o), \sigma^2_{\psi_y}(t_o), \sigma^2_{\psi_z}(t_o), \right.$$
$$\left. \sigma^2_{\epsilon_x}, \sigma^2_{\epsilon_y}, \sigma^2_{\epsilon_z}, \sigma^2_{\alpha_x}, \sigma^2_{\alpha_y}, \sigma^2_{b_{V1}}, \sigma^2_{b_{D1}}, \sigma^2_{b_{V2}}, \sigma^2_{b_{D2}} \right\} , \tag{5.9}$$

$$\sigma^2_{R_x R_y} = P_{12}(t_o) = P_{21}(t_o) = E\left[\delta R_x(t_o)\delta R_y(t_o)\right] = E\left[\delta x_1(t_o)\delta y_1(t_o)\right] . \tag{5.10}$$

In Eq. (5.9) and (5.10), the initial position error statistics may be those associated with a VOR/DME reading (see Section 4.3) or those determined from another estimate of position. The variances of the velocity and platform attitude errors will depend on the state of the INS when the filter is initialized, and the values of the remainder of the variances appearing in Eq. (5.8) are readily determined from the error models derived in Chapter III.

5.2 Discretization

For the purposes of simulation, the continuous, time-varying, linear system under consideration will be approximated by a multistage system. Thus, a multistage process described by

$$\underline{x}_{i+1} = \Phi_i \underline{x}_i + \Gamma_i \underline{n}_i , \qquad i = 0, 1, 2, \ldots , \tag{5.11}$$

is sought such that

$$\left.\begin{aligned} &\underline{x}_o \cong \underline{x}(t_o) , \\ &\underline{x}_1 \cong \underline{x}(t_1) , \qquad t_1 = t_o + \Delta T , \\ &\underline{x}_2 \cong \underline{x}(t_2) , \qquad t_2 = t_1 + \Delta T , \\ &\quad \vdots \end{aligned}\right\} \tag{5.12}$$

where ΔT is a time increment. The continuous process described by Eqs. (5.1) can be approximated to first order in ΔT by the process described by Eq. (5.11) if ([32], Section 11.5)

$$\Phi_i = \left[I + F(t_i)\Delta T \right] , \tag{5.13}$$

$$\Gamma_i = \Delta T , \tag{5.14}$$

$$\underline{n}_i = \underline{n}(t_i) , \qquad t_i \leq t < t_{i+1} , \tag{5.15}$$

with

$$E\left[\underline{n}_i \underline{n}_j^T \right] = Q' \delta_{ij} = \frac{Q}{\Delta T} \delta_{ij} , \tag{5.16}$$

where δ_{ij}, the Kronecker delta function, is equal to zero unless $i = j$, in which case it equals one. Furthermore, the discrete approximation to the continuous measurement system described by Eqs. (5.2) is given by

$$\underline{z}_i = H_i \underline{x}_i + \underline{v}_i , \qquad i = 0, 1, 2, \ldots , \tag{5.17}$$

with

$$\underline{v}_i = \underline{v}(t_i) , \qquad t_i \leq t < t_{i+1} , \tag{5.18}$$

where

$$E\left[\underline{v}_i \underline{v}_j^T \right] = R' \delta_{ij} = \frac{R}{\Delta T} \delta_{ij} . \tag{5.19}$$

The approximation holds only if ΔT is small compared to the characteristic times of the system.

5.3 Filter Equations

The Kalman filter equations [40] for the linear multistage approximation described by Eqs. (5.11) through (5.19) are:

Time update:

$$\hat{\underline{x}}_{i+1} = \Phi_i \hat{\underline{x}}_{i+} \quad , \tag{5.20}$$

$$P_{i+1} = \Phi_i P_{i+} \Phi_i^T + \Gamma_i Q' \Gamma_i^T \quad . \tag{5.21}$$

Measurement update:

$$\hat{\underline{x}}_{i+} = \hat{\underline{x}}_i + K_i (\underline{z}_i - H_i \hat{\underline{x}}_i) \quad , \tag{5.22}$$

$$P_{i+} = (I - K_i H_i) P_i (I - K_i H_i)^T + K_i R' K_i^T \quad , \tag{5.23}$$

$$K_i = P_i H_i^T \left(H_i P_i H_i^T + R' \right)^{-1} \quad , \tag{5.24}$$

where $\hat{\underline{x}}_i$ and P_i, and $\hat{\underline{x}}_{i+}$ and P_{i+} denote the state estimate and covariance matrix at stage i before and after processing the measurement at stage i, respectively.

Note that in the absence of measurements, the propagation of the state estimate and covariance matrix are described by Eqs. (5.20) and (5.21). This would correspond to the propagation of errors in unaided-inertial operation.

The error estimates obtained from the above filter are, in practice, used in two ways [54]. In the feed-forward configuration shown in Fig. 5.1, the estimates of the position and velocity errors obtained from the filter are simply subtracted from the position and velocity indicated by the INS computer, which essentially solves Eqs. (A.28). Using this configuration, the uncorrected output of the INS computer corresponds to the output obtained in unaided-inertial operation.

In the feedback configuration shown in Fig. 5.2, the error estimates obtained from the filter are used to correct the values of position and velocity in the INS computer as well as to compensate for the estimated sensor errors and apply torques to zero the estimated platform tilts and azimuth error. This configuration has the advantage of keeping the INS errors small, thus reinforcing the assumption of a linear error model.

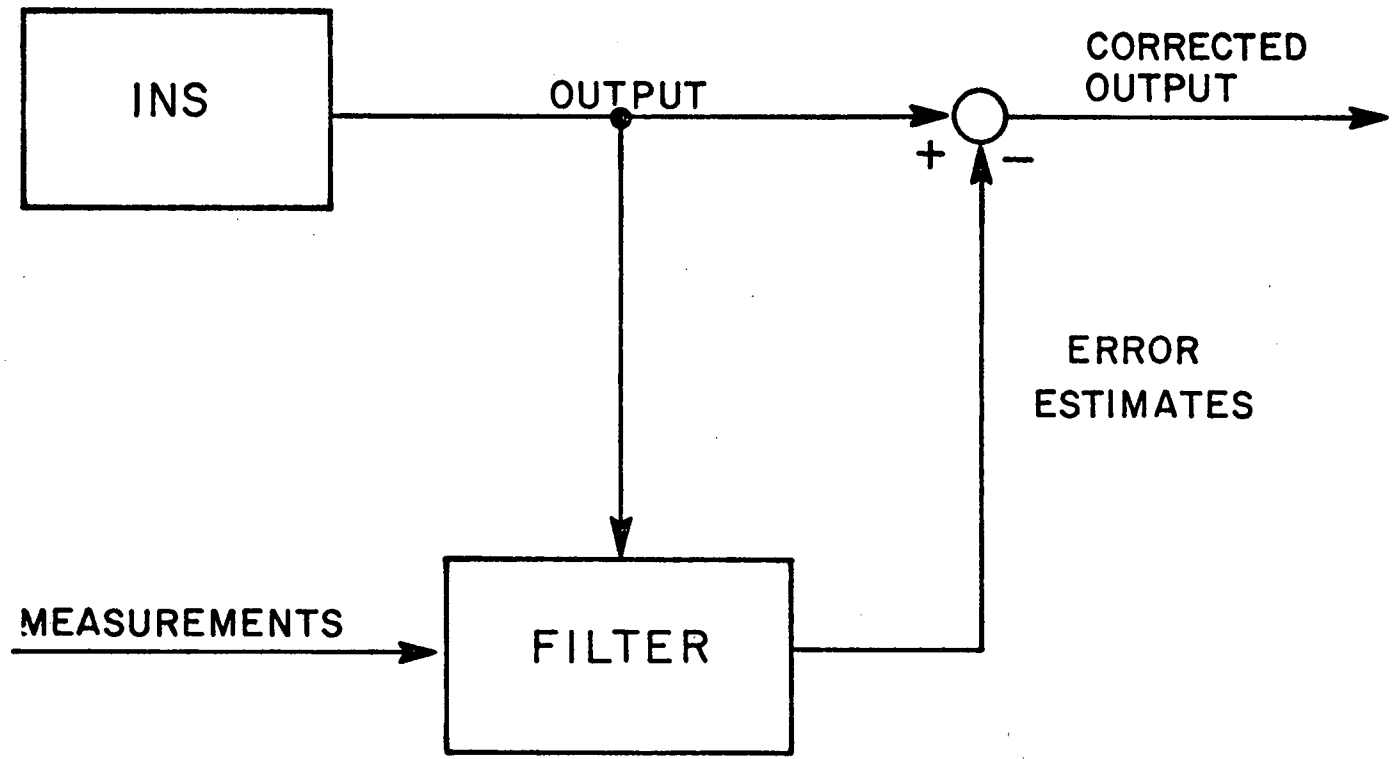

Fig. 5.1. FEED-FORWARD CONFIGURATION OF AIDED-INERTIAL SYSTEM.

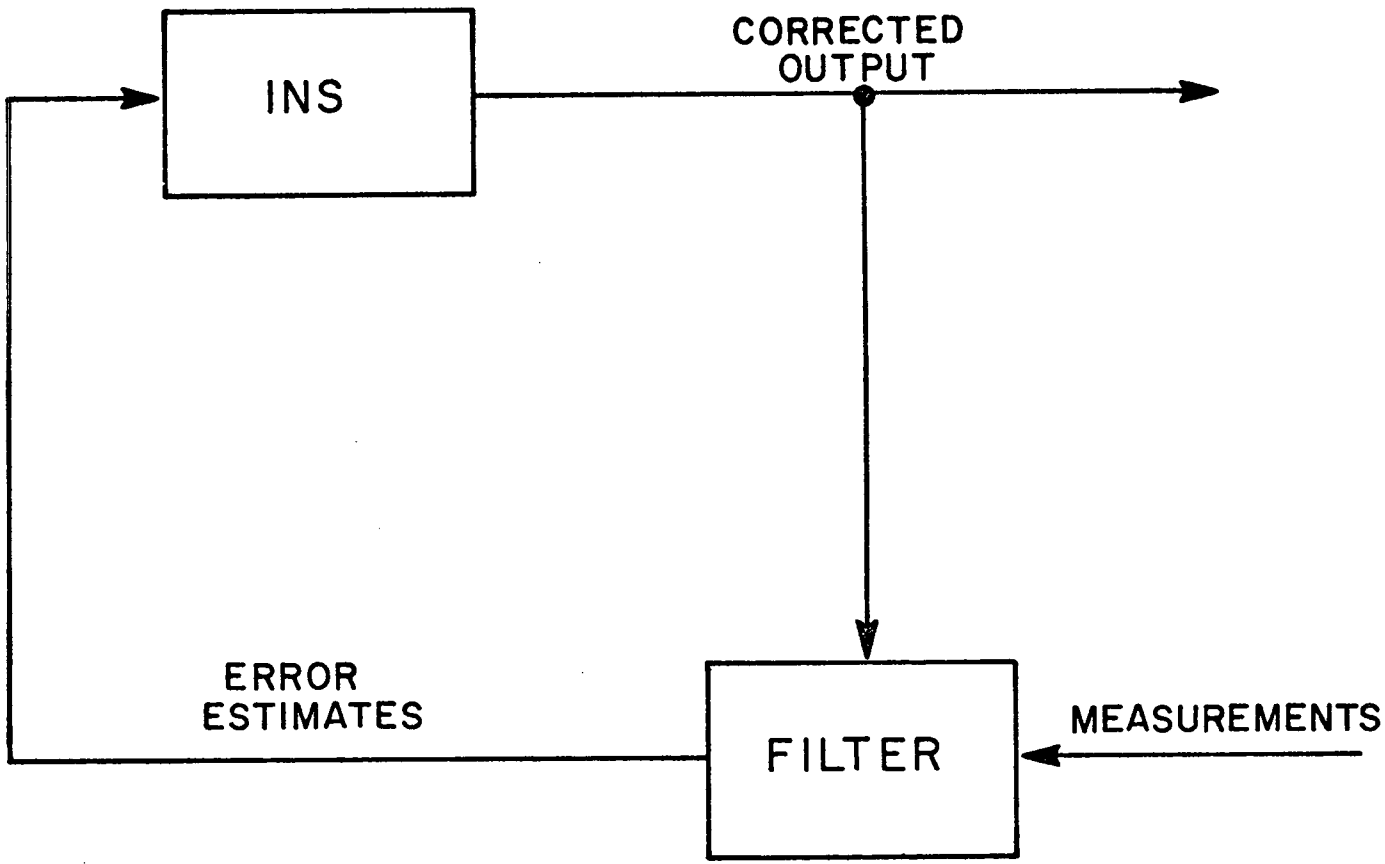

Fig. 5.2. FEEDBACK CONFIGURATION OF AIDED-INERTIAL SYSTEM.

An alternative to the filter assumed here, that is, one which estimates only system and sensor errors, is a filter which treats vehicle position and velocity as state variables. The state equations would then be of the form of Eqs. (A.27). Such a filter would be an integral part of the INS mechanization equations with the output of the INS computer yielding the best estimate of position and velocity.

5.4 Summary

The continuous process which describes the INS updated with VOR/DME information is approximated by a linear multistage process. This approximation is based on a first-order approximation of the state transition matrix. The associated multistage filter estimates the easterly and northerly components of the position and velocity errors, the angles of rotation about the east, north, and vertical axes which relate the platform and computer axes, the gyro drift in each of the three gyros, the errors in the east and north accelerometers, and the bias in each VOR and each DME. In deriving the measurement equations the rotation between the true and reference station coordinate axes, due to the curvature of the earth, is neglected. Upon tuning in a new VOR/DME station, the associated VOR and DME biases must be re-initialized.

VI. ESTIMATOR FOR COMBINING INFORMATION FROM TWO VOR/DME's WITHOUT AIR OR INERTIAL DATA

Combining VOR/DME information without air or inertial data reduces to the problem of finding the maximum-likelihood estimates of x_1 and y_1 (see Fig. 4.1). Thus, the vector of parameters to be estimated, $\underline{x}$, is

$$\underline{x} = \begin{bmatrix} x_1 \\ y_1 \end{bmatrix} . \tag{6.1}$$

The measurements are given by [see Eqs. (4.3)]

$$\underline{z} = h(\underline{x}) + \underline{v} ,$$

that is,

(6.2)

$$\begin{bmatrix} V_1 \\ D_1 \\ V_2 \\ D_2 \end{bmatrix} = \begin{bmatrix} \arctan\,(x_1/y_1) \\ \left[x_1^2 + y_1^2 + h_1^2\right]^{1/2} \\ \arctan\left[(x_1 - x_{12})/(y_1 - y_{12})\right] \\ \left[(x_1 - x_{12})^2 + (y_1 - y_{12})^2 + (h_1 - h_{12})^2\right]^{1/2} \end{bmatrix} + \begin{bmatrix} b_{V1} + e_{V1} \\ b_{D1} + e_{D1} \\ b_{V2} + e_{D2} \\ b_{D2} + e_{D2} \end{bmatrix} ,$$

where V_1 and D_1, and V_2 and D_2 are the VOR and DME measurements from stations 1 and 2, respectively.

Equations (6.2) can be linearized about the nominal value of $\underline{x}$, $\bar{\underline{x}}$. Hence, denoting the perturbations of $\underline{x}$ and $\underline{z}$ about their nominal values by $\delta\underline{x}$ and $\delta\underline{z}$, respectively, the following linearized perturbation equation results:

$$\delta \underline{z} = H \delta \underline{x} + \underline{v} \quad , \tag{6.3}$$

with

$$H = \left.\frac{\partial \underline{h}}{\partial \underline{x}}\right|_{\underline{x}=\underline{\bar{x}}} = \begin{bmatrix} \dfrac{\bar{y}_1}{A} & \dfrac{-\bar{x}_1}{A} \\ \dfrac{\bar{x}_1}{\left[A + h_1^2\right]^{1/2}} & \dfrac{\bar{y}_1}{\left[A + h_1^2\right]^{1/2}} \\ \dfrac{\bar{y}_1 - y_{12}}{B} & \dfrac{x_{12} - \bar{x}_1}{B} \\ \dfrac{\bar{x}_1 - x_{12}}{\left[B + (h_1 - h_{12})^2\right]^{1/2}} & \dfrac{\bar{y}_1 - y_{12}}{\left[B + (h_1 - h_{12})^2\right]^{1/2}} \end{bmatrix} , \tag{6.4}$$

where

$$A = \bar{x}_1^2 + \bar{y}_1^2 , \qquad B = (\bar{x}_1 - x_{12})^2 + (\bar{y}_1 - y_{12})^2 \quad . \tag{6.5}$$

Letting $\hat{\underline{x}}$ denote the best estimate of $\underline{x}$, then ([32], Section 12.2)

$$\hat{\underline{x}} = \underline{\bar{x}} + P H^T R^{-1} \left[\underline{z} - \underline{h}(\underline{\bar{x}})\right] \quad . \tag{6.6}$$

Furthermore, the error covariance matrix, P, is given by

$$P = E\left[(\hat{\underline{x}} - \underline{x})(\hat{\underline{x}} - \underline{x})^T\right] = \left[H^T R^{-1} H\right]^{-1} \quad , \tag{6.7}$$

where

$$R = E\left[\underline{v}\underline{v}^T\right] = \text{diag}\left\{\sigma^2_{b_{V1}} + \sigma^2_{e_{V1}}, \sigma^2_{b_{D1}} + \sigma^2_{e_{D1}}, \sigma^2_{b_{V2}} + \sigma^2_{e_{V2}}, \sigma^2_{b_{D2}} + \sigma^2_{e_{D2}}\right\} . \tag{6.8}$$

The estimator for investigating the use of any combination of 0, 1, or 2 VOR's and 0, 1, or 2 DME's can be derived from the above estimator by deleting the measurements not taken.

VII. SIMULATION STUDIES

7.1 Computer Program

A computer program was written to calculate the state error covariance matrices associated with the filters of Chapters IV and V and the estimator of Chapter VI. This program can be used to study error propagation when using the information from 0, 1, or 2 VOR's and 0, 1, or 2 DME's with or without air or inertial data. The nominal flight path can consist of any series of straight-line segments.

The main inputs to the program are: (a) the combination of information to be used, (b) the model parameters, (c) the latitude, longitude, and altitude of each of the VOR/DME stations to be used, and (d) the latitude and longitude of each of the switching points, that is, points along the flight path where the aircraft tunes in a new VOR/DME station or changes its speed or directional heading. The outputs of the program are the RMS errors in the estimates of the states (i.e., position, velocity, etc.).

A listing of the program, which is written in FORTRAN IV programming language, appears in Appendix B. All the results presented were obtained from this program by properly choosing the input parameters.

7.2 Combining VOR/DME Information and Air Data

Using the computer program, the RMS error histories for various flight paths were calculated. The results presented here are for an aircraft flying due east at an altitude of 33,000 feet with a speed of 500 knots. The value of ΔT (the time between measurement updates) was taken to be 10 seconds.

7.2.1 RMS Errors

The RMS position errors which occur when using the information from one VOR/DME with and without air data are shown in Figs. 7.1 and 7.2 for a radial and an area flight, respectively. The improvement

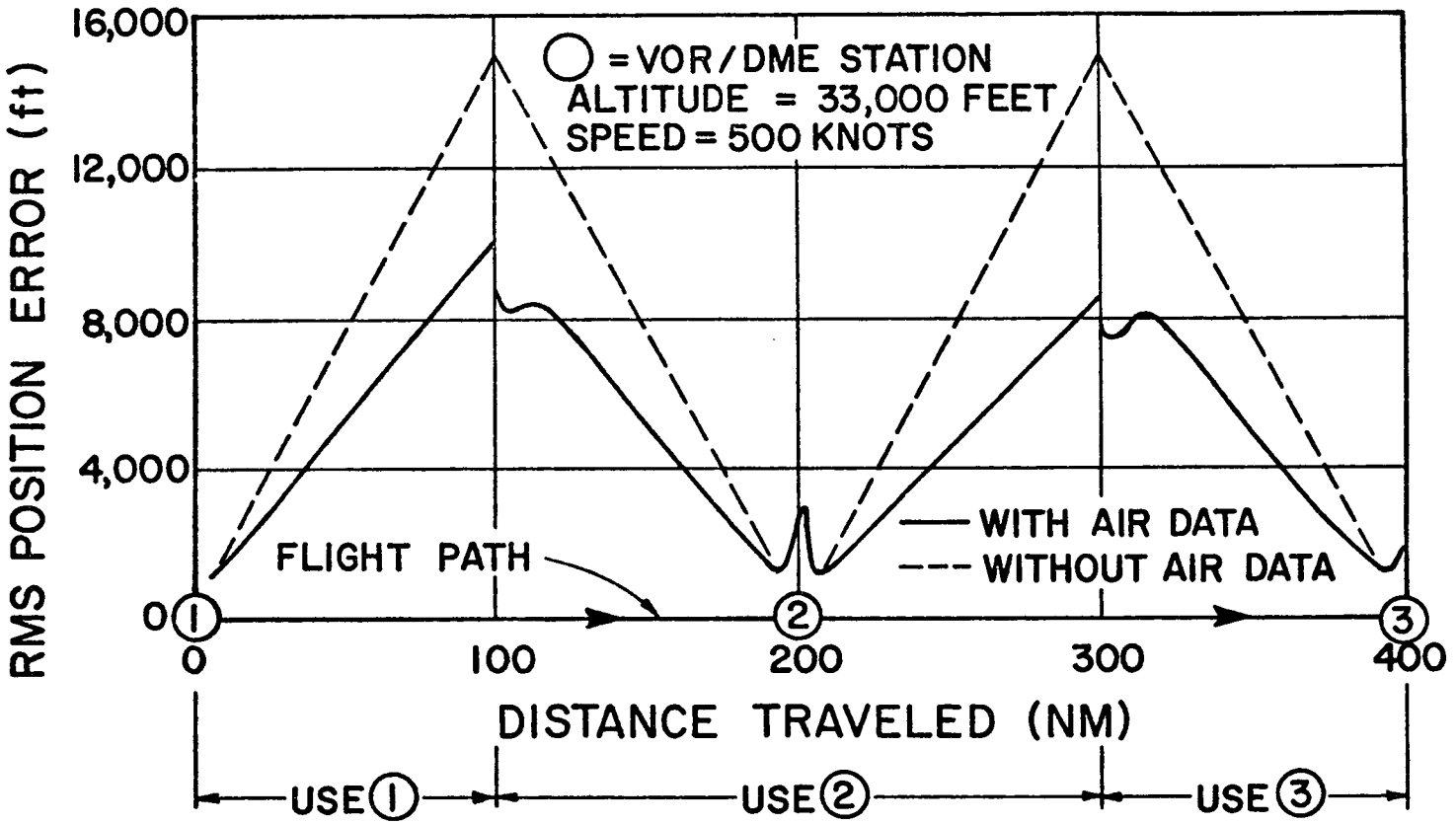

Fig. 7.1. RMS POSITION ERRORS FOR A RADIAL FLIGHT USING ONE VOR/DME WITH AND WITHOUT AIR DATA.

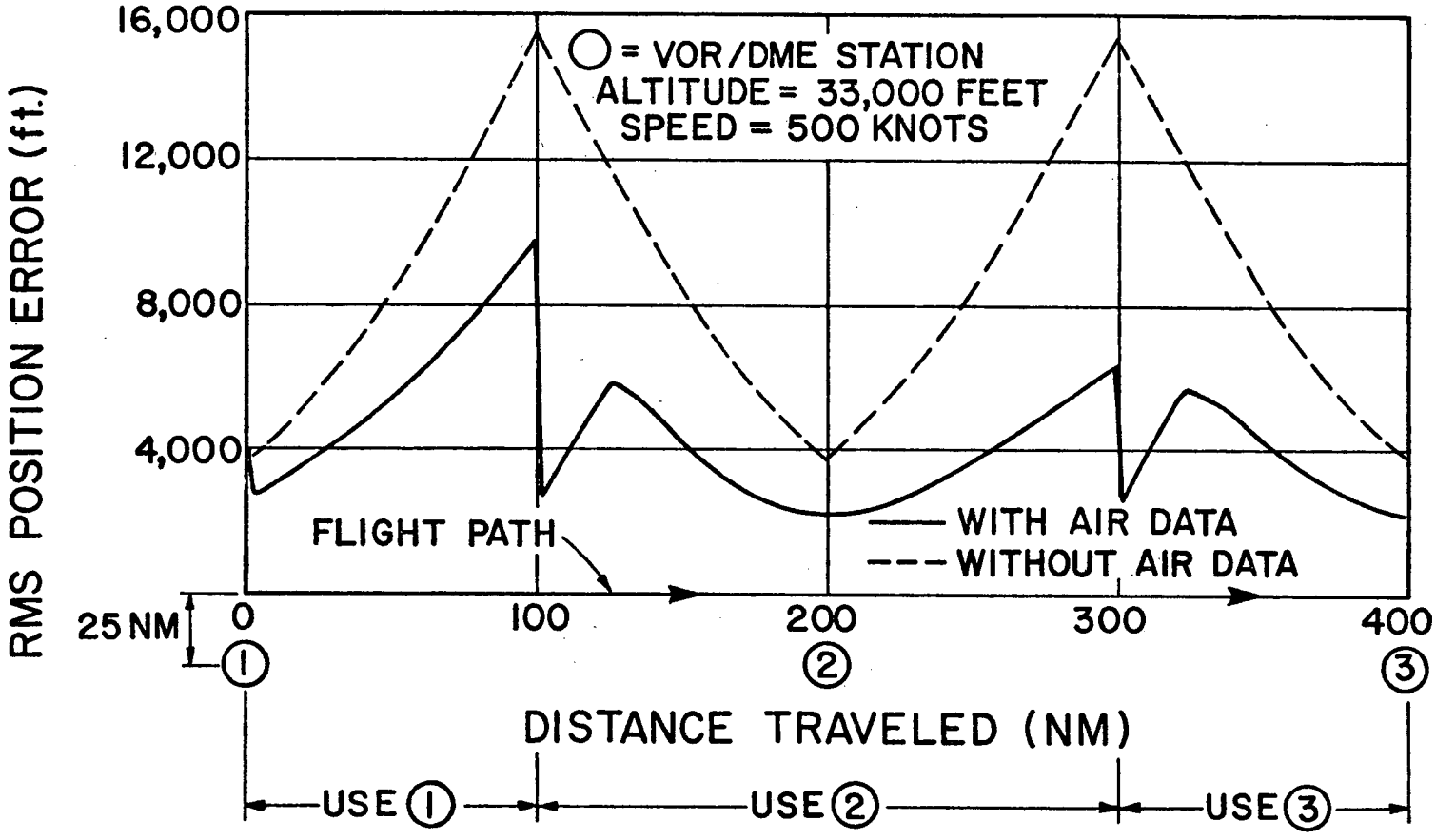

Fig. 7.2. RMS POSITION ERRORS FOR AN AREA FLIGHT USING ONE VOR/DME WITH AND WITHOUT AIR DATA.

in position accuracy which results when air data are added is larger for area than for radial flights. This is due to the fact that the filter can estimate the VOR bias more accurately for area than for radial flights, while just the opposite is true for the DME bias. This is shown in Figs. 7.3 and 7.4, respectively. Since the position error due to the VOR bias is larger, the factor of improvement is greater for area flights.

The sharp decreases in RMS position errors in Figs. 7.1 and 7.2 at the points where the aircraft switches from one VOR/DME station to another are of interest. The decreases which occur in the radial flight (as well as a portion of the decreases for the area flight) are due to a transient effect which is introduced when, upon tuning in a new station, the variances of the biases are re-initialized and the off-diagonal terms involving the biases are set to zero in the covariance matrix. The larger decreases occurring in the area flight are explained by the fact that the DME position information is more accurate than the VOR position information (except when very near the station), and the fact that the lines-of-sight to the new and old stations at the switching points for the area flight (Fig. 7.2) are not parallel.

Also of interest is the rapidity with which the RMS VOR and DME bias errors tend to nearly constant values after switching to a new station (see Figs. 7.3 and 7.4). The reason for this is that the aircraft has a rather good estimate of its position as a result of filtering data from the previous station; and hence, as the aircraft switches to the new station, the filter can estimate the new bias errors quickly.

At elevation angles above 60 degrees, the VOR signals are usually unusable due to excessive interference. Hence, when using only VOR/DME information, the RMS position error becomes large when overflying a VOR/DME station. However, when air data are added, the RMS position error remains relatively small as shown in Fig. 7.1.

In Fig. 7.5, the RMS position errors for various combinations of the information from two VOR/DME's and air data are shown. When a second VOR is added to the case of one VOR and two DME's, with or without air data, the decreases in the RMS position errors are negligible (less than five feet).

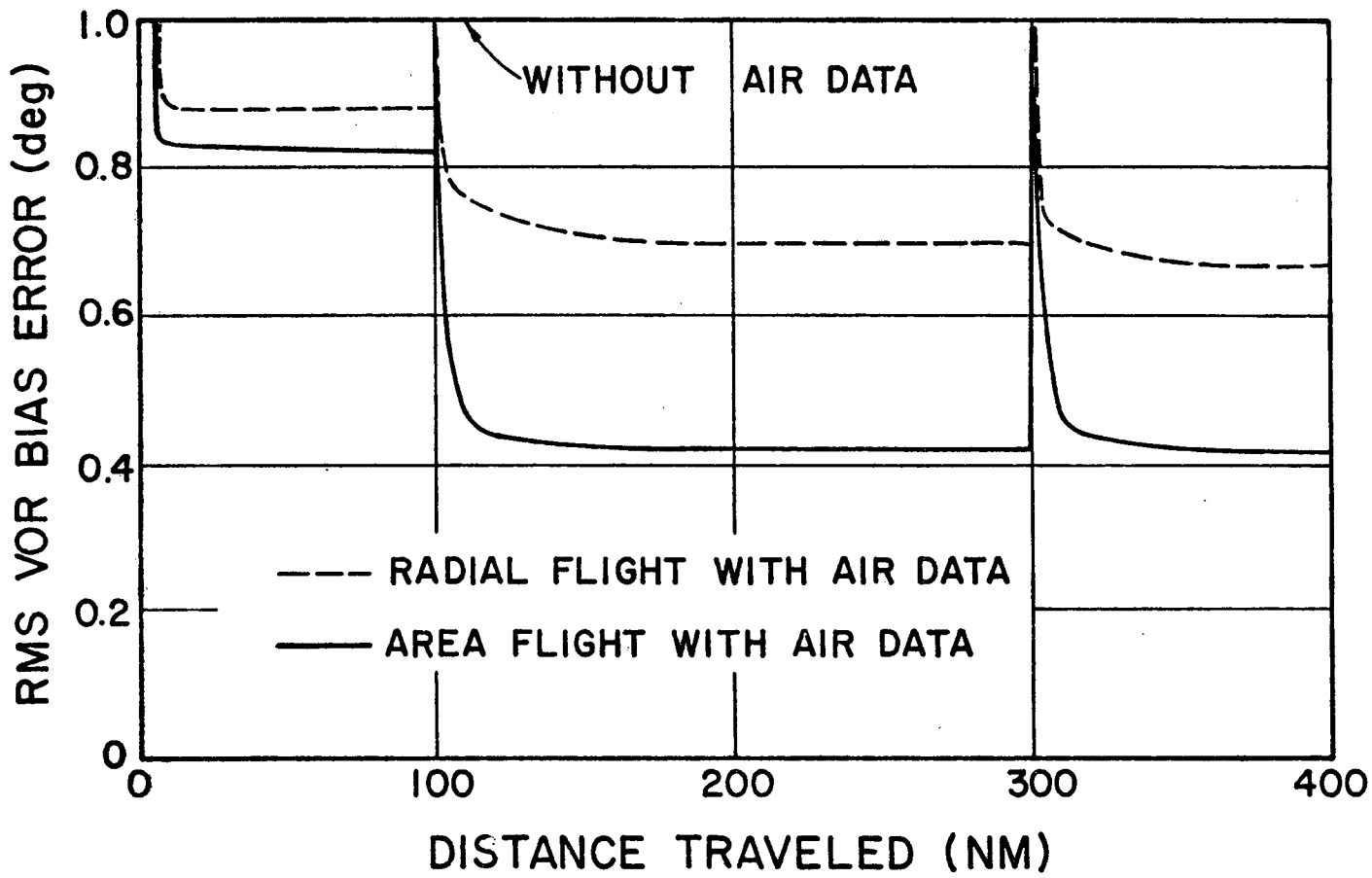

Fig. 7.3. COMPARISON OF RMS VOR BIAS ERRORS FOR THE RADIAL AND AREA FLIGHTS OF FIGS. 7.1 AND 7.2.

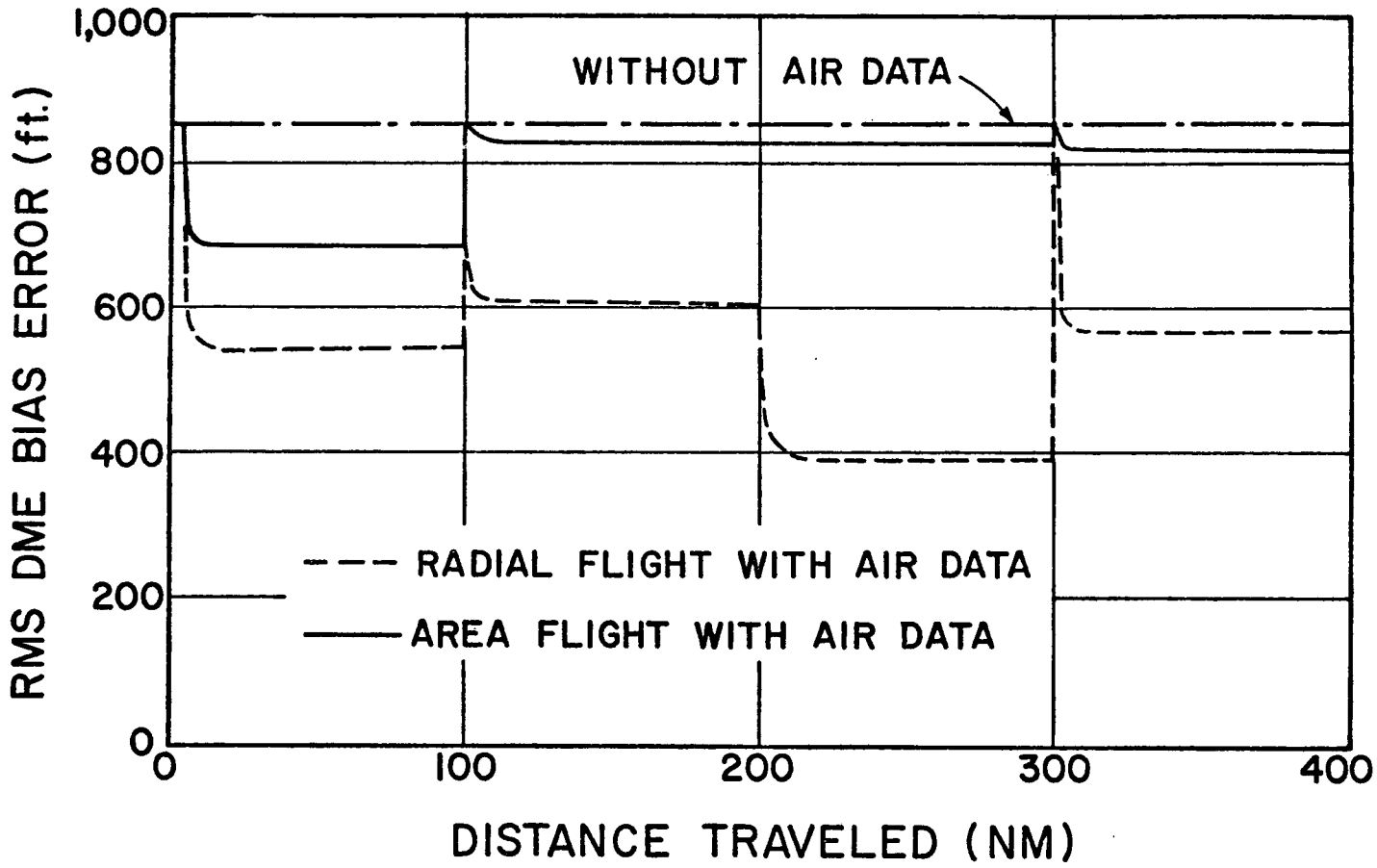

Fig. 7.4. COMPARISON OF RMS DME BIAS ERRORS FOR THE RADIAL AND AREA FLIGHTS OF FIGS. 7.1 AND 7.2.

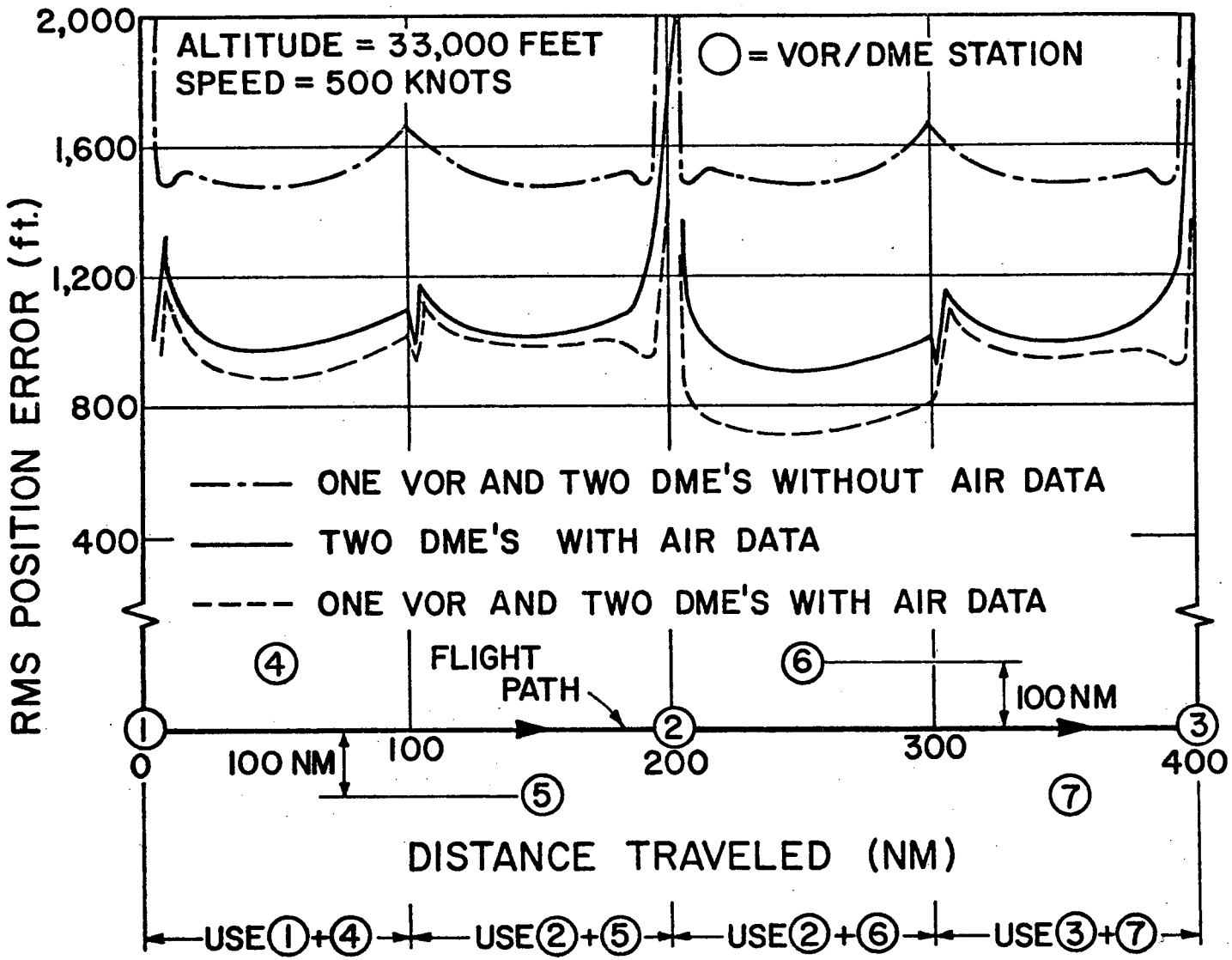

Fig. 7.5. RMS POSITION ERRORS FOR VARIOUS COMBINATIONS OF THE INFORMATION FROM TWO VOR/DME's AND AIR DATA.

Since the position error due to VOR error is much greater than that due to DME error, the best position accuracy, when using two stations, occurs when the crossing angle between the lines-of-sight from the aircraft to the two stations is 90 degrees. For the flight path of Fig. 7.5, the crossing angle varied from about 60 to 120 degrees. As can be seen from Fig. 7.5, the RMS position errors increase as the crossing angle deviates from 90 degrees. The present network of VOR/DME stations would allow an aircraft flying almost anywhere in the U.S. at jet altitudes (24,000 to 45,000 feet) to choose stations so that the crossing angle lies between 60 and 120 degrees [6].

Factors of improvement in RMS position error over the use of a single VOR/DME are shown in Table 7.1 for various combinations of information. These factors were calculated for a point halfway between the second and third stations because at this point the error for the case of using a single VOR/DME is maximum; and hence, the factor of improvement at this point is of prime importance. The case where two DME's are used without air data is not included in Table 7.1 because there are generally two position fixes possible in this case. However, the addition of a VOR measurement to two DME measurements resolves the ambiguity,

Table 7.1

APPROXIMATE FACTORS OF IMPROVEMENT IN RMS POSITION ACCURACY OVER THE USE OF A SINGLE VOR/DME FOR VARIOUS COMBINATIONS OF VOR/DME INFORMATION AND AIR DATA

Combination of Information	Factor of Improvement
1 VOR, 1 DME, air data (radial flight)	1.8
1 VOR, 1 DME, air data (area flight)	2.5
1 (or 2) VOR's, 2 DME's	9
2 DME's, air data	15
1 (or 2) VOR's, 2 DME's air data	19

although it does not substantially improve the accuracy of the position fixes. From these results, it is seen that the navigational accuracy resulting from the use of a given combination of VOR/DME information is improved by roughly a factor of two by the addition of air data.

RMS velocity errors are reduced from roughly 60 to 30 knots when one VOR, one DME, and air data are combined, and to about 20 knots for combinations involving the information from two VOR/DME's and air data.

Jet flights along approved radial and area routes between San Francisco and Chicago were simulated and the results checked with those presented here between the second and third stations of these short flights. The position error histories resulting between the second and third stations will repeat if the flight paths discussed above are extended and similar configurations of stations are encountered.

7.2.2 Sensitivity Analysis

The design of the filter was based on "nominal" values for the error model parameters. Since some of these parameters are quite uncertain, it is desirable to establish how the filter performs when the error statistics are not nominal. The equations required to determine the sensitivity of the filter to variations in the initial covariance matrix and the spectral densities of the process and measurement noises are derived in Appendix C.

There is considerable uncertainty in the correlation times as well as in the RMS values of the air data errors (σ_{wx} and σ_{wy}) and the white noise component of the VOR error (σ_{e_V}). In order to determine the sensitivity of the filter performance to variations in these error parameters, certain parameters were assumed to be "non-nominal," and the performance degradation was calculated. Here performance degradation is defined as the difference between the factors of improvement in RMS position accuracy obtained from the nominal filter and the optimal filter (the filter designed using the fact that certain parameters were not nominal) divided by the nominal factor of improvement. The results are shown in Table 7.2. The flight path was that of Fig. 7.1 with the performance degradation calculated at the midpoint between the second

Table 7.2

FILTER SENSITIVITY TO VARIATIONS
IN ERROR MODEL PARAMETERS

Non-nominal Parameters	Performance Degradation (%)
all correlation times halved	2
all correlation times doubled	3
σ_{wx} = 20 knots σ_{wy} = 60 knots	4
σ_{wx} = 60 knots σ_{wy} = 20 knots	11
σ_{e_V} = 0.5 deg.	5
σ_{e_V} = 2.0 deg.	8

and third stations. From these results, it appears that the performance of the (nominal) filter may be insensitive to fairly wide variations in error model parameters.

7.2.3 Suboptimal Filters

The gains associated with the filter which combines VOR/DME information with air data are time-varying. Since this filter must be implemented in real-time using an onboard computer, computation time and computer storage are severely limited. Hence, it would seem desirable to design a suboptimal filter with constant and/or linearly-varying gains which would behave nearly optimally. However, the filter gains associated with the VOR and DME measurements were found to be highly dependent upon the location of the VOR/DME stations relative to the flight path. Because of the nature of the gains, the search for a suboptimal filter with constant and/or linearly-varying gains proved fruitless.

Another possible method of reducing the required computer storage and computation time is to reduce the order of the filter by neglecting states which are not of primary interest. In particular, the performances of the suboptimal filters resulting when certain VOR and DME biases are neglected were investigated. The effect on filter performance of neglecting states is discussed in Appendix D. For the case where information from one VOR/DME and air data is used (for the flight path shown in Fig. 7.1), the performance degradation of the suboptimal filter resulting when the DME bias is neglected is less than 1%, whereas if both the VOR and DME biases are neglected, the performance degradation is about 31%. For the case of using two DME's with air data (for the flight path of Fig. 7.5), the performance degradation resulting when both DME biases are neglected is approximately 25%. In general, neglecting VOR biases results in great performance degradation while neglecting DME biases does not. Note that although the 25% degradation stated for the case of two DME's and air data is a significant percentage, the degradation in terms of feet of RMS position error is small (see Fig. 7.5). The above performance degradations were calculated at the midpoint between the second and third stations.

7.3 Combining VOR/DME Information and Inertial Data

7.3.1 In-flight Alignment

The possibility of performing the fine alignment* of the INS platform while in the air by using VOR/DME information was investigated. Figures 7.6 and 7.7 show the RMS errors in the estimates of position, velocity, and platform attitude (ϕ_x = tilt about east axis, ϕ_y = tilt about north axis, and ϕ_z = azimuth error) for a 30-minute flight (200 NM at 400 knots) using one VOR/DME to update a high-quality INS (0.01 deg/hr gyro drift). In Figs. 7.8 and 7.9 these same errors are shown for a flight using two DME's. The time between measurement updates was

*Although platform alignment usually refers to physically rotating the platform to a desired orientation, in this context platform alignment simply means the estimation of the platform attitude errors.

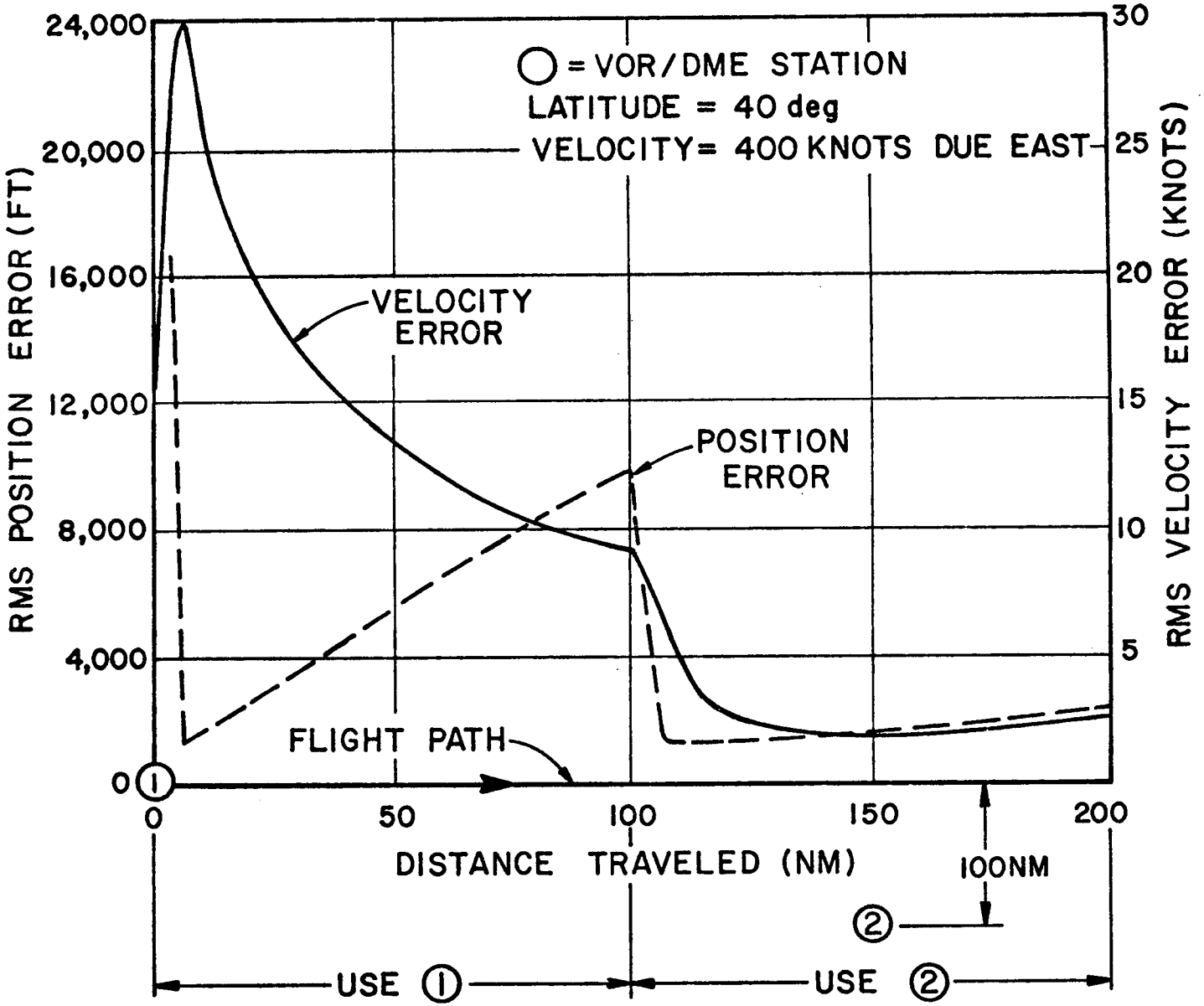

Fig. 7.6. POSITION AND VELOCITY ERRORS FOR IN-FLIGHT ALIGNMENT USING THE INFORMATION FROM ONE VOR/DME.

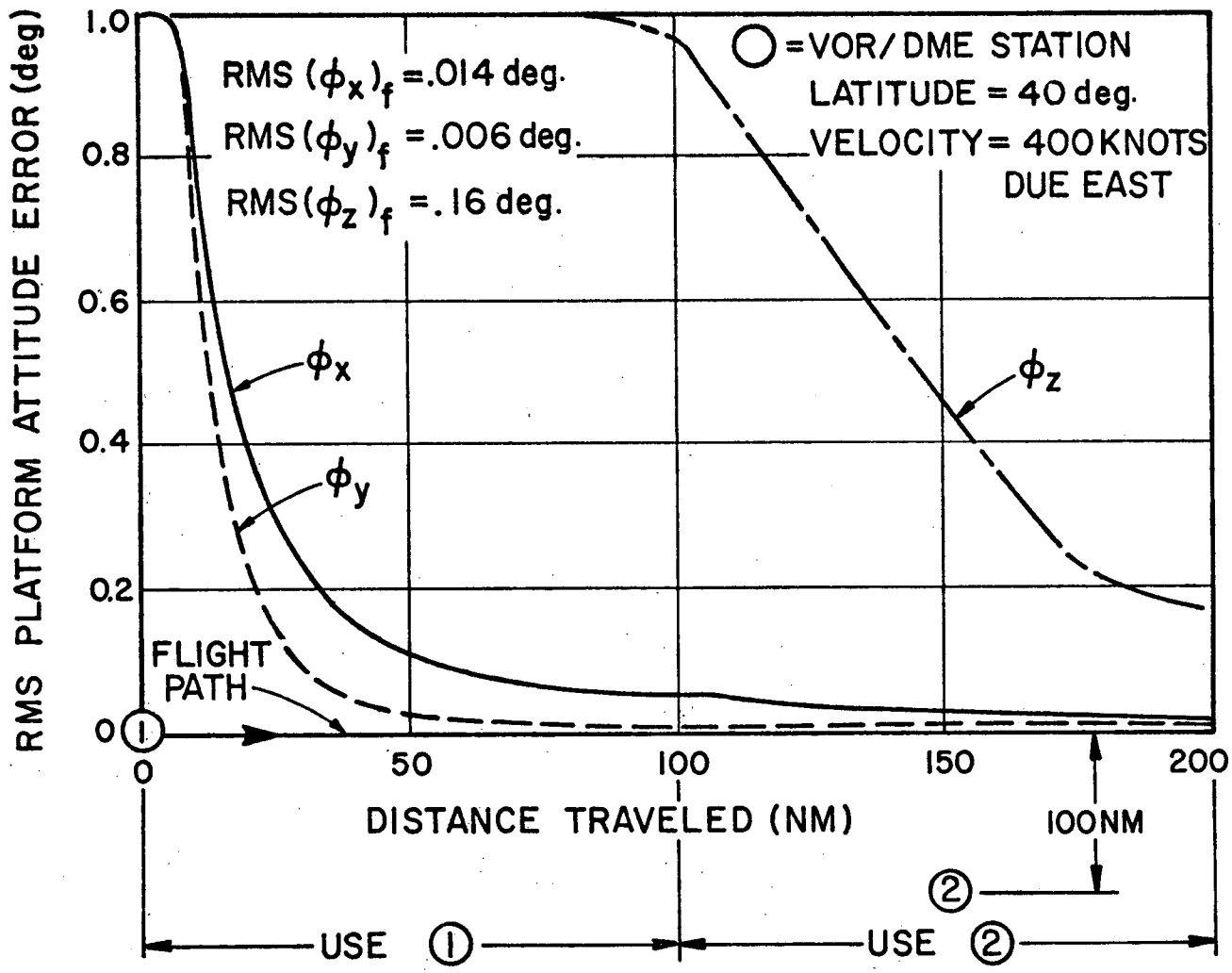

Fig. 7.7. PLATFORM ATTITUDE ERRORS FOR IN-FLIGHT ALIGNMENT USING THE INFORMATION FROM ONE VOR/DME.

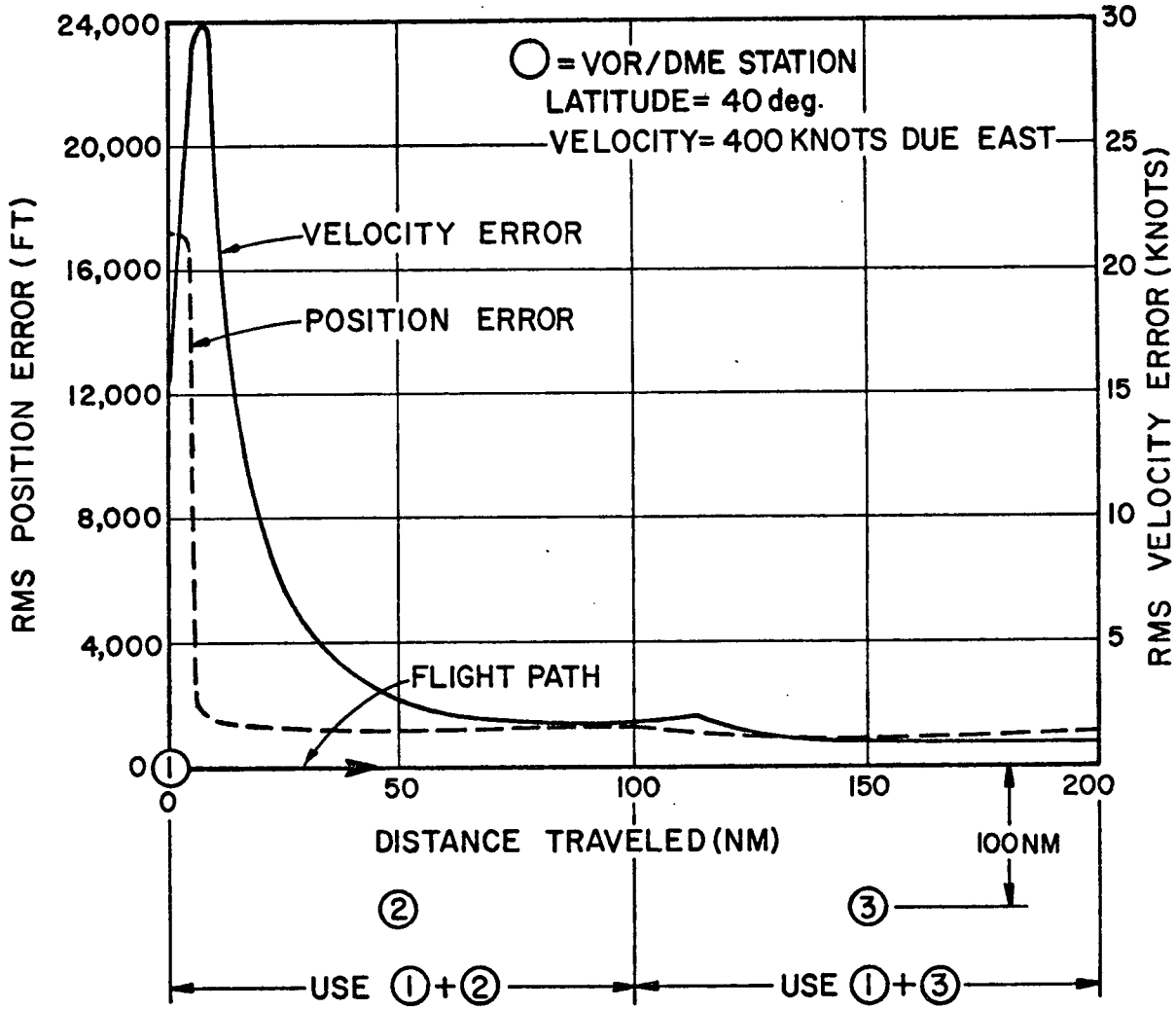

Fig. 7.8. POSITION AND VELOCITY ERRORS FOR IN-FLIGHT ALIGNMENT USING THE INFORMATION FROM TWO DME's.

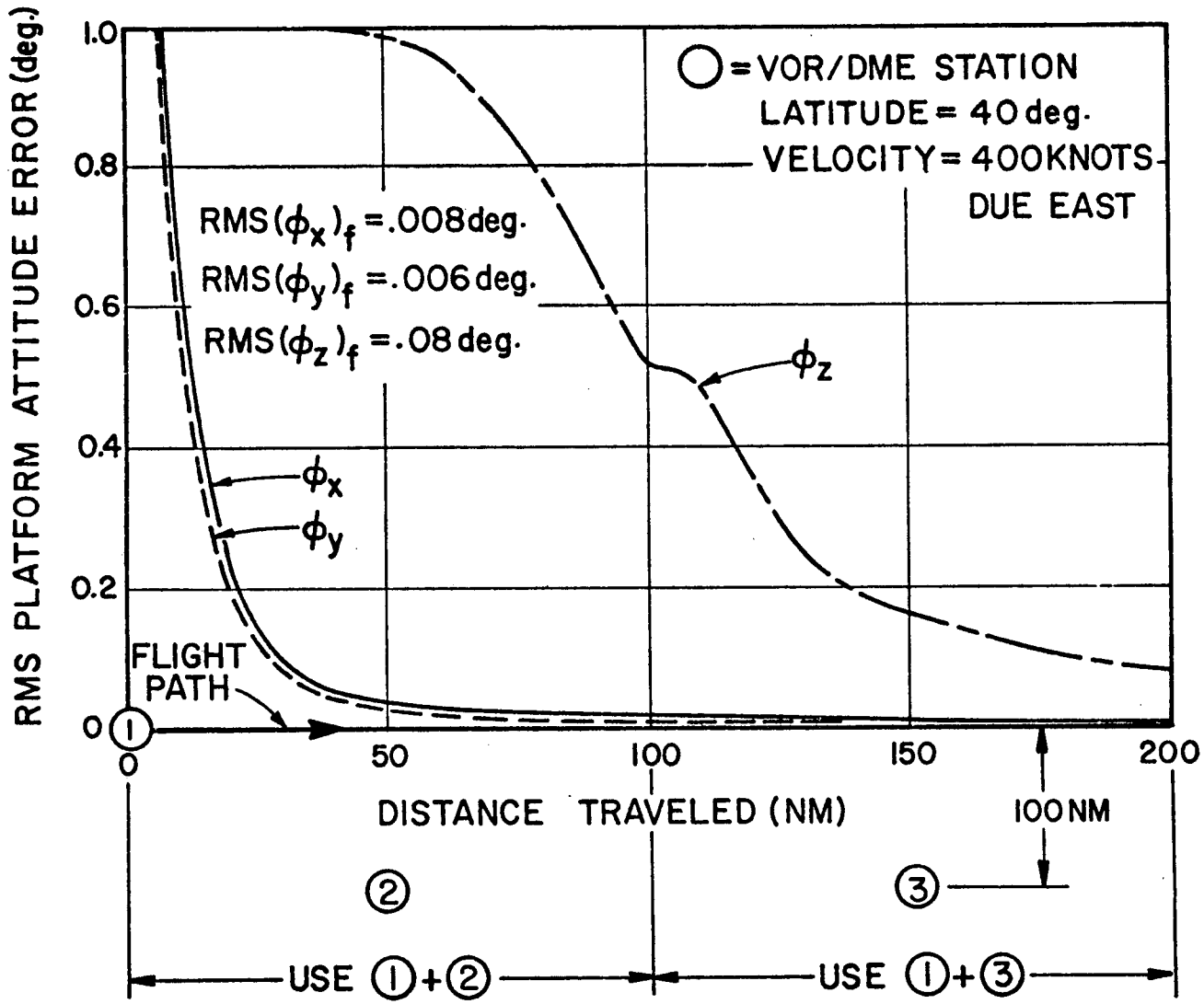

Fig. 7.9. PLATFORM ATTITUDE ERRORS FOR IN-FLIGHT ALIGNMENT USING THE INFORMATION FROM TWO DME's.

60 seconds and the attitude was 33,000 feet. The present method of ground alignment takes about 15 minutes with the final RMS error in the platform tilts, RMS $(\phi_x)_f$ and RMS $(\phi_y)_f$, equal to about 0.005 degrees and the final RMS azimuth error, RMS $(\phi_z)_f$, equal to about 0.05 degrees. Thus, the accuracy of in-flight alignment using two DME's is about the same as for ground alignment, whereas in-flight alignment using one VOR/DME is less accurate by a factor of 2 or 3. In Fig. 7.10 the RMS position errors during an unaided-inertial flight preceded by ground alignment are compared with errors during a flight with in-flight alignment (using two DME's, the station configuration being that of Fig. 7.9).

In-flight alignment using combinations of VOR/DME information other than the two previously discussed were also considered. The use of only the DME measurements during the flight of Fig. 7.7 yields much less accurate alignment than when both the VOR and DME measurements are used. The addition of VOR measurements during the flight of Fig. 7.9 does not significantly improve the accuracy of alignment.

Station configurations other than the two simple configurations of Figs. 7.7 and 7.9 were also studied. It was found that more complex configurations with more frequent switching between stations does not result in a significant improvement in alignment accuracy. Note that the results of Figs. 7.7 and 7.9 are not restricted to the specific flight paths considered. For example, if during a 30-minute flight, the information from one VOR/DME is used for in-flight alignment where the line-of-sight to the station used during half of the flight is, in general, orthogonal to the line-of-sight to the station used during the other half of the flight, the resulting alignment will essentially be that of Fig. 7.7. Similarly, if the information from two DME's is used where the crossing angles between the lines-of-sight from the aircraft to the stations lies between 60 and 120 degrees, the resulting alignment will be about the same as that of Fig. 7.9.

Although the need for initial in-flight alignment of inertial systems onboard commercial aircraft is questionable, the in-flight realignment of the system before leaving the U.S. airspace on a transoceanic flight (e.g., from Los Angeles to London or Chicago to Hawaii) could result in significant improvements in navigational accuracy. Also,

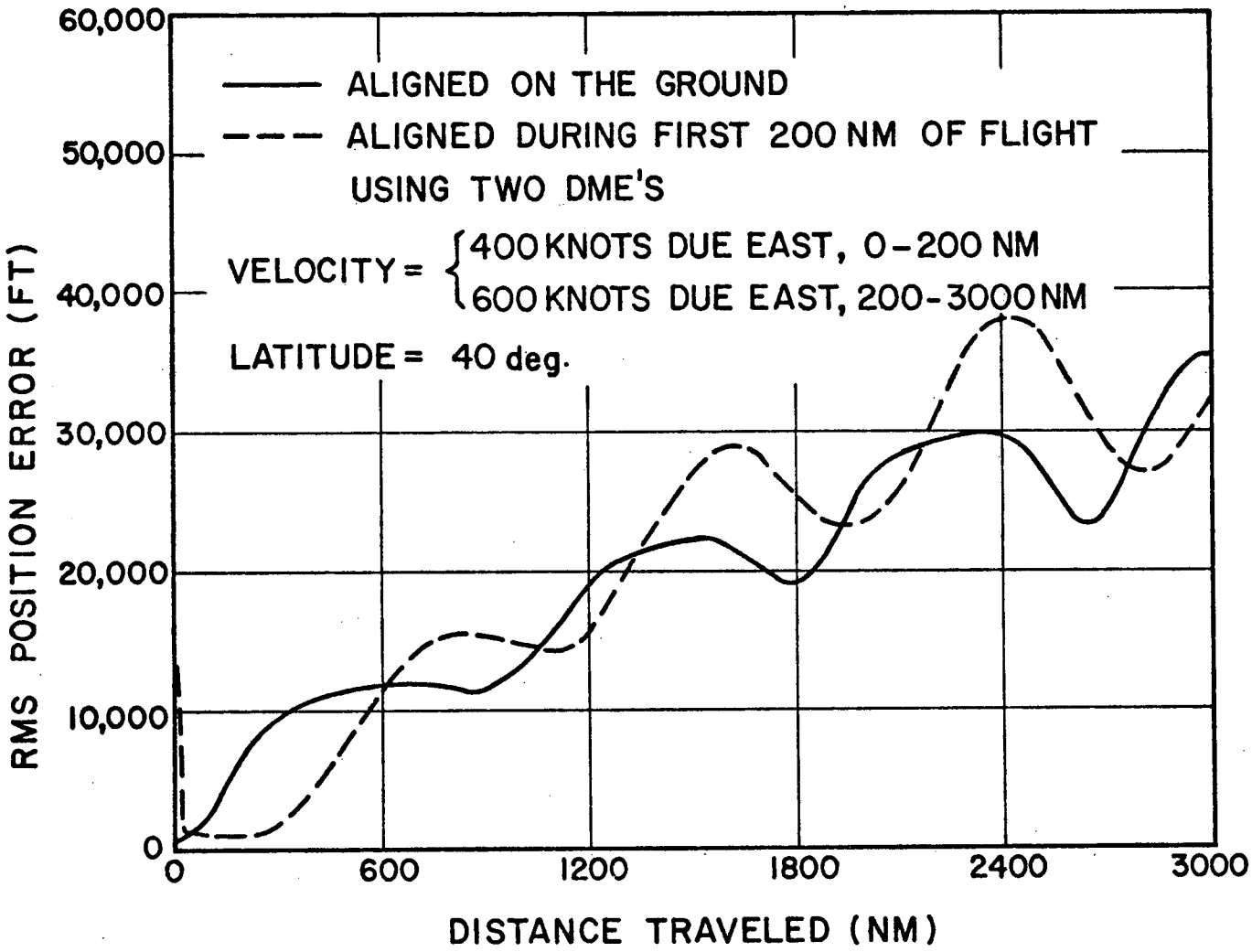

Fig. 7.10. RMS POSITION ERRORS RESULTING DURING AN UNAIDED-INERTIAL FLIGHT PRECEDED BY GROUND AND IN-FLIGHT ALIGNMENT.

in-flight realignment of the system after a transoceanic flight could be useful in providing more accurate position, velocity, and attitude information in the terminal area and for approach and landing.

7.3.2 Periodic Updating

The use of VOR/DME information to update a high-quality INS during a five-hour transcontinental flight was investigated. The system is assumed to be initially aligned on the ground with 0.005 degree RMS error in the platform tilts and a 0.05 degree RMS azimuth error. Furthermore, the initial position and velocity errors are taken to be 0.1 NM and 0.1 knot, respectively, in both the easterly and northerly directions. The altitude is 33,000 feet and the time between measurement updates is two minutes. The RMS position and velocity errors are shown in Figs. 7.11 and 7.12 for the unaided-inertial case as well as for the cases where the system is realigned twice during the flight (from 800 to 1000 NM and from 1800 to 2000 NM). Realignment is done using one VOR/DME with the station configuration of Fig. 7.7 and using two DME's with the station configuration of Fig. 7.9. Obviously, periodic realignment of the INS results in more accurate position and velocity information than that resulting from unaided-inertial operation. There is not much difference between the errors resulting from the use of one VOR/DME and the use of two DME's. If the final realignment is performed just prior to entering the terminal area, accurate position, velocity, and attitude information will be available for approach and landing.

Also shown in Figs. 7.11 and 7.12 are the position and velocity errors resulting if two position resets are performed during the flight (at 950 and 1950 NM). Here position reset means that the position display is reset to correspond to a position fix from two DME's (whose lines-of-sight are perpendicular). Thereafter, the increments of position change calculated by the INS are simply added to the display. The position used in the routine which integrates the outputs of the accelerometers is not changed because such a change causes large amplitude oscillations in the RMS position and velocity error histories. The effect of such position resets upon the covariance is described in Appendix E. Position resets

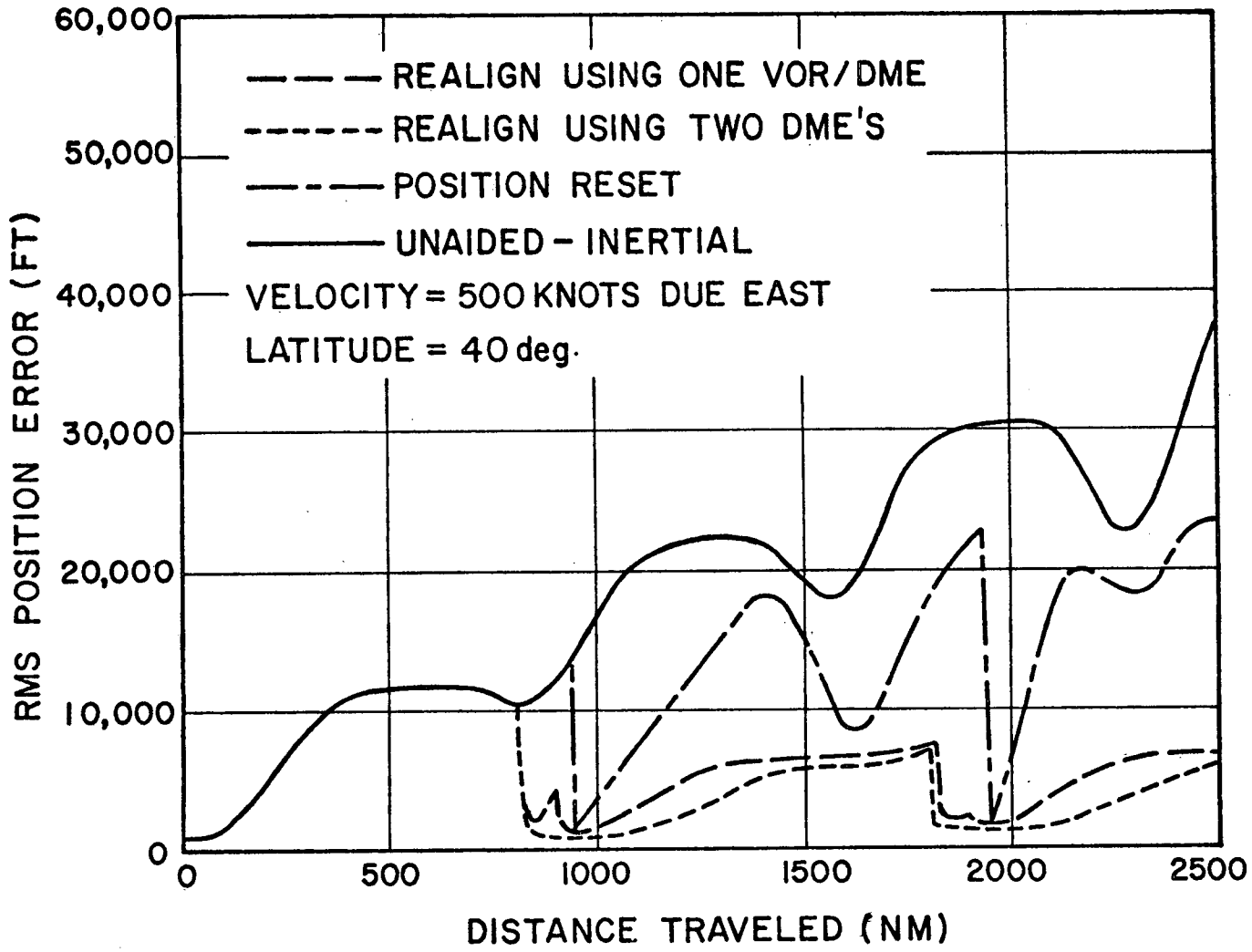

Fig. 7.11. RMS POSITION ERRORS FOR REALIGNMENT, POSITION RESET, AND UNAIDED-INERTIAL MODES OF OPERATION DURING A TRANSCONTINENTAL FLIGHT.

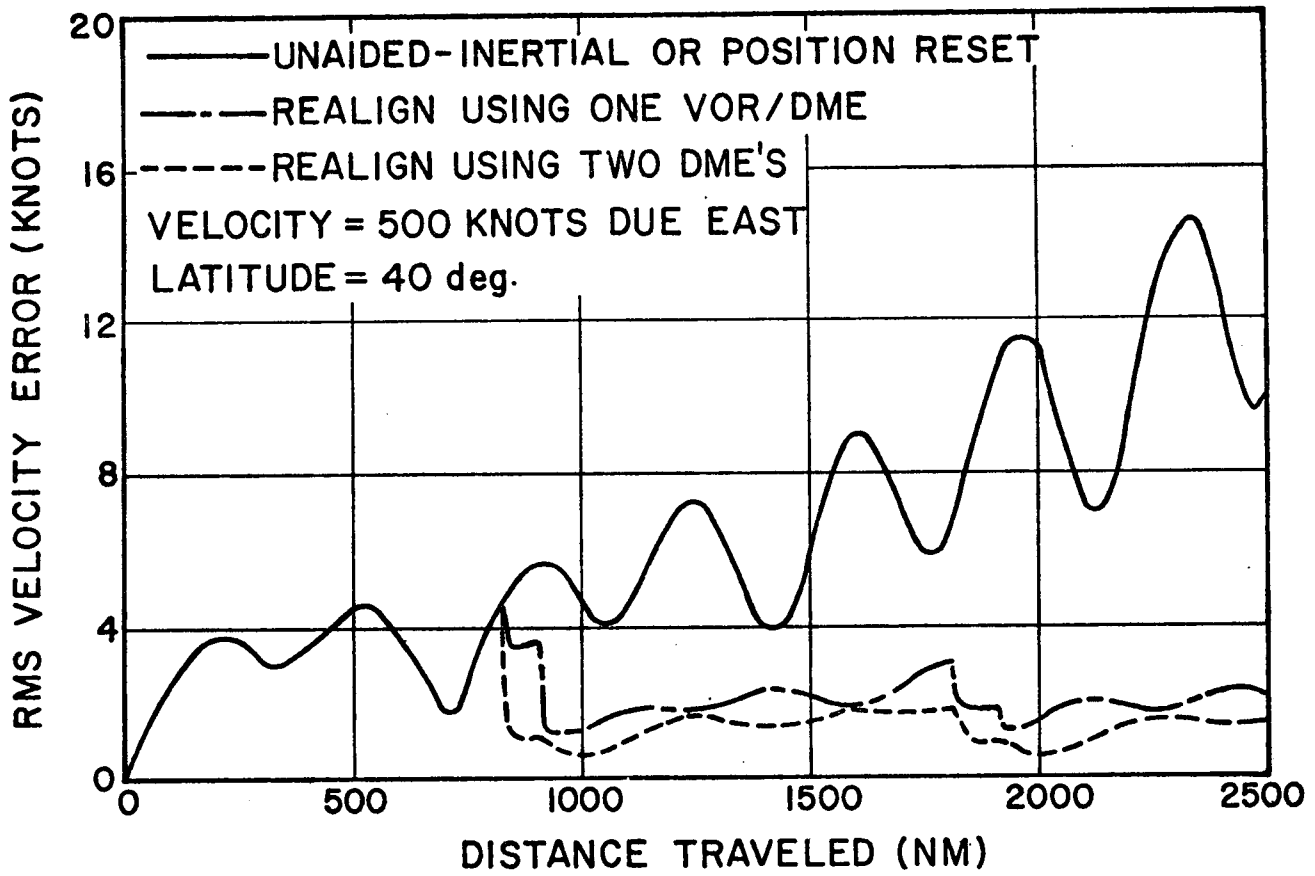

Fig. 7.12. RMS VELOCITY ERRORS FOR REALIGNMENT, POSITION RESET, AND UNAIDED-INERTIAL MODES OF OPERATION DURING A TRANSCONTINENTAL FLIGHT.

must be performed frequently (every few minutes) to obtain position accuracy comparable to the case where the system is realigned. Obviously, position resets do not result in decreased velocity or platform drift errors.

7.3.3 Continuous Updating

Since the VOR/DME system provides nationwide coverage in the U.S., there exists the possibility of continuously updating an INS with VOR/DME information during domestic flights. For such flights it may be possible to use a low-quality INS instead of the high-quality system required for unaided-inertial operation.

In Fig. 7.13, the RMS position errors for a radial flight using the information from one VOR/DME with a high-quality INS (0.01 deg/hr gyro drift), a low-quality INS (1.0 deg/hr gyro drift), and without an INS are shown. These same error histories are shown in Fig. 7.14 for an area flight. The time between measurement updates is 90 seconds and the altitude is 33,000 feet. The RMS value of the initial position error is that of a VOR/DME reading taken at the beginning of the flight while the RMS velocity error is 10 knots in the northerly and easterly directions. The RMS value of the initial platform tilts and azimuth error are 0.05 and 0.1 degrees, and 0.5 and 5.0 degrees for the high-quality and low-quality systems, respectively. As can be seen in Figs. 7.13 and 7.14, there is considerable improvement in position accuracy when inertial data are added to the information from one VOR/DME. However, the improvement in position accuracy when using a high-quality INS is not much greater than when using a low-quality INS. The estimates of the VOR and DME biases resulting when using inertial data with VOR/DME information are essentially the same as when air data were used with VOR/DME information. Also, the reasons for the sharp decreases in RMS position errors at the points where the aircraft switches from one VOR/DME station to another are the same as for the air-data case.

In Fig. 7.15, the RMS position errors are shown for various combinations of the information from two VOR/DME's and data from a low-quality INS. The use of a high-quality INS yields only a small improvement over the position accuracy obtained when using a low-quality INS. When a

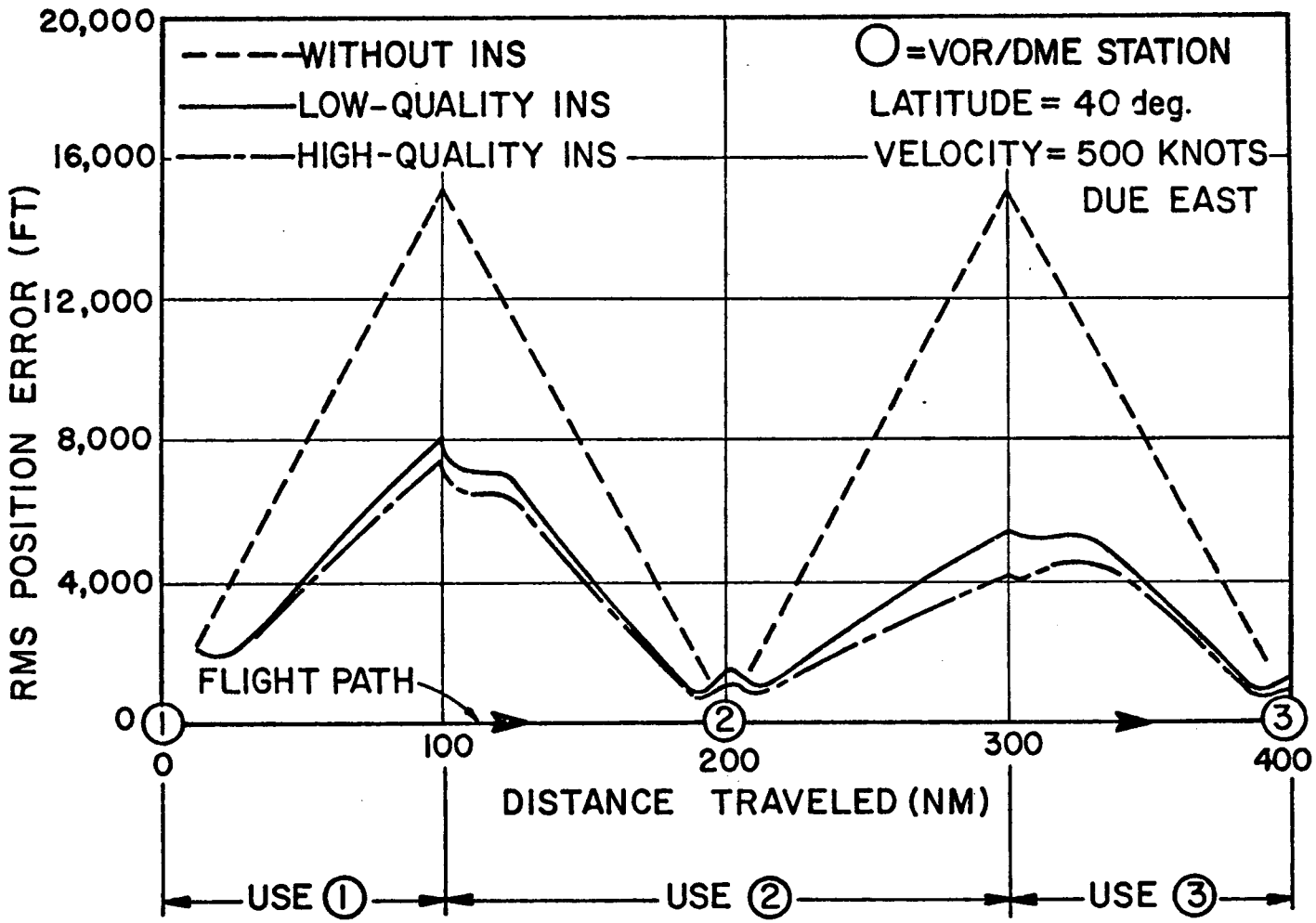

Fig. 7.13. RMS POSITION ERRORS FOR A RADIAL FLIGHT USING ONE VOR/DME WITH A HIGH-QUALITY INS, A LOW-QUALITY INS, AND WITHOUT AN INS.

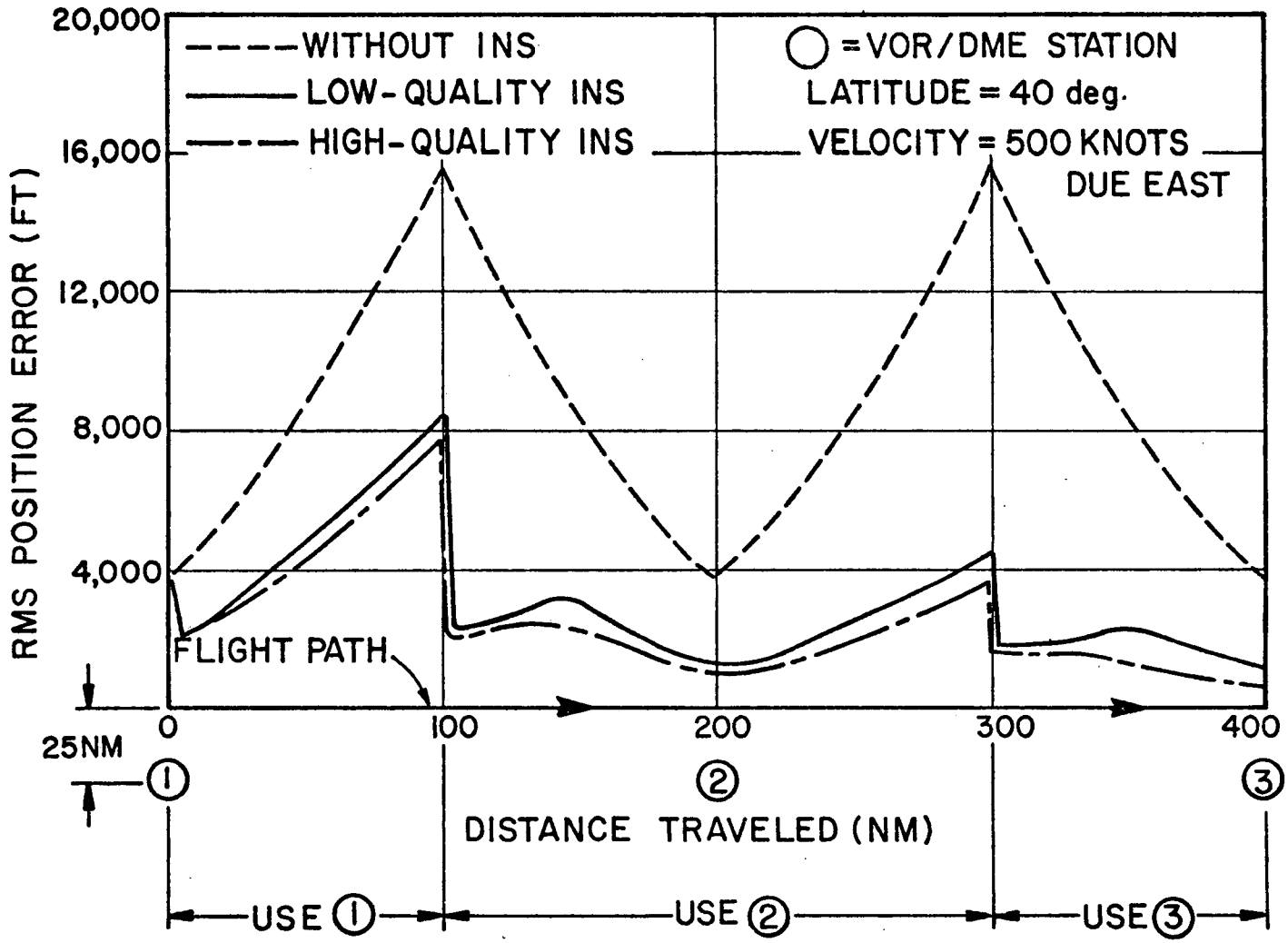

Fig. 7.14. RMS POSITION ERRORS FOR AN AREA FLIGHT USING ONE VOR/DME WITH A HIGH-QUALITY INS, A LOW-QUALITY INS, AND WITHOUT AN INS.

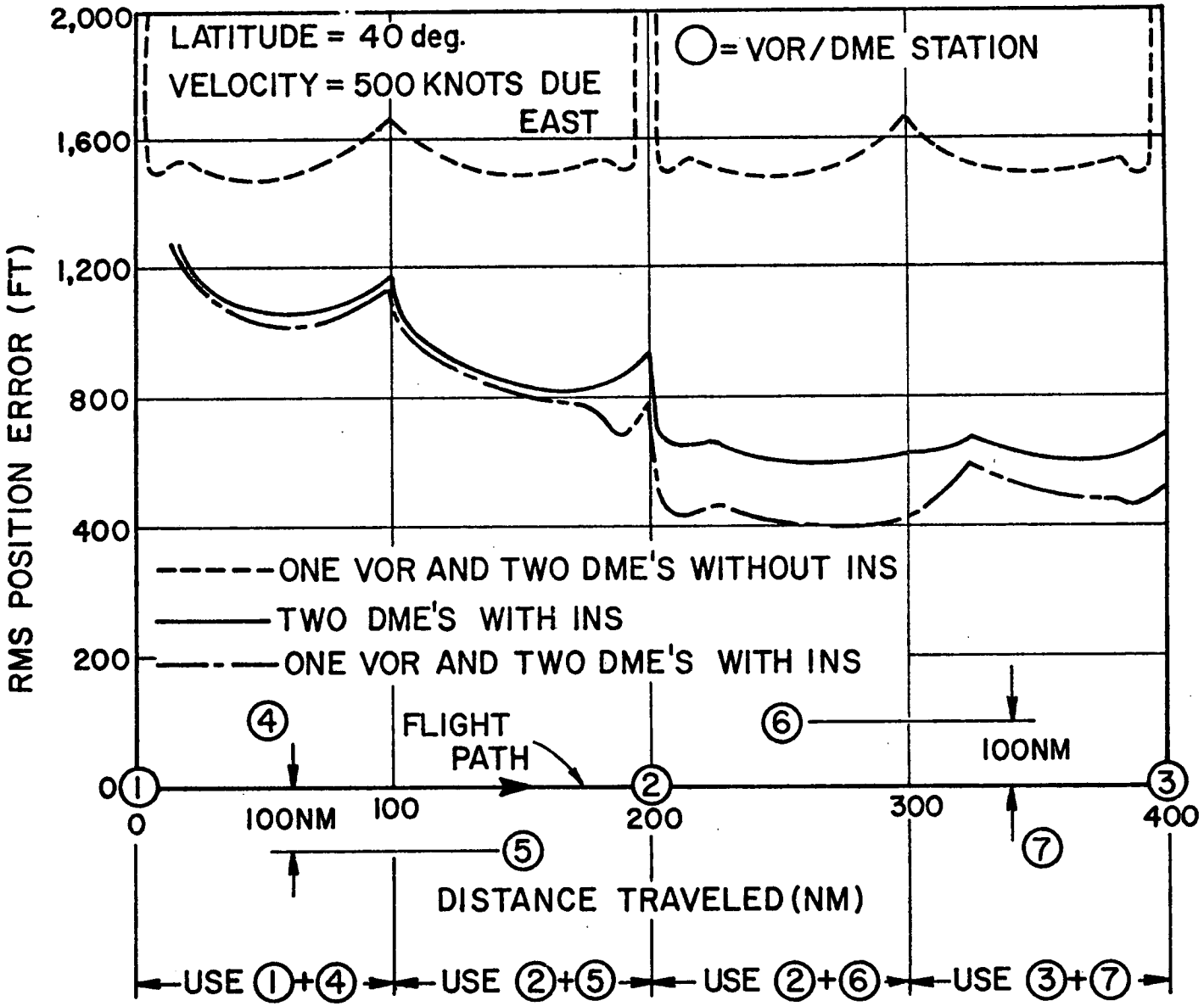

Fig. 7.15. RMS POSITION ERRORS FOR VARIOUS COMBINATIONS OF THE INFORMATION FROM TWO VOR/DME's AND DATA FROM A LOW-QUALITY INS.

second VOR is added to the case of one VOR, two DME's and inertial data, the decrease in the RMS position error is negligible.

Factors of improvement in RMS position error over the use of a single VOR/DME are shown in Table 7.3 for various combinations of the information from two VOR/DME's and inertial data from a low-quality INS. These factors were calculated for a point midway between the second and third stations because at this point the error for the case of using a single VOR/DME is maximum; and hence, the factor of improvement is of prime importance. From these results, it is seen that the navigational accuracy resulting from the use of a given combination of VOR/DME information is improved by roughly a factor of 3 by the addition of inertial data.

Table 7.3

APPROXIMATE FACTORS OF IMPROVEMENT IN RMS POSITION ACCURACY OVER THE USE OF A SINGLE VOR/DME FOR VARIOUS COMBINATIONS OF VOR/DME INFORMATION AND DATA FROM A LOW-QUALITY INS

Combination of Information	Factor of Improvement
1 VOR, 1 DME, INS (radial flight)	2.8
1 VOR, 1 DME, INS (area flight)	3.5
1 (or 2) VOR's, 2 DME's	9
2 DME's, INS	24
1 (or 2) VOR's, 2 DME's INS	37

When using the information from one VOR/DME to update a low-quality INS, RMS velocity errors of 7 or 8 knots can be expected, whereas, when using a high-quality INS, velocity errors of 3 or 4 knots occur. The use of the information from two VOR/DME stations to update an INS yields RMS velocity errors of roughly one and two knots for a high-quality and a low-quality system, respectively.

If the flight paths of Figs. 7.13, 7.14, and 7.15 were extended and similar configurations of stations were encountered, the error histories between the second and third stations would repeat.

7.3.4 Suboptimal Filters

Since the correlation times of the gyro drift and accelerometer errors are long (5 hours and 10 hours, respectively), these errors behave as biases over short periods of time (one-half hour or so). Hence, the method for determining the effect of neglecting states derived in Appendix D applies when the filter operates for short periods of time. Using this method, it was found that for the alignment or realignment of a high-quality INS (which takes from 20 to 30 minutes), the suboptimal filter resulting when the gyro drifts, accelerometer errors, and DME biases are neglected performs nearly optimally. Hence, when using one VOR/DME, the alignment accuracy shown in Fig. 7.7 can be obtained by using an eighth-order filter, whereas, when using two DME's, the alignment accuracy shown in Fig. 7.9 is obtainable with a seventh-order filter. This seventh or eighth order suboptimal filter also behaves nearly optimally when using VOR/DME information to periodically update a high-quality INS.

When using VOR/DME information to continuously update an INS, the performances of the suboptimal filters resulting when certain VOR and DME biases are neglected were investigated. As in the air-data case, neglecting VOR biases generally results in great performance degradation, while neglecting DME biases does not.

VIII. CONCLUSION

Combining VOR/DME information (from one or two stations) with air or inertial data by means of a maximum-likelihood filter results in substantial improvements in navigational accuracy over that obtained by the use of a single VOR/DME, as is the current practice.

The addition of air data (airspeed and heading) to the information from a single VOR/DME station reduces the RMS position error by a factor of about 2, whereas the RMS velocity error is reduced from roughly 60 to 30 knots. The use of a low-quality INS with one VOR/DME reduces the RMS position error by a factor of roughly 3, and yields RMS velocity errors of about 8 knots. When using VOR/DME information continuously throughout the flight, the use of a high-quality INS (0.01 deg/hr gyro drift) instead of a low-quality INS (1.0 deg/hr gyro drift) does not substantially improve position accuracy, but does reduce the RMS velocity error to about 4 knots. Some of the improvement due to the use of air or inertial data results from the ability of the filter to estimate the bias errors associated with the VOR/DME measurements. Estimates of VOR bias error are better for area than for radial flights while the opposite is true for the DME bias error.

The use of information from two VOR/DME stations with air or inertial data yields large factors of improvement in RMS position accuracy over the use of a single VOR/DME station, roughly 15 to 20 for the air-data case and 25 to 35 for the inertial-data case. In general, the RMS position error obtained when using a given combination of the VOR/DME information from two stations is decreased by factors of about 2 and 3 by the addition of air and inertial data, respectively. When using information from two VOR/DME stations, the RMS velocity error in the air-data case was about 20 knots, whereas when using a high-quality and a low-quality INS, the velocity errors were 1 and 2 knots, respectively. As far as position and velocity accuracy are concerned, at most one VOR station need be used.

Accurate in-flight alignment of an INS platform by using VOR/DME information is possible. The accuracy of in-flight alignment using two DME's is about the same as for ground alignment, whereas, when using one VOR/DME, alignment is less accurate by a factor of 2 or 3. In-flight

alignment takes about 30 minutes. Although the need for initial in-flight alignment of inertial systems onboard commercial aircraft is questionable, the in-flight realignment of the system before a trans-oceanic flight (e.g., from Los Angeles to London or Chicago to Hawaii) results in significant improvement in navigational accuracy. This might permit a reduction of separation requirements over the North Atlantic routes. Also, realignment of the system after a transoceanic flight could prove useful since the result would be accurate position, velocity, and attitude information in the terminal area and for approach and landing.

Periodic realignment (every one or two hours) of a high-quality INS during a transcontinental flight results in significant improvements in position and velocity errors over unaided-inertial operation or the use of periodic position display resets. The use of a periodically-realigned, high-quality INS would make it possible to fly great circle routes between cities since the locations of VOR/DME stations would not substantially restrict the flight paths (as they do when using a continuously-updated INS). If the final realignment is performed just prior to entering the terminal area, accurate position, velocity, and attitude information would be available for approach and landing without reliance upon VOR/DME information.

In general, when combining VOR/DME information with air or inertial data, the suboptimal filter resulting when the DME biases are neglected, performs nearly optimally. However, neglecting VOR biases results in great performance degradation. During the period of time that it takes for in-flight alignment (or realignment) of a high-quality INS (20 to 30 minutes), the suboptimal filter resulting when the gyro drifts, accelerometer errors, and DME biases are neglected performs nearly optimally. Hence, alignment can be accomplished by using an eighth-order filter when using one VOR/DME or a seventh-order filter when using two DME's.

The performance of the air-data filter was found to be rather insensitive to wide variations in error model parameters. However, more information regarding the error statistics should be acquired.

Appendix A

DERIVATION OF INS ERROR EQUATIONS

The approach used here is basically the one used by Pinson [33]. The INS consists of a computer and a gyro-stabilized platform on which are mounted three accelerometers with their sensitive axes mutually perpendicular. Three sets of coordinate axes enter into the error analysis:

(1) platform coordinate axes, the axes lying along the nominal accelerometer sensitive axes,

(2) true coordinate axes, the axes representing the ideal alignment of the platform axes at the location of the platform, and

(3) computer coordinate axes, the axes corresponding to the true coordinate axes established at the location indicated by the computer.

For a perfectly operating system, the platform, true, and computer sets of axes coincide. However, in actual operation these coordinate systems are generally rotated relative to each other through small angles.* Let $\underline{\delta\theta}$ denote the vector angle required to rotate the true coordinates into the computer coordinates, $\underline{\phi}$ the vector angle required to rotate the true coordinates into the platform coordinates, and $\underline{\psi}$ the vector angle required to rotate the computer coordinates into the platform coordinates.

The true set of axes rotates at a certain rate $\underline{\omega}$ with respect to inertial space. Since the computer contains the computer set of axes as its estimate of the true set and $\underline{\omega}_c$ as its estimate of $\underline{\omega}$, it rotates the computer axes at $\underline{\omega}_c$. Since the platform and computer coordinates differ by an angle $\underline{\psi}$, the gyro-torquing signals equivalent to $\underline{\omega}_c$ result in a platform angular velocity of $\underline{\omega}_c + \underline{\psi} \times \underline{\omega}_c$. In addition to the

*Hence, the theory of infinitesimal rotations is assumed to be applicable.

intentionally induced platform angular velocity, there exists a platform drift rate $\underline{\epsilon}$ due mainly to gyro drifts. Hence, the angular velocity of the platform coordinate axes in inertial space, $\underline{\omega}_p$, is given by

$$\underline{\omega}_p = \underline{\omega}_c + \underline{\Psi} \times \underline{\omega}_c + \underline{\epsilon} \quad . \tag{A.1}$$

Now,

$$\underline{\omega}_p = \underline{\omega}_c + (\dot{\underline{\Psi}})_c \quad , \tag{A.2}$$

where $(\dot{\underline{\Psi}})_c$ is the time rate of change of $\underline{\Psi}$ relative to the computer reference frame, that is, the angular velocity of the platform relative to the computer reference frame. Hence, from Eqs. (A.1) and (A.2) it follows that

$$(\dot{\underline{\Psi}})_c + \underline{\omega}_c \times \underline{\Psi} = \underline{\epsilon} \quad , \tag{A.3}$$

or

$$(\dot{\underline{\Psi}})_I = \underline{\epsilon} \quad , \tag{A.4}$$

where $(\dot{\underline{\Psi}})_I$ denotes the rate of change of $\underline{\Psi}$ relative to inertial space.

Ideally, the accelerometers of an INS sense an acceleration $\underline{A}$ which is given by

$$\underline{A} = (\ddot{\underline{R}})_I - \underline{g}_m \quad , \tag{A.5}$$

where $\underline{R}$ is the radius vector from the center of the earth to the true position of the vehicle, $\underline{g}_m$ is the gravitational force per unit mass vector, and $(\ddot{\underline{R}})_I$ is the second rate of change of $\underline{R}$ as viewed by an observer fixed in inertial space.* Letting $\underline{V}$ denote the velocity of the vehicle relative to the earth, that is,

---

*For near-earth operation, an inertial reference frame can be defined by a set of axes that is nonrotating with respect to the fixed stars and has its origin fixed at the center of the earth.

$$\underline{V} = (\dot{\underline{R}})_E \quad , \tag{A.6}$$

where $(\dot{\underline{R}})_E$ is the time rate of change of $\underline{R}$ as viewed by an observer fixed relative to the earth, Eq. (A.5) can be written in the following form:

$$(\dot{\underline{R}})_I = \underline{V} + \underline{\Omega} \times \underline{R} \quad , \tag{A.7}$$

$$(\dot{\underline{V}})_I = \underline{A} - \underline{\Omega} \times \underline{V} + \underline{g}(\underline{R}) \quad , \tag{A.8}$$

where

$$\underline{g}(\underline{R}) = \underline{g}_m - \underline{\Omega} \times (\underline{\Omega} \times \underline{R}) \quad . \tag{A.9}$$

The vector $\underline{g}(\underline{R})$ is the "plumb-bob" gravity vector composed of both mass attraction and centripetal components; $\underline{\Omega}$ is the angular velocity of the earth in inertial space.

The actual accelerometer output, $\underline{a}$, differs from the ideal accelerometer output, $\underline{A}$, because of accelerometer error, $\underline{\alpha}$, due to null shifts, scale-factor error, etc. Furthermore, since the accelerometers measure components of acceleration along platform axes but the computer processes these components as if they were along computer axes, the actual and ideal accelerometer outputs are related as follows:

$$\underline{A} = \underline{a} - \underline{\alpha} + \underline{\Psi} \times \underline{a} \quad . \tag{A.10}$$

Substitution of Eq. (A.10) into Eq. (A.8) yields:

$$(\dot{\underline{V}})_I = \underline{a} - \underline{\alpha} + \underline{\Psi} \times \underline{a} - \underline{\Omega} \times \underline{V} + \underline{g}(\underline{R}) \quad . \tag{A.11}$$

Thus, Eqs. (A.4), (A.7), and (A.11) are the true dynamical equations which must be solved in order to determine $\underline{R}$ and $\underline{V}$ from the actual accelerometer output $\underline{a}$.

In the INS computer, the actual accelerometer output is treated as though it were the ideal accelerometer output. Thus, from Eqs. (A.7) and (A.8), it is seen that the equations solved in the INS computer are

$$(\dot{\bar{\underline{R}}})_I = \bar{\underline{V}} + \underline{\Omega} \times \bar{\underline{R}} \quad , \tag{A.12}$$

$$(\dot{\bar{\underline{V}}})_I = \underline{a} - \underline{\Omega} \times \bar{\underline{V}} + \underline{g}(\bar{\underline{R}}) \quad , \tag{A.13}$$

where $\bar{\underline{R}}$ and $\bar{\underline{V}}$ are the computed values of $\underline{R}$ and $\underline{V}$, respectively.

The errors in the computed values of $\underline{R}$ and $\underline{V}$, $\underline{\delta R}$ and $\underline{\delta V}$, respectively, are defined by

$$\underline{\delta R} = \bar{\underline{R}} - \underline{R} \quad , \tag{A.14}$$

$$\underline{\delta V} = \bar{\underline{V}} - \underline{V} \quad . \tag{A.15}$$

Hence, subtracting Eqs. (A.7) and (A.11) from Eqs. (A.12) and (A.13), respectively, yields:

$$(\dot{\underline{\delta R}})_I = \underline{\delta V} + \underline{\Omega} \times \underline{\delta R} \quad , \tag{A.16}$$

$$(\dot{\underline{\delta V}})_I = \underline{\alpha} - \underline{\Psi} \times \underline{a} - \underline{\Omega} \times \underline{\delta V} + \underline{g}(\bar{\underline{R}}) - \underline{g}(\underline{R}) \quad . \tag{A.17}$$

The gravity vector $\underline{g}(\underline{R})$ is given by

$$\underline{g}(\underline{R}) = -\frac{g}{R}\underline{R} + (\text{ellipticity terms}) \quad , \tag{A.18}$$

where g and R are the magnitudes of $\underline{g}(\underline{R})$ and $\underline{R}$, respectively. For this study, the ellipticity terms were neglected. In this case, Eq. (A.18) becomes

$$\underline{g}(\underline{R}) = -\omega_s^2 \underline{R} \quad , \tag{A.19}$$

where

$$\omega_s^2 = \frac{g}{R} = \frac{g_o R_o^2}{R^3} \quad . \tag{A.20}$$

The quantity ω_s is the Schuler angular frequency while g_o is the value of g at the surface of the assumed spherical earth of radius R_o.

In view of Eqs. (A.19) and (A.20),

$$\underline{g}(\underline{\bar{R}}) = -\bar{\omega}_s^2 \underline{\bar{R}} = -\frac{g_o R_o^2}{\bar{R}^3} \underline{\bar{R}} \quad , \tag{A.21}$$

where $\bar{R}$ denotes the magnitude of $\underline{\bar{R}}$. Now, from Eqs. (A.19) and (A.21),

$$\underline{g}(\underline{\bar{R}}) - \underline{g}(\underline{R}) = -\bar{\omega}_s^2 \underline{\bar{R}} + \omega_s^2 \underline{R} \quad . \tag{A.22}$$

Expanding $\bar{\omega}_s^2$ in a Taylor series about $\underline{R}$ and retaining only first-order terms yields:

$$\bar{\omega}_s^2 = \omega_s^2 + 2\omega_s \frac{d\omega_s}{dR} \delta R \quad , \tag{A.23}$$

where, in view of Eq. (A.20),

$$\frac{d\omega_s}{dR} = -\frac{3}{2} \frac{\omega_s}{R} \quad . \tag{A.24}$$

Substituting from Eqs. (A.14), (A.23), and (A.24) into Eq. (A.22) yields:

$$\underline{g}(\underline{\bar{R}}) - \underline{g}(\underline{R}) = -\omega_s^2 \underline{\delta R} + 3 \frac{\omega_s^2}{R} \delta R(\underline{R} + \underline{\delta R}) \quad . \tag{A.25}$$

Thus, to first order,

$$\underline{g}(\bar{\underline{R}}) - \underline{g}(\underline{R}) = 3\,\frac{\omega_s^2}{R}\,\delta R\,\underline{R} - \omega_s^2\underline{\delta R} \quad . \tag{A.26}$$

Let $\underline{\omega}$ and $\underline{\rho}$ denote the angular velocity of the true set of axes relative to the inertial and earth-fixed reference frames, respectively. Then, from Eqs. (A.4), (A.7), (A.11), and (A.19), it is seen that the actual dynamic equations written in true coordinate axes are

$$\left.\begin{aligned} \dot{\underline{R}} &= \underline{V} - \underline{\rho} \times \underline{R} \quad , \\ \dot{\underline{V}} &= \underline{a} - \underline{\alpha} + \underline{\Psi} \times \underline{a} - \omega_s^2\underline{R} - (2\underline{\Omega} + \underline{\rho}) \times \underline{V} \quad , \\ \dot{\underline{\Psi}} &= \underline{\epsilon} - \underline{\omega} \times \underline{\Psi} \quad , \end{aligned}\right\} \tag{A.27}$$

where the time derivatives are taken with respect to the true reference frame. Furthermore, from Eqs. (A.12), (A.13), and (A.22), it is seen that the equations solved in the INS computer are

$$\left.\begin{aligned} \dot{\bar{\underline{R}}} &= \bar{\underline{V}} - \underline{\rho} \times \bar{\underline{R}} \quad , \\ \dot{\bar{\underline{V}}} &= \underline{a} - \bar{\omega}_s^2\bar{\underline{R}} - (2\underline{\Omega} + \underline{\rho}) \times \bar{\underline{V}} \quad , \end{aligned}\right\} \tag{A.28}$$

where the time derivatives are taken with respect to the true coordinates. Finally, from Eqs. (A.16), (A.17), and (A.26), it is seen that the error equations written in true coordinates are

$$\left.\begin{aligned} \dot{\underline{\delta R}} &= \underline{\delta V} - \underline{\rho} \times \underline{\delta R} \quad , \\ \dot{\underline{\delta V}} &= \underline{\alpha} - \underline{\Psi} \times \underline{a} - (2\underline{\Omega} + \underline{\rho}) \times \underline{\delta V} - \omega_s^2\underline{\delta R} + 3\,\frac{\omega_s^2}{R}\,\delta R\,\underline{R} \quad , \\ \dot{\underline{\Psi}} &= \underline{\epsilon} - \underline{\omega} \times \underline{\Psi} \quad . \end{aligned}\right\} \tag{A.29}$$

Note that Eqs. (A.27) through (A.29) are valid in any specified reference frame if the time derivatives are taken relative to that reference frame and $\underline{\omega}$ and $\underline{\rho}$ are replaced by the angular velocities of that specified reference frame relative to inertial and earth-fixed reference frames, respectively.

Appendix B

COMPUTER PROGRAM

A listing of the computer program that was used for the simulation studies performed in this work follows. All the results reported in this work were obtained from this program by reading in the proper values for the input parameters. The basic inputs are the particular combination of information to be used, the model parameters, the locations of the VOR/DME stations to be used, and the points where the stations are tuned in. The outputs of the program are the RMS errors in the estimates of the states (i.e., position, velocity, etc.).

```
C    THIS PROGRAM COMPUTES THE STATE ERROR COVARIANCE MATRIX ASSOCIATED
C    WITH THE FILTERS WHICH COMBINE VOR/DME INFORMATION WITH AIR AND
C    INERTIAL DATA
      REAL*4 Q(8,8)/64*0.0/,PHI(8,8)/64*0.0/,P(8,8)/64*0.0/,PHIQPH(8,8)/
     164*0.0/,X0(8,1)/8*0.0/,H(1,8),X(8,1),HNTRI(2,4),ALT1(20),ALT2(20),
     2LONG1(20),LONG2(20),LAT1(20),LAT2(20),SWLT1(20),SWLT2(20),LONG,LAT
     3,IDENT(8,8)/64*0.0/,SWLT3(20),SWLG3(20),KSTORE(9,1100),K(8,1),
     4LONGO,LATO,PO(9),PHIT(8,8),PPHIT(8,8),PHIPPH(8,8),HT(8,1),PHT(8,1)
     5,KH(8,8),KHP(8,8),KHT(8,8),PER(8,8),KT(1,8),KRKT(8,8),KR(8,1)
      REAL*8 FLIGHT(10)
      DIMENSION MEAS(6),SWLG1(20),SWLG2(20),HN(4,2),HNT(2,4),RI(4,4)
    1 FORMAT(1HO,'TIME-MIN',2X,'DIST-NM',6X,'LAT-DEG',5X,'X-NM',6X,'R-NM
     1',3X,'THETA-DEG',2X,'RMSX-FT',3X,'RMSY-FT',2X,'RMSRAD-FT',2X,'RMSV
     2WX-KT',2X,'RMSW-KT',2X,'RMSBV-DEG',2X,'RMSBD-FT'/1H ,22X,'LONG-DEG
     3',5X,'Y-NM',54X,'RMSVWY-KT')
    2 FORMAT(1HO,'DATA:'/1HO,'RMSVWX=',F7.2,' KT'/1H ,'RMSVWY=',F7.2,' K
     1T'/1H ,'RMSBV =',F7.2,' DEG'/1H ,'RMSBD =',F7.2,' NM'/1H ,'RMSVOR=
     2',F7.2,' DEG'/1H ,'RMSDME=',F7.2,' NM'/1H ,'CORVWX=',F7.2,' NM'/1H
     3 ,'CORVWY=',F7.2,' NM'/1H ,'CORVOR=',F7.2,' NM'/1H ,'CORDME=',F7.2
     4,' NM'/1H ,'DISTO =',F7.2,' NM'  /' TO    =',F7.2,' MIN'/' DELTAT=
     5',F7.2,' SEC'/' V     =',F7.2,' KT'/1H ,'ALT   =',F7.0,' FT'/1H ,
     6'LATO  =',F10.5,' DEG'/1H ,'LONGO =',F10.5,' DEG'/1H ,'NPRINT=',I3
     7/1H ,'NST1  =',I3/1H ,'NST2  =',I3/1H ,'NST3  =',I3/1H ,'NP    =',
     8I3/1H ,'ISEN  =',I3/1H ,'NSEN  =',I3/1H ,'IGAIN =',I3/1H ,'IRESET=
     9',I3/' NEST  =',I3/' IDISP =',I3/' MEAS  =',I3,5I5/////)
    3 FORMAT(1HO,'IST1',2X,'ALT1-FT',5X,'LAT1-DEG',4X,'LONG1-DEG',4X,
     1'SWLT1-DEG',4X,'SWLG1-DEG'//)
    4 FORMAT(' NO MEASUREMENT TAKEN FROM THE STATION BEING OVERFLOWN')
    5 FORMAT(//1HO,16X,'IST1=',I2,5X,'VX=',F7.2,' KT',5X,'XO=',F7.2,' NM
     1',5X,'TSWIT=',F6.2,' MIN',5X,'X2TO1=',F7.2,' NM',5X,'AT1=',F6.0,'
     2FT'/1H ,16X,'IST2=',I2,5X,'VY=',F7.2,' KT',5X,'YO=',F7.2,' NM',5X,
     3'VBRNG=',F6.2,' DEG',5X,'Y2TO1=',F7.2,' NM',5X,'AT2=',F6.0,' FT'//
     4)
    6 FORMAT(10F8.2)
    7 FORMAT(20I4)
    8 FORMAT(/////1H ,'IST2',2X,'ALT2-FT',5X,'LAT2-DEG',4X,'LONG2-DEG',
     14X,'SWLT2-DEG',4X,'SWLG2-DEG'//)
    9 FORMAT(1H+,I3,F10.0,4F13.5/)
   10 FORMAT(1H1,52X,'BEGINNING OF FLIGHT')
   11 FORMAT(1HO,55X,'END OF FLIGHT')
   12 FORMAT(8F10.5)
   13 FORMAT(/////1H ,'IST3',3X,'SWLT3-DEG',4X,'SWLG3-DEG'//)
   14 FORMAT(1H+,I3,2F13.5/)
   15 FORMAT(10A8)
   16 FORMAT(1H1,10A8//)
   17 FORMAT(1H1,62X,'GAINS:'//1HO,6X,'TIME',8X,'KX',13X,'KY',12X,'KVWX'
     1,11X,'KVWY',11X,'KBV1',11X,'KBD1',11X,'KBV2',11X,'KBD2')
   18 FORMAT(1HO,F10.2,8E15.7/(1H ,10X,8E15.7))
      IRUN=1
   20 NUM=1
      INSEN=0
      ITER=1
      READ(5,15) (FLIGHT(I),I=1,10)
   23 READ(5,6) RMSVWX,RMSVWY,RMSBV,RMSBD,RMSVOR,RMSDME,CORVWX,CORVWY,
```

```
     1CORVOR,CORDME
      IF(ITER.EQ.2) GO TO 24
      READ(5,7) NP,NPRINT,NST1,NST2,NST3,ISEN,NSEN,IGAIN,IRESET,NEST,
     1IDISP,(MEAS(J),J=1,6)
      IF(NSEN.GT.1.AND.IGAIN.EQ.1) INSEN=1
      READ(5,12) LATO,LONGO,TO,DELTAT,V,ALT,DISTO
      TOO=TO
      READ(5,6) (ALT1(I),I=1,NST1)
      READ(5,12) (LAT1(I),LONG1(I),I=1,NST1)
      READ(5,12) (SWLT1(I),SWLG1(I),I=1,NST1)
   24 WRITE(6,16) (FLIGHT(I),I=1,10)
      IF(MEAS(6).EQ.1) CALL INS1(RMSVWX,RMSVWY,RMSBV,RMSBD,RMSVOR,RMSDME
     1,CORVWX,CORVWY,CORVOR,CORDME,DISTO,TO,DELTAT,V,ALT,LATO,LONGO,
     2NPRINT,NST1,NST2,NST3,NP,ISEN,NSEN,IGAIN,MEAS,IRESET,NEST,IDISP,&2
     35)
      WRITE(6,2) RMSVWX,RMSVWY,RMSBV,RMSBD,RMSVOR,RMSDME,CORVWX,CORVWY,
     1CORVOR,CORDME,DISTO,TO,DELTAT,V,ALT,LATO,LONGO,NPRINT,NST1,NST2,
     2NST3,NP,ISEN,NSEN,IGAIN,IRESET,NEST,IDISP,(MEAS(J),J=1,6)
   25 WRITE(6,3)
      WRITE(6,9) (I,ALT1(I),LAT1(I),LONG1(I),SWLT1(I),SWLG1(I),I=1,NST1)
      IF(ITER.NE.1) GO TO 27
      N=0
      DO 26 I=1,4
   26 N=N+MEAS(I)
      MODE=1
      IF(MEAS(3).EQ.1) MODE=2
      IF(MEAS(4).EQ.1) MODE=2
   27 IF(MODE.EQ.1) GO TO 29
      IF(ITER.EQ.2) GO TO 28
      READ(5,6) (ALT2(I),I=1,NST2)
      READ(5,12) (LAT2(I),LONG2(I),I=1,NST2)
      READ(5,12) (SWLT2(I),SWLG2(I),I=1,NST2)
   28 WRITE(6,8)
      WRITE(6,9) (I,ALT2(I),LAT2(I),LONG2(I),SWLT2(I),SWLG2(I),I=1,NST2)
   29 IF(IRUN.EQ.2) GO TO 31
      IF(MEAS(6).EQ.1) CALL INS10(&31)
      DO 30 I=1,8
      DO 30 J=1,8
      PER(I,J)=0.0
   30 P(I,J)=0.0
   31 ISWV=0
      J1=0
      J2=0
      J3=0
      IF(NST3.EQ.0) GO TO 33
      IF(ITER.NE.1) GO TO 32
      READ(5,12) (SWLT3(I),SWLG3(I),I=1,NST3)
   32 ISWV=1
      IST3=1
      IF(ITER.EQ.3) GO TO 33
      WRITE(6,13)
      WRITE(6,14) (I,SWLT3(I),SWLG3(I),I=1,NST3)
   33 WRITE(6,10)
      IST1=1
      TO=TO*60.0
      T=TO
      DIST=DISTO
```

```
      LAT=LAT0
      LONG=LONG0
      AT1=(ALT-ALT1(1))/6076.10
      DTR=3.141592/180.0
      RE=(2.090E+07)/6076.10
      RCONE=0.7*AT1
      KS=1
      IF(MODE.EQ.1) GO TO 34
      IST2=1
      AT2=(ALT-ALT2(1))/6076.10
      GO TO 35
   34 IST2=0
      AT2=0.0
      X2TO1=0.0
      Y2TO1=0.0
   35 IF(MEAS(6).EQ.1) GO TO 36
      IF(MEAS(5).EQ.0) GO TO 37
   36 IN=1
      IPRINT=0
      JJ=0
      L=0
      IF(NP.EQ.0.AND.IRESET.NE.0) L=1
      IF(L.EQ.1.AND.IDISP.EQ.0) NP=1
      L=0
      IF(NP.NE.0) GO TO 37
      NP=1
      JJ=1
C    CALCULATE THE SYSTEM PARAMETERS
   37 IF(ITER.EQ.3) GO TO 39
      CORVOR=CORVOR*3600.0/V
      CORDME=CORDME*3600.0/V
      RMSBV=RMSBV*DTR
      RMSVOR=RMSVOR*DTR
      VARVOR=RMSBV**2+RMSVOR**2
      VARDME=RMSBD**2+RMSDME**2
      RVOR=2.0*CORVOR*RMSVOR**2/DELTAT
      RDME=2.0*CORDME*RMSDME**2/DELTAT
      IF(MEAS(6).EQ.1) CALL INS2(DTR,DELTAT,NP,RE,ALT,RMSBV,RMSBD,&39)
      RMSVWX=RMSVWX/3600.0
      RMSVWY=RMSVWY/3600.0
      CORVWX=CORVWX*3600.0/V
      CORVWY=CORVWY*3600.0/V
      IF(MEAS(5).EQ.0) GO TO 39
      Q(3,3)=2.0*(RMSVWX**2)/CORVWX
      Q(4,4)=2.0*(RMSVWY**2)/CORVWY
      DO 38 I=1,8
      PHI(I,I)=1.0
   38 IDENT(I,I)=1.0
      EX=1.0/EXP(DELTAT/CORVWX/NP)
      EY=1.0/EXP(DELTAT/CORVWY/NP)
      PHI(1,3)=CORVWX*(1.0-EX)
      PHI(2,4)=CORVWY*(1.0-EY)
      PHI(3,3)=EX
      PHI(4,4)=EY
      PHIQPH(1,1)=Q(3,3)*(DELTAT/NP-0.5*CORVWX*(3.0-EX)*(1.0-EX))*CORVWX
     1**2
      PHIQPH(2,2)=Q(4,4)*(DELTAT/NP-0.5*CORVWY*(3.0-EY)*(1.0-EY))*CORVWY
```

```
     1**2
      PHIQPH(1,3)=(Q(3,3)*0.5*CORVWX**2)*(1.0-EX)**2
      PHIQPH(2,4)=(Q(4,4)*0.5*CORVWY**2)*(1.0-EY)**2
      PHIQPH(3,1)=PHIQPH(1,3)
      PHIQPH(4,2)=PHIQPH(2,4)
      PHIQPH(3,3)=Q(3,3)*0.5*CORVWX*(1.0-EX**2)
      PHIQPH(4,4)=Q(4,4)*0.5*CORVWY*(1.0-EY**2)
C    INITIALIZE THE COVARIANCE MATRIX P
   39 LL=0
      CALL SWITCH(TSWIT,  IST1,IST2,NST1,NST2,   J1,   J2,LAT1,LAT2,LONG
     11,LONG2,LAT,LONG,SWLT1,SWLT2,SWLG1,SWLG2,RE,DTR,MODE,TO,T,LL,X2TO1
     2,Y2TO1,VX,VY,XO,MEAS(5),ALT,AT1,AT2,ALT1,ALT2,RCONE,ISW,VBRNG,V,
     3SWLT3,SWLG3,ISWV,IST3,NST3,&100)
      LL=1
      CALL ANGLE(XO(1,1),XO(2,1),THETA)
      R2=XO(1,1)**2+XO(2,1)**2
      R1=SQRT(R2)
      CALL RMS2(IN,R2,A,B,C,THETA,AT1,VARVOR,VARDME)
      IF(IRUN.EQ.2) GO TO 42
      IF(MEAS(6).EQ.1) CALL INS3(ITER,A,B,C,&42)
      P(1,1)=(A/6076.1)**2
      P(2,2)=(B/6076.1)**2
      P(1,2)=C
      P(2,1)=C
   40 P(3,3)=RMSVWX**2
      P(4,4)=RMSVWY**2
      P(5,5)=RMSBV**2
      P(6,6)=RMSBD**2
      P(7,7)=P(5,5)
      P(8,8)=P(6,6)
      IF(NEST.EQ.8) GO TO 42
      NEST1=NEST+1
      DO 41 I=NEST1,8
      PER(I,I)=P(I,I)
   41 P(I,I)=0.0
   42 TSWITM=TSWIT/60.0
      VBRNGD=VBRNG/DTR
      AT1FT=AT1*6076.1
      AT2FT=AT2*6076.1
      WRITE(6,5) IST1,VX,XO(1,1),TSWITM,X2TO1,AT1FT,IST2,VY,XO(2,1),
     1VBRNGD,Y2TO1,AT2FT
      IF(MEAS(6).EQ.0) GO TO 44
      CALL INS4(S)
      IF(IDISP.EQ.0.OR.IRESET.EQ.0) GO TO 43
      X(1,1)=XO(1,1)
      X(2,1)=XO(2,1)
      GO TO 56
   43 CALL INS5(XO(1,1),XO(2,1),THETA,T,R1,MODE,LONG,LAT,DIST)
      GO TO 46
   44 WRITE(6,1)
      IF(MEAS(5).EQ.0) CALL NOAIR(MEAS,T-DELTAT,XO(1,1),XO(2,1),VX,VY,
     1RCONE,X2TO1,Y2TO1,N,AT1,AT2,MODE,DELTAT,VARVOR,VARDME,P,HN,HNT,RI,
     2HNTRI,TO,X(1,1),X(2,1),LONG1(IST1),LAT1(IST1),LONG,LAT,DTR,RE,V,
     3DIST-V*DELTAT/3600.0,&79)
      CALL RMS1(P,DTR,XO(1,1),XO(2,1),THETA,T,R1,MODE,LONG,LAT,DIST)
      IF(NEST.EQ.8) GO TO 45
      CALL GMADD(PER,P,PHIT,8,8)
```

```
      CALL RMS1(PHIT,DTR,X0(1,1),X0(2,1),THETA,T,R1,MODE,LONG,LAT,DIST)
C     CALCULATE THE NOMINAL POSITION AND PERFORM THE TIME UPDATING OF P
   45 IF(MEAS(6).EQ.1) GO TO 46
      IF(MEAS(5).EQ.0) CALL NOAIR(MEAS,T,X0(1,1),X0(2,1),VX,VY,RCONE,X2T
     101,Y2T01,N,AT1,AT2,MODE,DELTAT,VARVOR,VARDME,P,HN,HNT,R1,HNTR1,T0,
     2X(1,1),X(2,1),LONG1(IST1),LAT1(IST1),LONG,LAT,DTR,RE,V,DIST,&79)
   46 DO 50 J=1,NP
      IF(MEAS(6).EQ.1) CALL INS6(LAT,LONG,VX,VY)
      T=T+DELTAT/NP
      X(1,1)=X0(1,1)+VX*(T-T0)/3600.0
      X(2,1)=X0(2,1)+VY*(T-T0)/3600.0
      DIST=DIST+V*DELTAT/3600.0/NP
      LONG=-(X(1,1)/RE/COS(LAT1(IST1)*DTR)/DTR)+LONG1(IST1)
      LAT=X(2,1)/RE/DTR+LAT1(IST1)
      R2=X(1,1)**2+X(2,1)**2
      R1=SQRT(R2)
      IF(MEAS(6).EQ.1) GO TO 47
      CALL GMTRA(PHI,PHIT,8,8)
      CALL GMPRD(P,PHIT,PPHIT,8,8,8)
      CALL GMPRD(PHI,PPHIT,PHIPPH,8,8,8)
      CALL GMADD(PHIPPH,PHIQPH,P,8,8)
      IF(NEST.EQ.8) GO TO 47
      CALL GMPRD(PER,PHIT,PPHIT,8,8,8)
      CALL GMPRD(PHI,PPHIT,PER,8,8,8)
   47 CALL ANGLE(X(1,1),X(2,1),THETA)
      IF(NP.NE.1) GO TO 48
      IF(JJ.EQ.1) GO TO 50
      IF(IPRINT+1.NE.NPRINT) GO TO 50
   48 IF(MEAS(6).EQ.0) GO TO 49
      CALL INS5(X(1,1),X(2,1),THETA,T,R1,MODE,LONG,LAT,DIST)
      GO TO 50
   49 CALL RMS1(P,DTR,X(1,1),X(2,1),THETA,T,R1,MODE,LONG,LAT,DIST)
      IF(NEST.EQ.8) GO TO 50
      CALL GMADD(PER,P,PHIT,8,8)
      CALL RMS1(PHIT,DTR,X(1,1),X(2,1),THETA,T,R1,MODE,LONG,LAT,DIST)
   50 CONTINUE
      IF(N.EQ.0) GO TO 51
      IF(R1.GT.RCONE) GO TO 55
      IF(MODE.EQ.1) GO TO 51
      IF(IRESET.NE.0) GO TO 51
      NH=2
      L=1
      GO TO 56
   51 IPRINT=IPRINT+1
      IF(IPRINT.NE.NPRINT) GO TO 79
      IPRINT=0
      IF(JJ.NE.1) GO TO 53
      IF(MEAS(6).EQ.0) GO TO 52
      CALL INS5(X(1,1),X(2,1),THETA,T,R1,MODE,LONG,LAT,DIST)
      GO TO 53
   52 CALL RMS1(P,DTR,X(1,1),X(2,1),THETA,T,R1,MODE,LONG,LAT,DIST)
      IF(NEST.EQ.8.OR.ICOMP.EQ.1) GO TO 53
      CALL GMADD(PER,P,PHIT,8,8)
      CALL RMS1(PHIT,DTR,X(1,1),X(2,1),THETA,T,R1,MODE,LONG,LAT,DIST)
   53 IF(N.NE.0) WRITE(6,4)
      GO TO 79
C     CALCULATE THE MEASUREMENT MATRIX AND PERFORM THE MEASUREMENT
```

```
C   UPDATING OF P
   55 NH=0
   56 IF(IRESET.NE.0) CALL INS11(N,IRESET,X(1,1),X(2,1),R2,X2TO1,Y2TO1,
     1AT1,AT2,HN,HNT,RI,HNTRI,VARVOR,VARDME,&66)
      IF(MEAS(6).EQ.1) CALL INS7(NH,X(1,1),X(2,1),AT1,AT2,R2,X2TO1,Y2TO1
     1,KS,ITER,RVOR,RDME,&66)
      DO 58 I=1,8
      DO 58 J=1,8
      IF(ABS(P(I,J)).LE.1.0E-25) P(I,J)=0.0
   58 CONTINUE
   60 NH=NH+1
      IF(MEAS(NH).EQ.0) GO TO 65
      CALL FINDH(NH,H,X(1,1),X(2,1),AT1,AT2,R2,X2TO1,Y2TO1,8)
      IF(ITER.NE.2) GO TO 62
      DO 61 I=1,8
   61 K(I,1)=KSTORE(I,KS)
      KS=KS+1
   62 CALL MEASUP(NH,H,P,RVOR,RDME,IDENT,ITER,K,8,HT,PHT,KH,KHP,KHT,KT,K
     1RKT,KR)
      IF(NEST.EQ.8) GO TO 63
      CALL GMTRA(KH,KHT,8,8)
      CALL GMPRD(KH,PER,KHP,8,8,8)
      CALL GMPRD(KHP,KHT,PER,8,8,8)
   63 IF(ISEN.EQ.0.AND.IGAIN.EQ.0) GO TO 65
      IF(ITER.EQ.2) GO TO 65
      IF(ITER.EQ.3.AND.IGAIN.EQ.0) GO TO 65
      DO 64 I=1,8
   64 KSTORE(I,KS)=K(I,1)
      IF(IGAIN.EQ.1) KSTORE(9,KS)=T
      KS=KS+1
   65 IF(NH.NE.4) GO TO 60
   66 IPRINT=IPRINT+1
      IF(IPRINT.NE.NPRINT) GO TO 75
      IPRINT=0
      IF(MEAS(6).EQ.0) GO TO 67
      CALL INS5(X(1,1),X(2,1),THETA,T,R1,MODE,LONG,LAT,DIST)
      GO TO 68
   67 CALL RMS1(P,DTR,X(1,1),X(2,1),THETA,T,R1,MODE,LONG,LAT,DIST)
      IF(NEST.EQ.8) GO TO 68
      CALL GMADD(PER,P,PHIT,8,8)
      CALL RMS1(PHIT,DTR,X(1,1),X(2,1),THETA,T,R1,MODE,LONG,LAT,DIST)
   68 IF(L.EQ.1) GO TO 70
      IF(ITER.EQ.2) GO TO 79
      IF(MEAS(6).EQ.1) GO TO 79
      CALL RMS2(IN,R2,A,B,C,THETA,AT1,VARVOR,VARDME)
      GO TO 79
   70 WRITE(6,4)
   75 L=0
   79 IF(ABS(T-TSWIT).GT.DELTAT/2.0) GO TO 45
      CALL SWITCH(TSWIT,  IST1,IST2,NST1,NST2,  J1,    J2,LAT1,LAT2,LONG
     11,LONG2,LAT,LONG,SWLT1,SWLT2,SWLG1,SWLG2,RE,DTR,MODE,TO,T,LL,X2TO1
     2,Y2TO1,VX,VY,XO,MEAS(6),ALT,AT1,AT2,ALT1,ALT2,RCONE,ISW,VBRNG,V,
     3SWLT3,SWLG3,ISWV,IST3,NST3,&80)
      GO TO 81
   80 J1=1
      J2=1
      J3=1
```

```
   81 IF(MEAS(6).EQ.1) CALL INS8(J1,J2,&92)
      IF(J1.EQ.0) GO TO 85
C    RE-INITIALIZE THE ELEMENTS OF P RELATING TO THE STATION BIASES
      DO 82 J=5,6
      DO 82 I=1,8
      P(I,J)=0.0
      P(J,I)=0.0
      PER(I,J)=0.0
   82 PER(J,I)=0.0
      P(5,5)=RMSBV**2
      P(6,6)=RMSBD**2
      J1=0
      IF(NEST.EQ.8) GO TO 85
      IF(NEST1-6)83,84,85
   83 PER(5,5)=P(5,5)
      P(5,5)=0.0
   84 PER(6,6)=P(6,6)
      P(6,6)=0.0
   85 IF(J2.EQ.0) GO TO 92
      DO 86 J=7,8
      DO 86 I=1,8
      P(I,J)=0.0
      P(J,I)=0.0
      PER(I,J)=0.0
   86 PER(J,I)=0.0
      P(7,7)=RMSBV**2
      P(8,8)=RMSBD**2
      J2=0
      IF(NEST.EQ.8) GO TO 92
      IF(NEST.EQ.7) GO TO 88
      PER(7,7)=P(7,7)
      P(7,7)=0.0
   88 PER(8,8)=P(8,8)
      P(8,8)=0.0
   92 IF(J3.EQ.1) GO TO 100
      TSWITM=TSWIT/60.0
      VBRNGD=VBRNG/DTR
      AT1FT=AT1*6076.1
      AT2FT=AT2*6076.1
      R1=SQRT(X0(1,1)**2+X0(2,1)**2)
      CALL ANGLE(X0(1,1),X0(2,1),THETA)
      WRITE(6,5) IST1,VX,X0(1,1),TSWITM,X2TO1,AT1FT,IST2,VY,X0(2,1),
     1VBRNGD,Y2TO1,AT2FT
      IF(MEAS(6).EQ.1) GO TO 95
      WRITE(6,1)
      IF(MEAS(5).EQ.0) CALL NOAIR(MEAS,T,X0(1,1),X0(2,1),VX,VY,RCONE,X2T
     1O1,Y2TO1,N,AT1,AT2,MODE,DELTAT,VARVOR,VARDME,P,HN,HNT,RI,HNTRI,TO,
     2X(1,1),X(2,1),LONG1(IST1),LAT1(IST1),LONG,LAT,DTR,RE,V,DIST,&79)
      CALL RMS1(P,DTR,X0(1,1),X0(2,1),THETA,T,R1,MODE,LONG,LAT,DIST)
      IF(NEST.EQ.8) GO TO 45
      CALL GMADD(PER,P,PHIT,8,8)
      CALL RMS1(PHIT,DTR,X0(1,1),X0(2,1),THETA,T,R1,MODE,LONG,LAT,DIST)
      GO TO 45
   95 CALL INS4(S)
      CALL INS5(X0(1,1),X0(2,1),THETA,T,R1,MODE,LONG,LAT,DIST)
      GO TO 46
  100 WRITE(6,11)
```

```
      IF(IGAIN.EQ.0.OR.ITER.EQ.2) GO TO 140
      IF(MEAS(6).EQ.1) CALL INS9(KS,&140)
      KSTORE(9,KS)=-1.0
      WRITE(6,17)
      IPRINT=0
      KP=1
  110 IPRINT=IPRINT+1
      T=KSTORE(9,KP)
      TM=T/60.0
      NN=1
  115 IF(KSTORE(9,KP).NE.KSTORE(9,KP+NN)) GO TO 120
      NN=NN+1
      GO TO 115
  120 IF(IPRINT.NE.NPRINT) GO TO 125
      WRITE(6,18) TM,((KSTORE(I,KP-1+J),I=1,8),J=1,NN)
      IPRINT=0
  125 KP=KP+NN
      IF(KP.GE.KS) GO TO 140
      GO TO 110
  140 IF(ISEN.EQ.0) GO TO 150
      IF(NUM.EQ.NSEN.AND.ITER.EQ.3) GO TO 150
      IF(INSEN.EQ.1.AND.ITER.EQ.3) GO TO 160
      ITER=ITER+1
      IF(ITER.LT.4) GO TO 141
      NUM=NUM+1
      ITER=2
  141 IF(JJ.EQ.1) NP=0
      TO=TOO
      IF(ITER.EQ.2) GO TO 23
      GO TO 29
  150 READ(5,7) IRUN
      IF(IRUN.NE.0) GO TO 20
  160 STOP
      END


      SUBROUTINE RMS1(P,DTR,X,Y,THETA,T,R1,MODE,LONG,LAT,DIST)
C   CALCULATES THE RMS ERRORS IN THE AIR-DATA FILTER ESTIMATES
      REAL*4 P(8,8),LONG,LAT
    1 FORMAT(1H+,110X,F10.2,F10.0)
    2 FORMAT(1HO,F7.2,F10.2,F13.5,3F10.2,3F10.0,3F10.2,F10.0/1H ,17X,
     1F13.5,F10.2,50X,F10.2)
      RMSX=SQRT(P(1,1))*6076.1
      RMSY=SQRT(P(2,2))*6076.1
      RMSVWX=SQRT(P(3,3))*3600.0
      RMSVWY=SQRT(P(4,4))*3600.0
      RMSBV=SQRT(P(5,5))/DTR
      RMSBD=SQRT(P(6,6))*6076.1
      RMSRAD=SQRT(P(1,1)+P(2,2))*6076.1
      RMSW=SQRT(P(3,3)+P(4,4))*3600.0
      TIME=T/60.0
      THETAD=THETA/DTR
      WRITE(6,2) TIME,DIST,LAT,X,R1,THETAD,RMSX,RMSY,RMSRAD,RMSVWX,RMSW,
     1RMSBV,RMSBD,LONG,Y,RMSVWY
      IF(MODE.EQ.1) RETURN
      RMSBV2=SQRT(P(7,7))/DTR
```

```
      RMSBD2=SQRT(P(8,8))*6076.1
      WRITE(6,1) RMSBV2,RMSBD2
      RETURN
      END



      SUBROUTINE RMS2(IN,R2,RMSX,RMSY,COVXY,THETA,ALT,VARVOR,VARDME)
C     CALCULATES THE RMS POSITION ERRORS RESULTING WHEN USING THE
C     INFORMATION FROM A SINGLE VOR/DME STATION WITHOUT AIR OR
C     INERTIAL DATA
    1 FORMAT(1H+,60X,3F10.0)
      S2=SIN(THETA)**2
      C2=COS(THETA)**2
      RR=R2+ALT**2
      F=(1.0-0.5*ALT**2/RR)**2
      RMSX=SQRT(RR*F*C2*VARVOR+F*S2*VARDME)*6076.1
      RMSY=SQRT(RR*F*S2*VARVOR+F*C2*VARDME)*6076.1
      RMSRAD=SQRT(RMSX**2+RMSY**2)
      IF(IN.NE.1) GO TO 10
      IN=2
      S=SIN(THETA)
      C=COS(THETA)
      COVXY=-RR*F*S*C*VARVOR+F*C*S*VARDME
      RETURN
   10 WRITE(6,1) RMSX,RMSY,RMSRAD
      RETURN
      END



      SUBROUTINE RMS3(P,DTR,T,THETA,DIST,LAT,LONG,X,Y,R1,MODE,RE,ALT)
C     CALCULATES THE RMS ERRORS IN THE INS FILTER ESTIMATES
      REAL*4 P(16,16),LONG,LAT
    1 FORMAT(1H0,F7.2,F10.2,F11.5,2F9.2,F10.0,F10.2,F11.4,2F12.4,F12.6,
     1F7.2,F10.0/1H ,17X,F11.5, F9.2, 9X,F10.0,F10.2,F11.4,2F12.4,F12.6)
    2 FORMAT(1H+,113X,F7.2,F10.0)
    3 FORMAT(1H ,28X,F9.2,  9X,F10.0,F10.2,F11.4,2F12.4,F12.6)
      RMSX=SQRT(P(1,1))*6076.10
      RMSY=SQRT(P(2,2))*6076.10
      RMSVX=SQRT(P(3,3))*3600.0
      RMSVY=SQRT(P(4,4))*3600.0
      RMSPIX=SQRT(P(5,5))/DTR
      RMSPIY=SQRT(P(6,6))/DTR
      RMSPIZ=SQRT(P(7,7))/DTR
      RA=2.0/(RE+ALT/6076.10)
      RA2=(RA/2.0)**2
      RMSPHX=SQRT(P(5,5)-RA*P(2,5)+P(2,2)*RA2)/DTR
      RMSPHY=SQRT(P(6,6)+RA*P(1,6)+P(1,1)*RA2)/DTR
      RMSPHZ=SQRT(P(7,7)+RA*TAN(LAT*DTR)*P(1,7)+RA2*P(1,1)*TAN(LAT*DTR)*
     1*2)/DTR
      RMSGX=SQRT(P(8,8))/DTR*3600.0
      RMSGY=SQRT(P(9,9))/DTR*3600.0
      RMSGZ=SQRT(P(10,10))/DTR*3600.0
      RMSACX=SQRT(P(11,11))*6076.10/32.2
      RMSACY=SQRT(P(12,12))*6076.10/32.2
      RMSBV1=SQRT(P(13,13))/DTR
```

```
      RMSBD1=SQRT(P(14,14))*6076.10
      RMSRAD=SQRT(P(1,1)+P(2,2))*6076.10
      RMSV=SQRT(P(3,3)+P(4,4))*3600.0
      TIME=T/60.0
      THETAD=THETA/DTR
      WRITE(6,1) TIME,DIST,LAT,X,THETAD,RMSX,RMSVX,RMSPIX,RMSPHX,RMSGX,
     1RMSACX,RMSBV1,RMSBD1,LONG,Y,RMSY,RMSVY,RMSPIY,RMSPHY,RMSGY,RMSACY
      IF(MODE.EQ.1) GO TO 10
      RMSBV2=SQRT(P(15,15))/DTR
      RMSBD2=SQRT(P(16,16))*6076.10
      WRITE(6,2) RMSBV2,RMSBD2
   10 WRITE(6,3) R1,RMSRAD,RMSV,RMSPIZ,RMSPHZ,RMSGZ
      RETURN
      END


      SUBROUTINE ANGLE(X,Y,THETA)
C     CALCULATES THE BEARING OF THE AIRCRAFT RELATIVE TO NORTH AT A
C     REFERENCE VOR/DME STATION
      PI=3.141592
      IF(X)10,20,30
   10 IF(Y)11,12,13
   11 ARG=ABS(X)/ABS(Y)
      THETA=PI+ATAN(ARG)
      RETURN
   12 THETA=3.0*PI/2.0
      RETURN
   13 ARG=ABS(X)/Y
      THETA=2.0*PI-ATAN(ARG)
      RETURN
   20 IF(Y) 21,22,22
   21 THETA=PI
      RETURN
   22 THETA=0.0
      RETURN
   30 IF(Y)31,32,33
   31 ARG=X/ABS(Y)
      THETA=PI-ATAN(ARG)
      RETURN
   32 THETA=PI/2.0
      RETURN
   33 ARG=X/Y
      THETA=ATAN(ARG)
      RETURN
      END


      SUBROUTINE FINDH(NH,H,X,Y,AT1,AT2,R2,X2TO1,Y2TO1,NST)
C     CALCULATES THE MEASUREMENT MATRIX
      DIMENSION H(1,NST)
      DO 10 I=1,NST
   10 H(1,I)=0.0
      GO TO (20,30,40,50),NH
   20 H(1,1)=Y/R2
      H(1,2)=-X/R2
```

```
      H(1,NST-3)=1.0
      RETURN
   30 D=SQRT(R2+AT1**2)
      H(1,1)=X/D
      H(1,2)=Y/D
      H(1,NST-2)=1.0
      RETURN
   40 D=(X+X2TO1)**2+(Y+Y2TO1)**2
      H(1,1)=(Y+Y2TO1)/D
      H(1,2)=-(X+X2TO1)/D
      H(1,NST-1)=1.0
      RETURN
   50 D=SQRT((X+X2TO1)**2+(Y+Y2TO1)**2+AT2**2)
      H(1,1)=(X+X2TO1)/D
      H(1,2)=(Y+Y2TO1)/D
      H(1,NST)=1.0
      RETURN
      END


      SUBROUTINE MEASUP(NH,H,P,RVOR,RDME,IDENT,ITER,K,NST,HT,PHT,KH,KHP,
     1KHT,KT,KRKT,KR)
C     PERFORMS THE MEASUREMENT UPDATING OF P
      REAL*4 P(NST,NST),H(1,NST),HT(NST,1),PHT(NST,1),K(NST,1),KH(NST,NS
     1T),KHP(NST,NST),IDENT(NST,NST),KHT(NST,NST),KT(1,NST),KRKT(NST,NST
     2),KR(NST,1)
      IF(NH.EQ.2) GO TO 10
      IF(NH.EQ.4) GO TO 10
      R=RVOR
      GO TO 11
   10 R=RDME
   11 IF(ITER.EQ.2) GO TO 20
      CALL GMTRA(H,HT,1,NST)
      CALL GMPRD(P,HT,PHT,NST,NST,1)
      HPHT=0.0
      DO 15 I=1,NST
   15 HPHT=HPHT+H(1,I)*PHT(I,1)
      DO 19 I=1,NST
   19 K(I,1)=PHT(I,1)/(HPHT+R)
   20 CALL GMPRD(K,H,KH,NST,1,NST)
      CALL GMSUB(IDENT,KH,KH,NST,NST)
      CALL GMPRD(KH,P,KHP,NST,NST,NST)
      IF(ITER.NE.2) GO TO 40
      CALL GMTRA(KH,KHT,NST,NST)
      CALL GMPRD(KHP,KHT,P,NST,NST,NST)
      CALL GMTRA(K,KT,NST,1)
      DO 30 I=1,NST
   30 KR(I,1)=K(I,1)*R
      CALL GMPRD(KR,KT,KRKT,NST,1,NST)
      CALL GMADD(P,KRKT,P,NST,NST)
      RETURN
   40 DO 50 I=1,NST
      DO 50 J=1,NST
   50 P(I,J)=KHP(I,J)
      RETURN
      END
```

```
      SUBROUTINE SWITCH(TSWIT,  IST1,IST2,NST1,NST2,   J1,   J2,LAT1,
     1LAT2,LONG1,LONG2,LAT,LONG,SWLT1,SWLT2,SWLG1,SWLG2,RE,DTR,MODE,T0,
     2T,LL,X2T01,Y2T01,VX,VY,X0,MEAS5,ALT,AT1,AT2,ALT1,ALT2,RCONE,ISW,
     3VBRNG,V,SWLT3,SWLG3,ISWV,IST3,NST3,*)
C    TUNES IN A NEW VOR/DME STATION OR CHANGES THE HEADING OF THE AIRCRAFT
      REAL*4         LAT1(20),LAT2(20),LONG1(20),LONG2(20),LAT,LONG,SWLT1
     1(20),SWLT2(20),SWLG1(20),SWLG2(20),X0(8,1),ALT1(20),ALT2(20),SWLT3
     2(20),SWLG3(20)
      IF(LL.EQ.0) GO TO 50
      T0=T
      IF(ISW.LT.4) GO TO 10
      IST3=IST3+1
      IF(IST3.GT.NST3) ISWV=0
      GO TO 50
   10 IF(ISW.EQ.2) GO TO 30
      IF(IST1.EQ.NST1) RETURN 1
      IST1=IST1+1
      AT1=(ALT-ALT1(IST1))/6076.1
      RCONE=0.7*AT1
      J1=1
   20 IF(ISW.EQ.1) GO TO 50
   30 IF(IST2.EQ.NST2) RETURN 1
      IST2=IST2+1
      AT2=(ALT-ALT2(IST2))/6076.1
      J2=1
   50 X0(1,1)=(LONG1(IST1)-LONG)*DTR*RE*COS(LAT1(IST1)*DTR)
      X0(2,1)=(LAT-LAT1(IST1))*DTR*RE
   60 IF(MODE.EQ.1) GO TO 70
      X2T01=(LONG2(IST2)-LONG1(IST1))*DTR*RE*COS(LAT1(IST1)*DTR)
      Y2T01=(LAT1(IST1)-LAT2(IST2))*DTR*RE
   70 XSW1=(LONG1(IST1)-SWLG1(IST1))*DTR*RE*COS(LAT1(IST1)*DTR)-X0(1,1)
      YSW1=(SWLT1(IST1)-LAT1(IST1))*DTR*RE-X0(2,1)
      RSW1=SQRT(XSW1**2+YSW1**2)
      IF(MODE.EQ.1.AND.ISWV.EQ.0) GO TO 80
      IF(MODE.EQ.1) GO TO 72
      XSW2=(LONG1(IST1)-SWLG2(IST2))*DTR*RE*COS(LAT1(IST1)*DTR)-X0(1,1)
      YSW2=(SWLT2(IST2)-LAT1(IST1))*DTR*RE-X0(2,1)
      RSW2=SQRT(XSW2**2+YSW2**2)
      IF(ISWV.EQ.0) GO TO 75
   72 XSW3=(LONG1(IST1)-SWLG3(IST3))*DTR*RE*COS(LAT1(IST1)*DTR)-X0(1,1)
      YSW3=(SWLT3(IST3)-LAT1(IST1))*DTR*RE-X0(2,1)
      RSW3=SQRT(XSW3**2+YSW3**2)
      IF(MODE.EQ.1) GO TO 76
      IF(RSW3.LT.RSW1.AND.RSW3.LT.RSW2) GO TO 85
      IF(RSW2.LT.RSW1.AND.RSW2.LT.RSW3) GO TO 90
      IF(RSW1.LT.RSW2.AND.RSW1.LT.RSW3) GO TO 80
      GO TO 79
   75 IF(RSW1-RSW2) 80,79,90
   76 IF(RSW1-RSW3) 80,80,85
   79 ISW=3
      GO TO 81
   80 ISW=1
   81 XSW=XSW1
      YSW=YSW1
```

C.3

```
      RSW=RSW1
      GO TO 95
   85 ISW=4
      XSW=XSW3
      YSW=YSW3
      RSW=RSW3
      GO TO 95
   90 ISW=2
      XSW=XSW2
      YSW=YSW2
      RSW=RSW2
   95 CALL ANGLE(XSW,YSW,VBRNG)
      TSWIT=T+RSW/V*3600.0
      IF(RSW.EQ.0.00) GO TO 100
      VX=V*XSW/RSW
      VY=V*YSW/RSW
      RETURN
  100 VX=V
      VY=0.0
      RETURN
      END


      SUBROUTINE NOAIR(MEAS,T,X0,Y0,VX,VY,RCONE,X2TO1,Y2TO1,N,AT1,AT2,
     1MODE,DELTAT,VARVOR,VARDME,PP,H,HT,RI,HTRI,TO,X,Y,LONG1,LAT1,LONG,
     2LAT,DTR,RE,V,DIST,*)
C    CALCULATES THE STATE ERROR COVARIANCE MATRIX ASSOCIATED WITH THE
C    ESTIMATOR USED TO OBTAIN MAXIMUM-LIKELIHOOD POSITION FIXES FROM
C    VOR/DME MEASUREMENTS
      REAL*4 LONG1,LAT1,LONG,LAT
      DIMENSION MEAS(5),H(N,2),HT(2,N),RI(N,N),HTRI(2,N),P(2,2),PP(8,8)
    1 FORMAT(' NO MEASUREMENT TAKEN FROM THE STATION BEING OVERFLOWN')
    2 FORMAT(1H0,F7.2,F10.2,F13.5,3F10.2/1H ,17X,F13.5,F10.2)
      IN=2
      DO 10 I=1,N
      DO 10 J=1,N
   10 RI(I,J)=0.0
      T=T+DELTAT
      X=X0+VX*(T-T0)/3600.0
      Y=Y0+VY*(T-T0)/3600.0
      DIST=DIST+V*DELTAT/3600.0
      LONG=-(X/RE/COS(LAT1*DTR)/DTR)+LONG1
      LAT=Y/RE/DTR+LAT1
      R2=X**2+Y**2
      R1=SQRT(R2)
      IF(R1.GT.RCONE) GO TO 20
      IF(MEAS(3).EQ.1.AND.MEAS(4).EQ.1) GO TO 15
      TIME=T/60.0
      CALL ANGLE(X,Y,THETA)
      THETAD=THETA/DTR
      WRITE(6,2) TIME,DIST,LAT,X,R1,THETAD,LONG,Y
      WRITE(6,1)
      GO TO 100
   15 CALL ANGLE(X,Y,THETA)
      CALL ANGLE(X+X2TO1,Y+Y2TO1,THETA2)
      RR2=(X+X2TO1)**2+(Y+Y2TO1)**2
```

```
      IN=1
      CALL RMS2(IN,RR2,A,B,C,THETA2,AT2,VARVOR,VARDME)
      PP(1,1)=(A/6076.1)**2
      PP(2,2)=(B/6076.1)**2
      CALL RMS1(PP,DTR,X,Y,THETA,T,R1,MODE,LONG,LAT,DIST)
      WRITE(6,1)
      GO TO 100
   20 I=1
      NH=0
   30 NH=NH+1
      IF(MEAS(NH).EQ.0) GO TO 90
      GO TO (40,50,60,70),NH
   40 H(I,1)=Y/R2
      H(I,2)=-X/R2
      GO TO 80
   50 D=SQRT(R2+AT1**2)
      H(I,1)=X/D
      H(I,2)=Y/D
      GO TO 80
   60 D=(X+X2TO1)**2+(Y+Y2TO1)**2
      H(I,1)=(Y+Y2TO1)/D
      H(I,2)=-(X+X2TO1)/D
      GO TO 80
   70 D=SQRT((X+X2TO1)**2+(Y+Y2TO1)**2+AT2**2)
      H(I,1)=(X+X2TO1)/D
      H(I,2)=(Y+Y2TO1)/D
   80 IF(NH.EQ.1) GO TO 85
      IF(NH.EQ.3) GO TO 85
      RI(I,I)=1.0/VARDME
      I=I+1
      GO TO 90
   85 RI(I,I)=1.0/VARVOR
      I=I+1
   90 IF(NH.NE.4) GO TO 30
      CALL GMTRA(H,HT,N,2)
      CALL GMPRD(HT,RI,HTRI,2,N,N)
      CALL GMPRD(HTRI,H,P,2,N,2)
      DET=P(1,1)*P(2,2)-P(1,2)*P(1,2)
      PP(1,1)=P(2,2)/DET
      PP(2,2)=P(1,1)/DET
      CALL ANGLE(X,Y,THETA)
      CALL RMS1(PP,DTR,X,Y,THETA,T,R1,MODE,LONG,LAT,DIST)
      CALL RMS2(IN,R2,A,B,C,THETA,AT1,VARVOR,VARDME)
  100 RETURN 1
      END



      SUBROUTINE INS(HI,HIT,RI,HITRI,N,LATO,LONGO,LAT,LONG,MEAS,X,Y,
     1IRESET)
C    PERFORMS INS FILTER COMPUTATIONS
      REAL*4 Q(16),LATO,LONGO,PHI(16,16),IDENT(16,16),P(16,16),KR(16,1),
     1RMS(12),LONG,LAT,PHIT(16,16),PPHIT(16,16),H(1,16),K(16,1),KSTORE(1
     27,1100),HT(16,1),PHT(16,1),KH(16,16),KHP(16,16),KHT(16,16),KT(1,16
     3),PER(16,16),M(2,2),   HI(N,2),HIT(2,N),RI(N,N),HITRI(2,N),PI(2,2)
     4,KRKT(16,16),AA(16,16),CC(16,16),DD(16,16)
      DIMENSION MEAS(6)
```

```
    1 FORMAT(1HO,'TIME-MIN',2X,'DIST-NM',4X,'LAT-DEG',4X,'X-NM',2X,
     1'THETA-DEG  ','RMSX-FT',2X,'RMSVX-KT',2X,'RMSPSIX-DEG',' RMSPHIX-D
     2EG RMSGX-DEG/HR  RMSAX-G ',     'RMSBV-DEG',1X,'RMSBD-FT'/1H ,
     320X,'LONG-DEG',4X,'Y-NM',13X,'RMSY-FT',2X,'RMSVY-KT',2X,'RMSPSIY-D
     4EG',1X,'RMSPHIY-DEG',1X,'RMSGY-DEG/HR',2X,'RMSAY-G'/1H ,32X,'R-NM'
     5,13X,'RMSR-FT',3X,'RMSV-KT',2X,'RMSPSIZ-DEG',1X,'RMSPHIZ-DEG',1X,
     6'RMSGZ-DEG/HR')
    2 FORMAT('0DATA:'/'0RMSGYO=',F7.4,' DEG/HR'/' RMSACC=',F7.4,' G'
     1  /1H ,'RMSBV =',F7.2,' DEG'/1H ,'RMSBD =',F7.2,' NM'/1H ,'RMSVOR=
     2',F7.2,' DEG'/1H ,'RMSDME=',F7.2,' NM'/1H ,'CORGYC=',F7.2,' HR'/1H
     3 ,'CORACC=',F7.2,' HR'/1H ,'CORVOR=',F7.2,' NM'/1H ,'CORDME=',F7.2
     4,' NM'/1H ,'DISTO =',F7.2,' NM'  /' TO    =',F7.2,' MIN'/' DELTAT=
     5',F7.2,' SEC'/' V     =',F7.2,' KT'/1H ,'ALT   =',F7.0,' FT'/1H ,
     6'LATO  =',F10.5,' DEG'/1H ,'LONGO =',F10.5,' DEG'/1H ,'NPRINT=',I3
     7/1H ,'NST1  =',I3/1H ,'NST2  =',I3/1H ,'NST3  =',I3/1H ,'NP    =',
     8I3/1H ,'ISEN  =',I3/1H ,'NSEN  =',I3/1H ,'IGAIN =',I3/1H ,'IRESET=
     9',I3/' NEST  =',I3/' IDISP =',I3/' MEAS  =',I3,5I5/////)
    3 FORMAT(I6,12F6.2)
    7 FORMAT(1H1,62X,'GAINS:'//1HO,6X,'TIME',8X,'KX',12X,'KVX',11X,
     1'KPSIX',10X,'KPSIZ',12X,'KGY',12X,'KAX',11X,'KBV1',11X,'KBD1'/
     21H ,18X,'KY',12X,'KVY',11X,'KPSIY',11X,'KGX',13X,'KGZ',12X,'KAY',
     311X,'KBV2',11X,'KBD2')
    8 FORMAT(1H+,10X,8E15.7/(1H ,10X,8E15.7))
    9 FORMAT(1HO,F10.2)
   10 FORMAT(' NO POSITION RESET PERFORMED')
      RETURN
C
      ENTRY INS1(RMSGYO,RMSACC,RMSBV,RMSBD,RMSVOR,RMSDME,CORGYO,CORACC,
     1CORVOR,CORDME,DISTO,TO,DELTAT,V,ALT,LATO,LONGO,NPRINT,NST1,NST2,
     2NST3,NP,ISEN,NSEN,IGAIN,MEAS,IRESET,NEST,IDISP,*)
      WRITE(6,2) RMSGYO,RMSACC,RMSBV,RMSBD,RMSVOR,RMSDME,CORGYO,CORACC,
     1CORVOR,CORDME,DISTO,TO,DELTAT,V,ALT,LATO,LONGO,NPRINT,NST1,NST2,
     2NST3,NP,ISEN,NSEN,IGAIN,IRESET,NEST,IDISP,(MEAS(J),J=1,6)
      RETURN 1
C
      ENTRY INS2(DTR,DELTAT,NP,RE,ALT,RMSBV,RMSBD,*)
      IBIASG=0
      IBIASA=0
      RMSGYO=RMSGYO*DTR/3600.0
      RMSACC=RMSACC/6076.10*32.2
      IF(CORGYO.GE.1000.0) IBIASG=1
      IF(CORACC.GE.1000.0) IBIASA=1
      CORGYO=CORGYO*3600.0
      CORACC=CORACC*3600.0
      DO 20 I=1,16
      DO 20 J=1,16
      PHI(I,J)=0.0
   20 IDENT(I,J)=0.0
      DO 25 I=1,16
      IDENT(I,I)=1.0
      PHI(I,I)=1.0
   25 Q(I)=0.0
      IF(IBIASG.EQ.1) GO TO 26
      Q(8)=2.0*(RMSGYO**2)/CORGYO*DELTAT/NP
      Q(9)=Q(8)
      Q(10)=Q(8)
   26 IF(IBIASA.EQ.1) RETURN 1
```

```
      Q(11)=2.0*(RMSACC**2)/CORACC*DELTAT/NP
      Q(12)=Q(11)
      RETURN 1
C
      ENTRY INS3(ITER,A,B,C,*)
      IF(ITER.EQ.3) GO TO 30
      READ(5,3) INIT,(RMS(J),J=1,12)
   30 IF(INIT.EQ.1) GO TO 32
      RMS(1)=A/6076.10
      RMS(2)=B/6076.10
      P(1,2)=C
      P(2,1)=C
   32 P(1,1)=RMS(1)**2
      P(2,2)=RMS(2)**2
      P(3,3)=(RMS(3)/3600.0)**2
      P(4,4)=(RMS(4)/3600.0)**2
      P(5,5)=(RMS(5)*DTR)**2
      P(6,6)=(RMS(6)*DTR)**2
      P(7,7)=(RMS(7)*DTR)**2
      P(8,8)=(RMS(8)*DTR/3600.0)**2
      P(9,9)=(RMS(9)*DTR/3600.0)**2
      P(10,10)=(RMS(10)*DTR/3600.0)**2
      P(11,11)=(RMS(11)*32.2/6076.10)**2
      P(12,12)=(RMS(12)*32.2/6076.10)**2
      P(13,13)=RMSBV**2
      P(14,14)=RMSBD**2
      P(15,15)=P(13,13)
      P(16,16)=P(14,14)
      IF(NEST.EQ.16) GO TO 39
      NEST1=NEST+1
      DO 33 I=NEST1,16
      PER(I,I)=P(I,I)
   33 P(I,I)=0.0
   39 RETURN 1
C
      ENTRY INS4(S)
      WRITE(6,1)
      RETURN
C
      ENTRY INS5(X,Y,THETA,T,R1,MODE,LONG,LAT,DIST)
      CALL RMS3(P,DTR,T,THETA,DIST,LAT,LONG,X,Y,R1,MODE,RE,ALT)
      IF(NEST.EQ.16.AND.IDISP.EQ.0) GO TO 55
      IF(IDISP.EQ.1) GO TO 54
      CALL GMADD(PER,P,PHIT,16,16)
   54 CALL RMS3(PHIT,DTR,T,THETA,DIST,LAT,LONG,X,Y,R1,MODE,RE,ALT)
   55 RETURN
C
      ENTRY INS6(LAT,LONG,VXX,VYY)
      VX=VXX/3600.0
      VY=VYY/3600.0
      VXDOT=0.0
      VYDOT=0.0
      VZDOT=0.0
      VZ=0.0
      GX=0.0
      GY=0.0
      GZ=-32.2/6076.10*(RE**2)/(RE+ALT/6076.1)**2
```

```
      OMEGA=15.04107*DTR/3600.0
      OMEGAX=0.0
      OMEGAY=OMEGA*COS(LAT*DTR)
      OMEGAZ=OMEGA*SIN(LAT*DTR)
      RHOX=-VY/RE
      RHOY=VX/RE
      RHOZ=VX/RE*TAN(LAT*DTR)
      OMEGAS=32.2/6076.10/RE
      AX=VXDOT+(2.0*OMEGAY+RHOY)*VZ-(2.0*OMEGAZ+RHOZ)*VY-GX
      AY=VYDOT+(2.0*OMEGAZ+RHOZ)*VX-(2.0*OMEGAX+RHOX)*VZ-GY
      AZ=VZDOT+(2.0*OMEGAX+RHOX)*VY-(2.0*OMEGAY+RHOY)*VX-GZ
      PHI(1,2)=RHOZ*DELTAT/NP
      PHI(1,3)=DELTAT/NP
      PHI(2,1)=-RHOZ*DELTAT/NP
      PHI(2,4)=DELTAT/NP
      PHI(3,1)=-OMEGAS*DELTAT/NP
      PHI(3,4)= (2.0*OMEGAZ+RHOZ)*DELTAT/NP
      PHI(3,6)=-AZ*DELTAT/NP
      PHI(3,7)=AY*DELTAT/NP
      PHI(3,11)=DELTAT/NP
      PHI(4,2)=-OMEGAS*DELTAT/NP
      PHI(4,3)=-(2.0*OMEGAZ+RHOZ)*DELTAT/NP
      PHI(4,5)=AZ*DELTAT/NP
      PHI(4,7)=-AX*DELTAT/NP
      PHI(4,12)=DELTAT/NP
      PHI(5,6)=(OMEGAZ+RHOZ)*DELTAT/NP
      PHI(5,7)=-(OMEGAY+RHOY)*DELTAT/NP
      PHI(5,8)=DELTAT/NP
      PHI(6,5)=-(OMEGAZ+RHOZ)*DELTAT/NP
      PHI(6,7)=(OMEGAX+RHOX)*DELTAT/NP
      PHI(6,9)=DELTAT/NP
      PHI(7,5)=(OMEGAY+RHOY)*DELTAT/NP
      PHI(7,6)=-(OMEGAX+RHOX)*DELTAT/NP
      PHI(7,10)=DELTAT/NP
      IF(IBIASG.EQ.1) GO TO 62
      PHI(8,8)=1.0-(1.0/CORGYO)*DELTAT/NP
      PHI(9,9)=PHI(8,8)
      PHI(10,10)=PHI(8,8)
   62 IF(IBIASA.EQ.1) GO TO 64
      PHI(11,11)=1.0-(1.0/CORACC)*DELTAT/NP
      PHI(12,12)=PHI(11,11)
   64 CALL GMTRA(PHI,PHIT,16,16)
      CALL GMPRD(P,PHIT,PPHIT,16,16,16)
      CALL GMPRD(PHI,PPHIT,P,16,16,16)
      DO 66 I=8,12
   66 P(I,I)=P(I,I)+Q(I)
      IF(IDISP.EQ.0) GO TO 69
      CALL GMPRD(PHI,AA,PHIT,16,16,16)
      DO 68 I=1,16
      DO 68 J=1,16
   68 AA(I,J)=PHIT(I,J)
      CALL GMTRA(AA,PHIT,16,16)
      CALL GMADD(AA,PHIT,PHIT,16,16)
      CALL GMSUB(P,PHIT,PHIT,16,16)
      CALL GMADD(PHIT,CC,PHIT,16,16)
   69 IF(NEST.EQ.16) RETURN
      CALL GMPRD(PER,PHIT,PPHIT,16,16,16)
```

```
      CALL GMPRD(PHI,PPHIT,PER,16,16,16)
      RETURN
C
      ENTRY INS7(NH,X,Y,AT1,AT2,R2,X2TO1,Y2TO1,KS,ITER,RVOR,RDME,*)
      DO 70 I=1,16
      DO 70 J=1,16
      IF(ABS(P(I,J)).LE.1.0E-25) P(I,J)=0.0
   70 CONTINUE
   71 NH=NH+1
      IF(MEAS(NH).EQ.0) GO TO 78
      CALL FINDH(NH,H,X,Y,AT1,AT2,R2,X2TO1,Y2TO1,16)
      IF(ITER.NE.2) GO TO 75
      DO 73 I=1,16
   73 K(I,1)=KSTORE(I,KS)
      KS=KS+1
   75 CALL MEASUP(NH,H,P,RVOR,RDME,IDENT,ITER,K,16,HT,PHT,KH,KHP,KHT,KT,
     1KRKT,KR)
      IF(NEST.EQ.16) GO TO 76
      CALL GMTRA(KH,KHT,16,16)
      CALL GMPRD(KH,PER,KHP,16,16,16)
      CALL GMPRD(KHP,KHT,PER,16,16,16)
   76 IF(ISEN.EQ.0.AND.IGAIN.EQ.0) GO TO 78
      IF(ITER.EQ.2) GO TO 78
      IF(ITER.EQ.3.AND.IGAIN.EQ.0) GO TO 78
      DO 77 I=1,16
   77 KSTORE(I,KS)=K(I,1)
      IF(IGAIN.EQ.1) KSTORE(17,KS)=T
      KS=KS+1
   78 IF(NH.NE.4) GO TO 71
      RETURN 1
C
      ENTRY INS8(J1,J2,*)
      IF(J1.EQ.0) GO TO 83
      DO 80 J=13,14
      DO 80 I=1,16
      P(I,J)=0.0
      P(J,I)=0.0
      PER(I,J)=0.0
   80 PER(J,I)=0.0
      P(13,13)=RMSBV**2
      P(14,14)=RMSBD**2
      J1=0
      IF(NEST.EQ.16) GO TO 83
      IF(NEST1-14)81,82,83
   81 PER(13,13)=P(13,13)
      P(13,13)=0.0
   82 PER(14,14)=P(14,14)
      P(14,14)=0.0
   83 IF(J2.EQ.0) RETURN 1
      DO 84 J=15,16
      DO 84 I=1,16
      P(I,J)=0.0
      P(J,I)=0.0
      PER(I,J)=0.0
   84 PER(J,I)=0.0
      P(15,15)=RMSBV**2
      P(16,16)=RMSBD**2
```

```
      J2=0
   85 IF(NEST.EQ.16) RETURN 1
      IF(NEST.EQ.15) GO TO 86
      PER(15,15)=P(15,15)
      P(15,15)=0.0
   86 PER(16,16)=P(16,16)
      P(16,16)=0.0
      RETURN 1
C
      ENTRY INS9(KS,*)
      KSTORE(17,KS)=-1.0
      WRITE(6,7)
      IPRINT=0
      KP=1
   90 IPRINT=IPRINT+1
      T=KSTORE(17,KP)
      TM=T/60.0
      NN=1
   94 IF(KSTORE(17,KP).NE.KSTORE(17,KP+NN)) GO TO 95
      NN=NN+1
      GO TO 94
   95 IF(IPRINT.NE.NPRINT) GO TO 98
      WRITE(6,9)TM
      WRITE(6,8)((KSTORE(I,KP-1+J),I=1,15,2),(KSTORE(L,KP-1+J),L=2,16,2)
     1,J=1,NN)
      IPRINT=0
   98 KP=KP+NN
      IF(KP.GE.KS) GO TO 99
      GO TO 90
   99 RETURN 1
C
      ENTRY INS10(*)
      DO 100 I=1,16
      DO 100 J=1,16
      CC(I,J)=0.0
      DD(I,J)=0.0
      PER(I,J)=0.0
  100 P(I,J)=0.0
      RETURN 1
C
      ENTRY INS11(N,IRESET,X,Y,R2,X2TO1,Y2TO1,AT1,AT2,HI,HIT,RI,HITRI,
     1VARVOR,VARDME,*)
      DO 110 I=1,16
      DO 110 J=1,16
      IF(ABS(P(I,J)).LE.1.0E-25) P(I,J)=0.0
  110 CONTINUE
      DO 115 I=1,N
      DO 115 J=1,N
  115 RI(I,J)=0.0
      I=1
      NH=0
  130 NH=NH+1
      IF(MEAS(NH).EQ.0) GO TO 190
      GO TO (140,150,160,170),NH
  140 HI(I,1)=Y/R2
      HI(I,2)=-X/R2
      GO TO 180
```

```
150 D=SQRT(R2+AT1**2)
    HI(I,1)=X/D
    HI(I,2)=Y/D
    GO TO 180
160 D=(X+X2TO1)**2+(Y+Y2TO1)**2
    HI(I,1)=(Y+Y2TO1)/D
    HI(I,2)=-(X+X2TO1)/D
    GO TO 180
170 D=SQRT((X+X2TO1)**2+(Y+Y2TO1)**2+AT2**2)
    HI(I,1)=(X+X2TO1)/D
    HI(I,2)=(Y+Y2TO1)/D
180 IF(NH.EQ.1) GO TO 185
    IF(NH.EQ.3) GO TO 185
    RI(I,I)=1.0/VARDME
    L=I+1
    GO TO 190
185 RI(I,I)=1.0/VARVOR
    I=I+1
190 IF(NH.NE.4) GO TO 130
    CALL GMTRA(HI,HIT,N,2)
    CALL GMPRD(HIT,RI,HITRI,2,N,N)
    CALL GMPRD(HITRI,HI,PI,2,N,2)
    IF(IRESET.EQ.1) GO TO 192
    DET=P(1,1)*P(2,2)-P(1,2)*P(1,2)
    M(1,1)=P(2,2)/DET
    M(2,2)=P(1,1)/DET
    M(1,2)=-P(1,2)/DET
    M(2,1)=M(1,2)
    CALL GMADD(M,PI,PI,2,2,2)
192 DET=PI(1,1)*PI(2,2)-PI(1,2)*PI(1,2)
    IF((P(1,1)+P(2,2)).LE.(PI(1,1)+PI(2,2))/DET) GO TO 198
    IF(IDISP.EQ.0) GO TO 195
    CC(1,1)=P(1,1)+PI(2,2)/DET
    CC(2,2)=P(2,2)+PI(1,1)/DET
    CC(1,2)=P(1,2)-PI(1,2)/DET
    CC(2,1)=CC(1,2)
    DO 193 J=1,2
    DO 193 I=1,16
193 DD(I,J)=P(I,J)
    DO 194 I=1,16
    DO 194 J=1,16
    PHIT(I,J)=P(I,J)-DD(I,J)-DD(J,I)+CC(I,J)
194 AA(I,J)=DD(I,J)
    GO TO 199
195 DO 196 I=1,2
    DO 196 J=1,16
    P(I,J)=0.0
196 P(J,I)=0.0
    P(1,1)=PI(2,2)/DET
    P(2,2)=PI(1,1)/DET
    P(1,2)=-PI(1,2)/DET
    P(2,1)=P(1,2)
    GO TO 199
198 WRITE(6,10)
199 RETURN 1
    END
```

Appendix C

FILTER SENSITIVITY ANALYSIS

The design of a maximum-likelihood filter is dependent upon knowledge of the error model statistics. Since the error model statistics are often not known precisely, a filter is designed assuming nominal error statistics. Hence, a desirable characteristic of the filter is that its performance be insensitive to variations in the error model statistics. In particular, consideration is given here to the sensitivity of the filter to variations in the initial state error covariance matrix and the spectral densities of the measurement and process noises.

C.1 Discrete Filter

Consider the linear multistage process described by

$$\underline{x}_{i+1} = \Phi_i \underline{x}_i + \Gamma_i \underline{n}_i , \qquad i = 0,1,2, \ \ldots , \tag{C.1}$$

where

$$E\left[\underline{x}_o\right] = 0 , \qquad E\left[\underline{x}_o \underline{x}_o^T\right] = P_o , \tag{C.2}$$

$$E\left[\underline{n}_i\right] = 0 , \qquad E\left[\underline{n}_i \underline{x}_o^T\right] = 0 , \qquad E\left[\underline{n}_i \underline{n}_j^T\right] = Q_i \delta_{ij} . \tag{C.3}$$

The vector measurement at stage i, $\underline{z}_i$, is related to the state vector $\underline{x}_i$ as follows:

$$\underline{z}_i = H_i \underline{x}_i + \underline{v}_i , \qquad i = 0,1,2, \ \ldots , \tag{C.4}$$

where

$$E\left[\underline{v}_i\right] = 0 , \qquad E\left[\underline{v}_i \underline{v}_j^T\right] = R_i \delta_{ij} , \tag{C.5}$$

$$E\left[\underline{n}_i \underline{v}_j^T\right] = 0 , \qquad E\left[\underline{x}_o \underline{v}_i^T\right] = 0 . \tag{C.6}$$

The discrete filter associated with the system described by Eqs. (C.1) through (C.6) which yields the maximum-likelihood estimate, $\hat{\underline{x}}$, of the state vector $\underline{x}$ is given by [40]:

Time update:

$$\hat{\underline{x}}_{i+1} = \Phi_i \hat{\underline{x}}_{i+} \quad , \tag{C.7}$$

$$P_{i+1} = \Phi_i P_{i+} \Phi_i^T + \Gamma_i Q_i \Gamma_i^T \quad . \tag{C.8}$$

Measurement update:

$$\hat{\underline{x}}_{i+} = \hat{\underline{x}}_i + K_i(\underline{z}_i - H_i \hat{\underline{x}}_i) \quad , \qquad \hat{\underline{x}}_o = 0 \quad , \tag{C.9}$$

$$P_{i+} = (I - K_i H_i) P_i (I - K_i H_i)^T + K_i R_i K_i^T \quad , \qquad P_o \text{ given,} \tag{C.10}$$

$$K_i = P_i H_i^T \left(H_i P_i H_i^T + R_i \right)^{-1} \quad , \tag{C.11}$$

where $\hat{\underline{x}}_i$ and P_i, and $\hat{\underline{x}}_{i+}$ and P_{i+} denote the state estimate and covariance matrix before and after taking the measurement at stage i, respectively.

Now, suppose that P_o^s and P_o^a, Q_i^s and Q_i^a, and R_i^s and R_i^a are the estimated and actual values of P_o, Q_i, and R_i, respectively. If only P_o^s, Q_i^s, and R_i^s are available and are used to design a filter, then from Eqs. (C.7) through (C.11), the filter equations are seen to be:

Time update:

$$\hat{\underline{x}}^s_{i+1} = \Phi_i \hat{\underline{x}}^s_{i+} \quad , \tag{C.12}$$

$$P^s_{i+1} = \Phi_i P^s_{i+} \Phi_i^T + \Gamma_i Q_i^s \Gamma_i^T \quad . \tag{C.13}$$

Measurement update:

$$\hat{\underline{x}}^s_{i+} = \hat{\underline{x}}^s_i + K^s_i\left(z_i - H_i\hat{\underline{x}}^s_i\right), \qquad \hat{\underline{x}}^s_o = 0 , \tag{C.14}$$

$$P^s_{i+} = \left(I - K^s_i H_i\right) P^s_i \left(I - K^s_i H_i\right)^T + K^s_i R^s_i \left(K^s_i\right)^T , \qquad P^s_o \text{ given}, \tag{C.15}$$

$$K^s_i = P^s_i H_i^T \left(H_i P^s_i H_i^T + R^s_i\right)^{-1} . \tag{C.16}$$

The problem is to determine how the suboptimal filter given by Eqs. (C.12) through (C.16) performs with $P_o = P^a_o$, $Q_i = Q^a_i$, and $R_i = R^a_i$, that is, to find the actual error covariance matrix associated with the state estimate, $\hat{\underline{x}}^s_i$ [42,43,44,45]. From Eqs. (C.1), (C.4), (C.12), and (C.14), it follows that

$$\hat{\underline{x}}^s_{i+1} - \underline{x}_{i+1} = \Phi_i\left(\hat{\underline{x}}^s_{i+} - \underline{x}_i\right) - \Gamma_i \underline{n}_i , \tag{C.17}$$

$$\hat{\underline{x}}^s_{i+} - \underline{x}_i = \left(I - K^s_i H_i\right)\left(\hat{\underline{x}}^s_i - \underline{x}_i\right) + K^s_i \underline{v}_i . \tag{C.18}$$

From Eqs. (C.17) and (C.18), it follows that

$$\bar{P}_{i+1} \triangleq E\left[\left(\hat{\underline{x}}^s_{i+1} - \underline{x}_{i+1}\right)\left(\hat{\underline{x}}^s_{i+1} - \underline{x}_{i+1}\right)^T\right] = \Phi_i \bar{P}_{i+} \Phi_i^T + \Gamma_i Q^a_i \Gamma_i^T , \tag{C.19}$$

$$\bar{P}_{i+} \triangleq E\left[\left(\hat{\underline{x}}^s_{i+} - \underline{x}_i\right)\left(\hat{\underline{x}}^s_{i+} - \underline{x}_i\right)^T\right] = \left(I - K^s_i H_i\right)\bar{P}_i \left(I - K^s_i H_i\right)^T + K^s_i R^a_i \left(K^s_i\right)^T . \tag{C.20}$$

Equations (C.19) and (C.20) describe the propagation of the error covariance matrix associated with the state estimates obtained by using the suboptimal filter which was designed using erroneous values of P_o, Q, and R. The sensitivity analysis for the case where uncertainty exists

in the state and measurement equations, that is, uncertainty in Φ_i, Γ_i, and H_i is treated in [46].

C.2 Continuous Filter

Consider the linear continuous process described by

$$\dot{\underline{x}}(t) = F(t)\underline{x}(t) + \underline{f}(t) + \underline{n}(t) , \qquad t \geq t_o , \tag{C.21}$$

where $\underline{f}(t)$ is a known vector forcing function and

$$E\left[\underline{x}(t_o)\right] = 0 , \qquad E\left[\underline{x}(t_o)\underline{x}^T(t_o)\right] = P_o , \tag{C.22}$$

$$E\left[\underline{n}(t)\underline{x}^T(t_o)\right] = 0 , \qquad E\left[\underline{n}(t)\right] = 0 , \qquad E\left[\underline{n}(t)\underline{n}^T(t+\tau)\right] = Q(t)\delta(\tau) . \tag{C.23}$$

Furthermore, the observation is described by

$$\underline{z}(t) = H(t)\underline{x}(t) + \underline{v}(t) , \tag{C.24}$$

where

$$E\left[\underline{v}(t)\right] = 0 , \qquad E\left[\underline{v}(t)\underline{v}^T(t+\tau)\right] = R(t)\delta(\tau) , \tag{C.25}$$

$$E\left[\underline{n}(t)\underline{v}^T(\tau)\right] = 0 , \qquad E\left[\underline{x}(t_o)\underline{v}^T(t)\right] = 0 . \tag{C.26}$$

The continuous filter associated with the system described by Eqs. (C.21) through (C.26) which yields the maximum-likelihood estimate, $\hat{\underline{x}}$, of the state vector $\underline{x}$ is given by [41]

$$\dot{\hat{\underline{x}}} = F\hat{\underline{x}} + \underline{f} + K(\underline{z} - H\hat{\underline{x}}) , \qquad \hat{\underline{x}}(t_o) = 0 , \tag{C.27}$$

$$\dot{P} = FP + PF^T + Q - KRK^T \quad , \qquad P(t_o) = P_o \quad , \tag{C.28}$$

with

$$K = PH^T R^{-1} \quad , \tag{C.29}$$

where P is the state error covariance matrix.

From Eqs. (C.27) through (C.29), it is seen that the filter which is designed using estimates of P_o, Q, and R, namely, P_o^s, Q^s, and R^s, respectively, is given by

$$\dot{\hat{\underline{x}}}^s = F\hat{\underline{x}}^s + \underline{f} + K^s(\underline{z} - H\hat{\underline{x}}^s) \quad , \qquad \hat{\underline{x}}^s(t_o) = 0 \quad , \tag{C.30}$$

$$\dot{P}^s = FP^s + P^sF^T + Q^s - K^sR^s\left(K^s\right)^T \quad , \qquad P^s(t_o) = P_o^s \quad , \tag{C.31}$$

with

$$K^s = P^sH^T\left(R^s\right)^{-1} \quad . \tag{C.32}$$

If the actual values of P_o, Q, and R are P_o^a, Q^a, and R^a, respectively, the actual error covariance matrix, $\bar{P}$, associated with the suboptimal estimates $\hat{\underline{x}}^s$ must be determined [47].

Now, let

$$\bar{P} \triangleq E\left[\left(\hat{\underline{x}}^s - \underline{x}\right)\left(\hat{\underline{x}}^s - \underline{x}\right)^T\right] \quad . \tag{C.33}$$

Taking the time derivative of Eq. (3.33) and interchanging the order of the differentiation and expectation operators yields:

$$\dot{\bar{P}} = E\left[\left(\dot{\hat{\underline{x}}}^s - \dot{\underline{x}}\right)\left(\hat{\underline{x}}^s - \underline{x}\right)^T\right] + E\left[\left(\hat{\underline{x}}^s - \underline{x}\right)\left(\dot{\hat{\underline{x}}}^s - \dot{\underline{x}}\right)^T\right] \quad . \tag{C.34}$$

From Eqs. (C.21), (C.24), and (C.30),

$$\dot{\underline{\hat{x}}}^s - \dot{\underline{x}} = (F - K^s H)(\underline{\hat{x}}^s - \underline{x}) + K^s \underline{v} - \underline{n} \quad . \tag{C.35}$$

Solutions for Eqs. (C.21) and (C.30) are given by (see e.g., [32], pp. 449-450)

$$\underline{x}(t) = \Phi(t, t_o)\underline{x}(t_o) + \int_{t_o}^{t} \Phi(t, \tau)\left[\underline{n}(\tau) + \underline{f}(\tau)\right] d\tau \quad , \tag{C.36}$$

$$\underline{\hat{x}}^s(t) = \Phi^s(t, t_o)\underline{\hat{x}}^s(t_o) + \int_{t_o}^{t} \Phi^s(t, \tau)\left[K^s(\tau)\underline{z}(\tau) + \underline{f}(\tau)\right] d\tau \quad , \tag{C.37}$$

where

$$\frac{d}{dt}\left[\Phi(t, t_o)\right] = F(t)\Phi(t, t_o) \quad , \qquad \Phi(t_o, t_o) = I \quad , \tag{C.38}$$

$$\frac{d}{dt}\left[\Phi^s(t, t_o)\right] = \left[F(t) - K^s(t)H(t)\right]\Phi^s(t, t_o) \quad , \quad \Phi^s(t_o, t_o) = I \quad . \tag{C.39}$$

Substituting Eqs. (C.35) through (C.37) into (C.34) and using Eqs. (C.22) through (C.26) and Eq. (C.33) yields:

$$\dot{\bar{P}} = (F - K^s H)\bar{P} + \bar{P}\left(F - K^s H\right)^T + Q^a + K^s R^a \left(K^s\right)^T \quad , \quad \bar{P}(t_o) = P_o^a \quad . \tag{C.40}$$

The sensitivity analysis for the case where uncertainty exists in the state and observation equations is treated in [48].

C.3 Continuous-Time Discrete-Data Filter

Consider the system described by Eqs. (C.21) through (C.26) where the continuous observation process is approximated by a discrete process. Denoting the time interval between measurement updates by ΔT, the filter which gives the best estimate of $\underline{x}$, $\underline{\hat{x}}$, is:

Between measurements:

$$\dot{\hat{\underline{x}}} = F\hat{\underline{x}} + \underline{f} \quad , \qquad \hat{\underline{x}}(t_o) = 0 \quad , \tag{C.41}$$

$$\dot{P} = FP + PF^T + Q \quad , \qquad P(t_o) = P_o \quad . \tag{C.42}$$

At a measurement:

$$\hat{\underline{x}}_+ = \hat{\underline{x}}_- + K\left[\underline{z} - H\hat{\underline{x}}_-\right] \quad , \tag{C.43}$$

$$P_+ = (I - KH)P_-(I - KH)^T + K(R/\Delta T)\, K^T \quad , \tag{C.44}$$

$$K = P_-H^T\left(HP_-H^T + R/\Delta T\right)^{-1} \quad , \tag{C.45}$$

where P is the state error covariance matrix and the $-$ and $+$ designate quantities before and after a measurement, respectively.

If the filter is designed using the estimates P_o^s, Q^s, and R^s, instead of the actual values P_o^a, Q^a, and R^a of P_o, Q, and R, respectively, then from the results of Sections C.1 and C.2, the performance of the suboptimal filter is given by:

Between measurements:

$$\dot{\hat{\underline{x}}}^s = F\hat{\underline{x}}^s + \underline{f} \quad , \qquad \hat{\underline{x}}^s = 0 \quad , \tag{C.46}$$

$$\dot{\overline{P}} = F\overline{P} + \overline{P}F^T + Q^a \quad , \qquad \overline{P}(t_o) = P_o^a \quad . \tag{C.47}$$

At a measurement:

$$\hat{\underline{x}}_+^s = \hat{\underline{x}}_-^s + K^s(\underline{z} - H\hat{\underline{x}}_-^s) \quad , \tag{C.48}$$

$$\bar{P}_{+} = (I - K^{s}H)\bar{P}_{-}\left(I - K^{s}H\right)^{T} + K^{s}(R^{a}/\Delta T)\left(K^{s}\right)^{T} \quad , \tag{C.49}$$

$$K^{s} = P_{-}^{s}H^{T}\left(HP_{-}^{s}H^{T} + R^{s}/\Delta T\right)^{-1} \quad , \tag{C.50}$$

where $\hat{\underline{x}}^{s}$ and P^{s} are the suboptimal estimate of the state vector and erroneous covariance matrix, respectively, associated with the suboptimal filter, and $\bar{P}$ is the actual state error covariance matrix.

Appendix D

EFFECT OF NEGLECTING STATES

When implementing a filter in real-time on an airborne computer, computer storage and computation time are limited. Hence, it is often desirable, if not necessary, to reduce the number of states in the filter by neglecting states which are not of primary interest (e.g., correlated noise). The problem considered here is to determine the effect of the neglected states upon the performance of the resulting suboptimal filter.

D.1 Discrete Filter

Consider the linear multistage system described by Eqs. (C.1) through (C.6) and the associated filter, Eqs. (C.7) through (C.11). Now, let the p-dimensional state vector $\underline{x}_i$ be partitioned as follows:

$$\underline{x}_i = \begin{bmatrix} \left(\underline{x}_e\right)_i \\ \hline \left(\underline{x}_n\right)_i \end{bmatrix} \begin{matrix} \} \, m \\ \} \, p-m \end{matrix} , \tag{D.1}$$

where $(\underline{x}_e)_i$ contains the m states to be estimated and $(\underline{x}_n)_i$ the (p-m) states to be neglected. This partition of the state vector induces the following partitions:

$$\Phi_i = \begin{bmatrix} \underbrace{\left(\Phi_{ee}\right)_i}_{m} & \underbrace{\left(\Phi_{en}\right)_i}_{p-m} \\ \hline \left(\Phi_{ne}\right)_i & \left(\Phi_{nn}\right)_i \end{bmatrix} \begin{matrix} \} \, m \\ \} \, p-m \end{matrix} , \qquad \underline{n}_i = \begin{bmatrix} \left(\underline{n}_e\right)_i \\ \hline \left(\underline{n}_n\right)_i \end{bmatrix} \begin{matrix} \} \, m \\ \} \, p-m \end{matrix} , \tag{D.2}$$

$$Q_i = \left[\begin{array}{c|c} \underbrace{\left(Q_{ee}\right)_i}_{m} & \underbrace{\left(Q_{en}\right)_i}_{p-m} \\ \hline \left(Q_{ne}\right)_i & \left(Q_{nn}\right)_i \end{array}\right] \begin{matrix} \}m \\ \}p-m \end{matrix} \quad , \qquad K_i = \left[\begin{array}{c} \left(K_e\right)_i \\ \hline \left(K_n\right)_i \end{array}\right] \begin{matrix} \}m \\ \}p-m \end{matrix} \quad , \tag{D.3}$$

$$P_i = \left[\begin{array}{c|c} \underbrace{\left(P_{ee}\right)_i}_{m} & \underbrace{\left(P_{en}\right)_i}_{p-m} \\ \hline \left(P_{ne}\right)_i & \left(P_{nn}\right)_i \end{array}\right] \begin{matrix} \}m \\ \}p-m \end{matrix} \quad , \qquad \hat{\underline{x}}_i = \left[\begin{array}{c} \left(\hat{\underline{x}}_e\right)_i \\ \hline \left(\hat{\underline{x}}_n\right)_i \end{array}\right] \begin{matrix} \}m \\ \}p-m \end{matrix} \quad , \tag{D.4}$$

$$H_i = \left[\underbrace{\left(H_e\right)_i}_{m} \;\middle|\; \underbrace{\left(H_n\right)_i}_{p-m}\right] \quad . \tag{D.5}$$

The following observation is made: If $(\Phi_{ne})_i = 0$,

$$Q_i = \left[\begin{array}{c|c} \left(Q_{ee}\right)_i & 0 \\ \hline 0 & 0 \end{array}\right] \quad , \qquad \text{and} \qquad P_o^s = \left[\begin{array}{c|c} \left(P_{ee}\right)_o & 0 \\ \hline 0 & 0 \end{array}\right] \quad ,$$

then the maximum-likelihood estimate, $\hat{\underline{x}}_i^s$, of the state vector $\underline{x}_i$ is given by [see Eqs. (C.7) through (C.11)*]:

Time update:

$$\left(\hat{\underline{x}}_e^s\right)_{i+1} = \left(\Phi_{ee}\right)_i \left(\hat{\underline{x}}_e^s\right)_{i+} \quad , \tag{D.6}$$

*Γ_i is taken to be the identity matrix.

$$\left(P^s_{ee}\right)_{i+1} = \left(\Phi_{ee}\right)_i \left(P^s_{ee}\right)_{i+} \left(\Phi_{ee}\right)^T_i + \left(Q_{ee}\right)_i \quad . \tag{D.7}$$

Measurement update:

$$\left(\underline{\hat{x}}^s_e\right)_{i+} = \left(\underline{\hat{x}}^s_e\right)_i + \left(K^s_e\right)_i \left[\underline{z}_i - \left(H_e\right)_i \left(\underline{\hat{x}}^s_e\right)_i\right] \quad , \qquad \left(\underline{\hat{x}}^s_e\right)_o = 0 \quad , \tag{D.8}$$

$$\left(P^s_{ee}\right)_{i+} = \left[I - \left(K^s_e\right)_i \left(H^s_e\right)_i\right] \left(P^s_{ee}\right)_i \left[I - \left(K^s_e\right)_i \left(H^s_e\right)_i\right]^T$$

$$+ \left(K^s_e\right)_i R_i \left(K^s_e\right)^T_i \quad , \qquad \left(P^s_{ee}\right)_o = \left(P_{ee}\right)_o \quad , \tag{D.9}$$

$$\left(K^s_e\right)_i = \left(P^s_{ee}\right)_i \left(H^s_e\right)^T_i \left[\left(H_e\right)_i \left(P^s_{ee}\right)_i \left(H_e\right)^T_i + R_i\right]^{-1} \quad , \tag{D.10}$$

where

$$\left(\underline{\hat{x}}_n\right)_i = \left(\underline{\hat{x}}_n\right)_{i+} = 0 \quad , \qquad \left(K^s_n\right)_i = 0 \quad , \qquad \left(P^s_{en}\right)_i = \left(P^s_{en}\right)_{i+} = 0 \quad , \tag{D.11}$$

$$\left(P^s_{ne}\right)_i = \left(P^s_{ne}\right)_{i+} = 0 \quad , \quad \text{and} \quad \left(P^s_{nn}\right)_i = \left(P^s_{nn}\right)_{i+} = 0 \quad , \quad \text{for all } i = 0, 1, 2, \ldots \quad . \tag{D.12}$$

The above filter is precisely that which would result if $(\underline{x}_n)_i$ were neglected. Thus, the following is true: If $(\Phi_{ne})_i$, $(Q_{en})_i$, $(Q_{ne})_i$, and $(Q_{nn})_i$ are equal to zero, then the effect of neglecting $(\underline{x}_n)_i$ is equivalent to the effect of assuming that P_o is

$$\left[\begin{array}{c|c} \left(P_{ee}\right)_o & 0 \\ \hline 0 & 0 \end{array}\right] ,$$

when in fact it is

$$\left[\begin{array}{c|c} \left(P_{ee}\right)_o & \left(P_{en}\right)_o \\ \hline \left(P_{ne}\right)_o & \left(P_{nn}\right)_o \end{array}\right] .$$

Therefore, in this case, the effect of neglecting $\underline{x}_n$ is equivalent to the effect of an error in P_o.

If view of the above observation, from the results of Section C.1, the actual error covariance matrix, $\bar{P}_i$, associated with the suboptimal filter resulting when $(\underline{x}_n)_i$ is neglected is given by

$$\bar{P}_{i+1} = \Phi_i \bar{P}_{i+} \Phi_i^T + Q_i \quad , \tag{D.13}$$

$$\bar{P}_{i+} = \left(I - K_i^s H_i\right)\bar{P}_i \left(I - K_i^s H_i\right)^T + K_i^s R_i \left(K_i^s\right)^T \quad , \qquad \bar{P}_o = P_o \quad , \tag{D.14}$$

with

$$K_i^s = \left[\begin{array}{c} \left(K_e^s\right)_i \\ \hline 0 \end{array}\right] \begin{array}{l} \Big\} m \\ \\ \Big\} p-m \end{array} . \tag{D.15}$$

Furthermore, defining

$$E_i \triangleq \bar{P}_i - P_i^s \quad , \tag{D.16}$$

$$E_{i+} \triangleq \bar{P}_{i+} - P_{i+}^s \quad , \tag{D.17}$$

from the above results, it is seen that

$$E_{i+1} = \Phi_i E_{i+} \Phi_i^T \quad , \tag{D.18}$$

$$E_{i+} = \left(I - K_i^s H_i\right) E_i \left(I - K_i^s H_i\right)^T \quad , \tag{D.19}$$

where

$$E_o = \left[\begin{array}{c|c} 0 & \left(P_{en}\right)_o \\ \hline \left(P_{ne}\right)_o & \left(P_{nn}\right)_o \end{array}\right] \quad . \tag{D.20}$$

Note that the conditions $(Q_{en})_i$, $(Q_{ne})_i$, and $(Q_{nn})_i$ equal zero simply mean that the states being neglected are uncorrelated biases while the condition $(\Phi_{ne})_i$ equals zero means that there is only one-way coupling between the estimated and neglected states (always true when the neglected states are biases). For more general results regarding the effect of neglecting states, see [49,50,51].

D.2 Continuous Filter

Consider the continuous system described by Eqs. (C.21) through (C.26) and the associated filter, Eqs. (C.27) through (C.29). Let the p-dimensional state vector $\underline{x}$ be partitioned as follows:

$$\underline{x} = \left[\begin{array}{c} \underline{x}_e \\ \hline \underline{x}_n \end{array}\right] \begin{array}{l} \} \, m \\ \\ \} \, p-m \end{array} \quad , \tag{D.21}$$

where $\underline{x}_e$ contains the m states to be estimated and $\underline{x}_n$ the (p-m) states to be neglected. This partition of the state vector induces the following partitions:

$$F = \begin{bmatrix} \underbrace{F_{ee}}_{m} & \underbrace{F_{en}}_{p-m} \\ F_{ne} & F_{nn} \end{bmatrix} \begin{matrix} \} m \\ \} p-m \end{matrix} , \quad \underline{f} = \begin{bmatrix} \underline{f}_e \\ \underline{f}_n \end{bmatrix} \begin{matrix} \} m \\ \} p-m \end{matrix} , \quad \underline{n} = \begin{bmatrix} \underline{n}_e \\ \underline{n}_n \end{bmatrix} \begin{matrix} \} m \\ \} p-m \end{matrix} , \tag{D.22}$$

$$H = \underset{m}{\begin{bmatrix} H_e & H_n \end{bmatrix}} \underset{p-m}{} , \quad Q = \begin{bmatrix} \underbrace{Q_{ee}}_{m} & \underbrace{Q_{en}}_{p-m} \\ Q_{ne} & Q_{nn} \end{bmatrix} \begin{matrix} \} m \\ \} p-m \end{matrix} , \tag{D.23}$$

$$\hat{\underline{x}} = \begin{bmatrix} \hat{\underline{x}}_e \\ \hat{\underline{x}}_n \end{bmatrix} \begin{matrix} \} n \\ \} p-m \end{matrix} , \quad K = \begin{bmatrix} K_e \\ K_n \end{bmatrix} \begin{matrix} \} n \\ \} p-m \end{matrix} , \quad P = \begin{bmatrix} \underbrace{P_{ee}}_{m} & \underbrace{P_{en}}_{p-m} \\ P_{ne} & P_{nn} \end{bmatrix} \begin{matrix} \} m \\ \} p-m \end{matrix} . \tag{D.24}$$

The following observation is made: If $F_{ne} = 0$, $\underline{f}_n = 0$,

$$Q = \begin{bmatrix} Q_{ee} & 0 \\ 0 & 0 \end{bmatrix} , \quad \text{and} \quad P^s(t_o) = \begin{bmatrix} \left(P_{ee}\right)_o & 0 \\ 0 & 0 \end{bmatrix} ,$$

then the maximum-likelihood estimate, $\hat{\underline{x}}^s$, of the state vector $\underline{x}$ is given by [see Eqs. (C.27) through (C.29)]:

$$\dot{\hat{\underline{x}}}^s_e = F_{ee}\hat{\underline{x}}^s_e + \underline{f}_e + K^s_e\left(\underline{z} - H_e\hat{\underline{x}}^s_e\right) , \quad \hat{\underline{x}}^s_e(t_o) = 0 , \tag{D.25}$$

$$\dot{P}^s_{ee} = F_{ee}P^s_{ee} + P^s_{ee}F^T_{ee} + Q_{ee} - K^s_{ee}R\left(K^s_{ee}\right)^T , \quad P^s_{ee}(t_o) = \left(P_{ee}\right)_o \tag{D.26}$$

$$K_e^s = P_{ee}^s (H_e)^T R^{-1} \quad , \tag{D.27}$$

where

$$\hat{\underline{x}}_n = 0 \ , \quad K_n^s = 0 \ , \quad P_{en}^s = 0 \ , \quad P_{ne}^s = 0 \ , \quad \text{and} \quad P_{nn}^s = 0 \ . \tag{D.28}$$

Since the above filter is precisely the one which would result if $\underline{x}_n$ were neglected, the following is true: If F_{ne}, $\underline{f}_n$, Q_{en}, Q_{ne}, and Q_{nn} are equal to zero, the effect of neglecting $\underline{x}_n$ is equivalent to the effect of assuming that P_o is

$$\begin{bmatrix} \left(P_{ee}\right)_o & 0 \\ 0 & 0 \end{bmatrix} ,$$

when in fact it is

$$\begin{bmatrix} \left(P_{ee}\right)_o & \left(P_{en}\right)_o \\ \left(P_{ne}\right)_o & \left(P_{nn}\right)_o \end{bmatrix} .$$

Thus, in this case, the effect of neglecting $\underline{x}_n$ is equivalent to the effect of an error in P_o.

In view of the above observation and the results of Section C.2, the actual error covariance matrix, $\bar{P}$, associated with the suboptimal filter resulting when $\underline{x}_n$ is neglected is given by

$$\dot{\bar{P}} = \left(F - K^s H\right)\bar{P} + \bar{P}\left(F - K^s H\right)^T + Q + K^s R \left(K^s\right)^T \ , \quad \bar{P}(t_o) = P_o \ , \tag{D.29}$$

where

$$K^s = \begin{bmatrix} K_e^s \\ \hline 0 \end{bmatrix} \begin{matrix} \} m \\ \} p-m \end{matrix} \quad . \tag{D.30}$$

Furthermore, defining

$$E \triangleq \bar{P} - P^s \quad , \tag{D.31}$$

from the above results,

$$\dot{E} = \left(F - K^s H\right)E + E\left(F - K^s H\right)^T \quad , \tag{D.32}$$

where

$$E(t_o) = \left[\begin{array}{c|c} 0 & \left(P_{en}\right)_o \\ \hline \left(P_{ne}\right)_o & \left(P_{nn}\right)_o \end{array}\right] \quad . \tag{D.33}$$

For more general results regarding the effect of neglecting states in continuous filters, see [51,52].

D.3 Continuous-Time, Discrete-Data Filter

Consider the system described by Eqs. (C.21) through (C.26) where the continuous measurement process is approximated by a discrete process. Letting ΔT denote the time interval between measurement updates, the maximum-likelihood filter is described by Eqs. (C.41) through (C.45). If F_{ne}, $\underline{f}_n$, Q_{en}, Q_{ne}, and Q_{nn} are zero, then from the results of Sections D.2 and D.3, it follows that the filter resulting when $\underline{x}_n$ is neglected is given by:

Between measurements:

$$\dot{\hat{\underline{x}}}_e^s = F_{ee}\hat{\underline{x}}_e^s + \underline{f}_e \quad , \qquad \hat{\underline{x}}_e(t_o) = 0 \quad , \tag{D.34}$$

$$\dot{P}_{ee}^s = F_{ee}P_{ee}^s + P_{ee}^s F_{ee}^T + Q_{ee} \quad , \qquad P_{ee}(t_o) = \left(P_{ee}\right)_o \quad . \tag{D.35}$$

At a measurement:

$$\left(\hat{\underline{x}}_e^s\right)_+ = \left(\hat{\underline{x}}_e^s\right)_- + K_e^s\left[\underline{z} - H_e\left(\hat{\underline{x}}_e^s\right)_-\right] \quad , \tag{D.36}$$

$$\left(P_{ee}^s\right)_+ = \left[I - K_e^s H_e\right]\left(P_{ee}^s\right)_-\left[I - K_e^s H_e\right]^T + K_e^s(R/\Delta T)\left(K_e^s\right)^T \quad , \tag{D.37}$$

$$K_e^s = \left(P_{ee}^s\right)_-\left(H_e\right)^T\left[H_e\left(P_{ee}^s\right)_- H_e^T + R/\Delta T\right]^{-1} \quad , \tag{D.38}$$

with

$$\hat{\underline{x}}_n = 0 \; , \quad K_n^s = 0 \; , \quad P_{en} = 0 \; , \quad P_{ne} = 0 \; , \quad \text{and} \quad P_{nn} = 0 \; . \tag{D.39}$$

The actual error covariance matrix, $\bar{P}$, associated with the state estimate, $\hat{\underline{x}}^s$, obtained from the suboptimal filter resulting when $\underline{x}_n$ is neglected is given by:

Between measurements:

$$\dot{\bar{P}} = F\bar{P} + \bar{P}F^T + Q \quad , \qquad \bar{P}(t_o) = P_o \quad . \tag{D.40}$$

At a measurement:

$$\bar{P}_+ = \left(I - K^s H\right)\bar{P}_-\left(I - K^s H\right)^T + K^s(R/\Delta T)\left(K^s\right)^T \quad , \tag{D.41}$$

where

$$K^S = \begin{bmatrix} K_e^S \\ \hline 0 \end{bmatrix} \begin{matrix} \} \, m \\ \} \, p-m \end{matrix} \quad . \tag{D.42}$$

Furthermore, if

$$E \triangleq \bar{P} - P^S \quad , \tag{D.43}$$

then E propagates as follows:

Between measurements:

$$\dot{E} = FE + EF^T \quad . \tag{D.44}$$

At a measurement:

$$E_+ = \left(I - K^S H\right) E_- \left(I - K^S H\right)^T \quad , \tag{D.45}$$

where

$$E(t_o) = \left[\begin{array}{c|c} 0 & \left(P_{en}\right)_o \\ \hline \left(P_{ne}\right)_o & \left(P_{nn}\right)_o \end{array}\right] \quad . \tag{D.46}$$

Appendix E

EFFECT OF POSITION RESETS ON INS ERRORS

The propagation of the errors in an INS is described by the following linear multistage process:

$$\underline{x}_{i+1} = \Phi_i \underline{x}_i + \Gamma_i \underline{n}_i \quad , \qquad i = 0,1,2, \ \ldots \ , \tag{E.1}$$

where

$$E\left[\underline{x}_o\right] = 0 \quad , \qquad E\left[\underline{x}_o \underline{x}_o^T\right] = P_o \quad , \tag{E.2}$$

$$E\left[\underline{n}_i\right] = 0 \quad , \qquad E\left[\underline{n}_i \underline{n}_j^T\right] = Q_i \delta_{ij} \quad , \tag{E.3}$$

and

$$E\left[\underline{x}_i \underline{n}_j^T\right] = 0 \quad \text{for} \quad i \leq j \quad . \tag{E.4}$$

Since $\underline{n}_i$ and $\underline{x}_o$ have zero means, $\underline{x}_i$ has a zero mean for all $i = 1,2,3, \ldots$. From Eqs. (E.1) through (E.4), it is seen that the covariance matrix, P_{i+1}, of the state vector at the $(i+1)^{th}$ stage, $\underline{x}_{i+1}$, is given by

$$P_{i+1} = E\left[\underline{x}_{i+1} \underline{x}_{i+1}^T\right] = \Phi_i P_i \Phi_i^T + \Gamma_i Q_i \Gamma_i^T \quad . \tag{E.5}$$

Thus, given $\underline{x}_o$ and P_o, Eqs. (E.1) and (E.5) describe the propagation of the INS errors and the covariance of these errors, respectively.

Now, consider the k^{th} stage of the process (E.1) with the associated state $\underline{x}_k$ and covariance P_k. Suppose that at this stage a position fix is determined by using VOR/DME measurements, and the INS position display is reset to correspond to the VOR/DME fix. Let the two elements of the zero mean vector $\underline{r}_k^1$ be the easterly and northerly components

of the error in the VOR/DME position fix. Then, the INS error vector immediately before the position display reset, $\underline{x}_k$, and the INS error immediately after the reset, $^r\underline{x}_k$, are given by

$$\underline{x}_k = \begin{bmatrix} \underline{x}_k^1 \\ --- \\ \underline{x}_k^2 \end{bmatrix} , \qquad ^r\underline{x}_k = \begin{bmatrix} ^r\underline{x}_k^1 \\ --- \\ \underline{x}_k^2 \end{bmatrix} , \tag{E.6}$$

where $\underline{x}_k^1$ contains the first two elements of $\underline{x}_k$, namely, the easterly and northerly components of position error.

Assuming that the position used in the integration routine which integrates the accelerometer outputs is not changed after taking the external position fix,* and that the increments of position change calcalculated by the INS computer are simply added to the position determined from the external fix, $^r\underline{x}_k$ propagates as follows:

$$^r\underline{x}_{k+n} = \underline{x}_{k+n} - \left(\underline{x}_k - {}^r\underline{x}_k\right) , \qquad n = 0,1,2, \ \ldots \ . \tag{E.7}$$

The problem now is to find the covariance matrix associated with $^r\underline{x}_{k+n}$, that is, to find

$$^rP_{k+n} \triangleq E\left[^r\underline{x}_{k+n} \ {}^r\underline{x}_{k+n}^T\right] , \qquad n = 0,1,2, \ \ldots \ . \tag{E.8}$$

The substitution of Eq. (E.7) into Eq. (E.8) yields:

*Resetting the position in the integration routine results in high amplitude oscillations in the RMS position error history. Thus, for part of the time such a reset will result in worse errors than would occur if an external position fix were not used.

$$
\begin{aligned}
{}^{r}P_{k+n} &= E\left[\underline{x}_{k+n} - \left(\underline{x}_k - {}^{r}\underline{x}_k\right)\right]\left[\underline{x}_{k+n} - \left(\underline{x}_k - {}^{r}\underline{x}_k\right)\right]^T \\
&= E\left[\underline{x}_{k+n}\underline{x}_{k+n}^T\right] - E\left[\underline{x}_{k+n}\left(\underline{x}_k - {}^{r}\underline{x}_k\right)^T\right] \\
&\quad - E\left[\left(\underline{x}_k - {}^{r}\underline{x}_k\right)\underline{x}_{k+n}^T\right] + E\left[\left(\underline{x}_k - {}^{r}\underline{x}_k\right)\left(\underline{x}_k - {}^{r}\underline{x}_k\right)^T\right] \quad , \qquad \text{(E.9)}
\end{aligned}
$$

where

$$
E\left[\underline{x}_{k+n}\underline{x}_{k+n}^T\right] = P_{k+n} \qquad \text{(E.10)}
$$

is given by Eq. (E.5). Furthermore, in view of Eqs. (E.6), it follows that

$$
E\left[\left(\underline{x}_k - {}^{r}\underline{x}_k\right)\left(\underline{x}_k - {}^{r}\underline{x}_k\right)^T\right] = C \quad , \qquad \text{(E.11)}
$$

where

$$
\left.
\begin{aligned}
C(i,j) &= 0 \quad , \quad \text{for all} \quad i,j, \quad \text{except}^* \quad , \\
C(1,1) &= P_k(1,1) + {}^{r}P_k(1,1) \quad , \\
C(2,2) &= P_k(2,2) + {}^{r}P_k(2,2) \quad , \\
C(1,2) &= C(2,1) = P_k(1,2) + {}^{r}P_k(1,2) \quad .
\end{aligned}
\right\} \qquad \text{(E.12)}
$$

From Eq. (E.1) it is seen that

$$
\underline{x}_{k+n} = A_n\underline{x}_k + B_n \quad , \qquad n = 0,1,2, \ \ldots \quad , \qquad \text{(E.13)}
$$

---

*${}^{r}P_k(1,1)$, ${}^{r}P_k(2,2)$, and ${}^{r}P_k(1,2)$ can be determined by using the estimator described in Chapter VI.

where

$$\left.\begin{aligned} A_o &= 1 , \qquad A_n = \Phi_{k+n-1} A_{n-1} , \\ \underline{B}_o &= 0 , \qquad \underline{B}_n = \Phi_{k+n} \underline{B}_{n-1} + \underline{n}_{k+n-1} . \end{aligned}\right\} \tag{E.14}$$

Using Eqs. (E.4), (E.6), and (E.13), it follows that

$$\begin{aligned} E\left[\underline{x}_{k+n}\left(\underline{x}_k - {}^r\underline{x}_k\right)^T\right] &= E\left[\left(A_n \underline{x}_k + \underline{B}_n\right)\left(\underline{x}_k - {}^r\underline{x}_k\right)^T\right] \\ &= A_n\left\{E\left[\underline{x}_k \underline{x}_k^T\right] - E\left[\underline{x}_k \, {}^r\underline{x}_k^T\right]\right\} \\ &= A_n D , \end{aligned} \tag{E.15}$$

where

$$D(i,j) = \begin{cases} P_k(i,j) , & \text{if} \quad j = 1 \text{ or } 2 , \\ 0 , & \text{if} \quad j \neq 1 \text{ or } 2 . \end{cases} \tag{E.16}$$

Using Eqs. (E.9) through (E.16), it is seen that the covariance matrix associated with the INS errors after a position display reset at the k^{th} stage of the process (E.1) is given by

$${}^rP_{k+n} = P_{k+n} - A_n D - (A_n D)^T + C , \tag{E.17}$$

for $n = 0, 1, 2, \ldots$.

It is important to note that because of the form of D [see Eq. (E.16)], the only nonzero elements of $A_n D$ are in the first two columns. Therefore, in view of the form of C [see Eq. (E.12)], from Eq. (E.17) it is seen that, except for the first two rows and first two columns, the elements of ${}^rP_{k+n}$ and P_{k+n} are identical. Hence, a position reset effects only position errors.

REFERENCES

[1] Cochran, M. V., "The Characteristics and Potential of VOR/DME Area Coverage Capability," IEEE Trans. on Aerospace and Navigational Electronics, Vol. ANE-12, No. 1, March 1965, pp. 83-89.

[2] Department of Transportation, Federal Aviation Administration, "Approval of Area Navigation Systems for Use in the U.S. Airspace System," FAA Advisory Circular AC No. 90-45, 18 August 1969.

[3] Martin, R. W., "Area Navigation in the Common System," Society of Automotive Engineers, National Air Transportation Meeting, New York, N.Y., April 21-24, 1969, Paper No. 690392.

[4] Hemesath, N. B., "Optimum Complementation of VOR/DME with Air Data," Journal of Aircraft, Vol. 8, No. 6, June 1971, pp. 456-460.

[5] Hemesath, N. B., "Optimal and Suboptimal Velocity-Aiding for VOR/DME Systems," AIAA Journal, Vol. 10, No. 1, January 1972, pp. 24-30.

[6] De Groot, L. E. and Larsen, J., "Extended Capability from Existing Navaids," Navigation, Vol. 15, No. 4, Winter 1968-69, pp. 391-405.

[7] Erzberger, H., "Application of Kalman Filtering to Error Correction of Inertial Navigators," NASA Technical Note TN D-3874, February 1967.

[8] Swik, R. and Schmidt, G., "Optimal Correction of Stochastic Errors of an Inertial Navigation System," in Hybrid Navigation Systems, AGARD Conference Proceedings No. 54, January 1970.

[9] Danik, B. and Stow, R. C., "Integrated Hybrid-Inertial Aircraft Navigation Systems," in Hybrid Navigation Systems, AGARD Conference Proceedings No. 54, January 1970.

[10] Faurre, P., "Systeme De Navigation A Inertie Hybride Optimise," in Hybrid Navigation Systems, AGARD Conference Proceedings No. 54, January 1970.

[11] Hollister, W. H. and Brayard, M. C., "Optimum Mixing of Inertial Navigator and Position Fix Data," Journal of Aircraft, Vol. 8, No. 9, September 1971, pp. 698-703.

[12] Schmidt, S. F., Weinberg, J. D. and Lukesh, J. S., "Case Study of Kalman Filtering in the C-5 Aircraft Navigation System," Joint Automatic Controls Conference, University of Michigan, Ann Arbor, Michigan, July 1968.

[13] Hemesath, N. B., Meyer, D. H. and Schweighofer, H. M., "Complementing VOR/DME with INS--An Improved Navigation System," Society of Automotive Engineers, National Business Aircraft Meeting, Wichita, Kansas, March 26-28, 1969, Paper No. 690338.

[14] Del Balzo, J. M., "Inertial Systems and Area Navigation in the U.S. Domestic Airspace," Navigation, Vol. 17, No. 4, Winter 1970-71, pp. 426-431.

[15] Holm, R. J., "Flight Evaluation of Inertial/DME/DME System," Federal Aviation Administration Report No. RD-70-24, May 1970.

[16] "Carousel IV Inertial Navigation System, System Technical Description and Operations Manual," AC Electronics, Division of General Motors, Milwaukee, Wisconsin, 1969.

[17] "Litton LTN-51 Inertial Navigation System for Commerical Aviation, Technical Description and Pilot's Guide," Litton Commerical Avionics, Woodland Hills, California, 1969.

[18] "International Standards and Recommended Practices--Aeronautical Telecommunications, Annex 10," Convention on International Civil Aviation, Second Edition of Vol. I, April 1968.

[19] Hawthorne, W. B. and Daugherty, L. C., "VOR/DME/TACAN Frequency Technology," IEEE Trans. on Aerospace and Navigational Electronics, Vol. ANE-12, No. 1, March 1965, pp. 11-15.

[20] Anderson, S. R., "VHF Omnirange Accuracy Improvements," IEEE Trans. on Aerospace and Navigational Electronics, Vol. ANE-12, No. 1, March 1965, pp. 26-35.

[21] Flint, R. B. and Hollm, E. R., "VOR Evolutionary System Improvements in the United States," IEEE Trans. on Aerospace and Navigational Electronics, Vol. ANE-12, No. 1, March 1965, pp. 46-56.

[22] Crone, W. J. and Kramer, E. L., "Development of the Doppler VOR in Europe," IEEE Trans. on Aerospace and Navigational Electronics, Vol. ANE-12, No. 1, March 1965, pp. 36-40.

[23] Hurley, H. C., Anderson, S. R., and Keary, H. F., "The Civil Aeronautics Administration VHF Omnirange," Proc. IRE, Vol. 39, December 1951, pp. 1506-1520.

[24] Feyer, L. H. W. and Nattrodt, K., "Test Results from a Tower VOR over a Forest Area," IEEE Trans. on Aerospace and Navigational Electronics, Vol. ANE-12, No. 1, March 1965, pp. 41-45.

[25] McFarland, R. H., "Experiments in the Determination of VOR Radial Stability," IEEE Trans. on Aerospace and Navigational Electronics, Vol. ANE-12, No. 1, March 1965, pp. 56-59.

[26] Dodington, S. H., "Recent Improvements in Today's DME," IEEE Trans. on Aerospace and Navigational Electronics, Vol. ANE-12, No. 1, March 1965, pp. 60-67.

[27] Hirsch, C. J., "A TACAN-Compatible Accurate DME for Short Ranges," IEEE Trans. on Aerospace and Navigational Electronics, Vol. ANE-12, No. 1, March 1965, pp. 68-76.

[28] Slater, J. M. and Ausman, J. S., "Inertial and Optical Sensors," in Guidance and Control of Aerospace Vehicles, edited by C. T. Leondes, McGraw-Hill Book Co., Inc., New York, 1963, Chapter 3.

[29] Pitman, G. R., Jr., Ed., Inertial Guidance, John Wiley and Sons, Inc., New York, 1962.

[30] Kayton, M. and Fried, W. R., Ed., Avionics Navigation Systems, John Wiley and Sons, Inc., New York, 1969.

[31] Faurre, P., Navigation Inertielle Optimale et Filtrage Statistique, Dunod, Paris, 1971.

[32] Bryson, A. E., Jr. and Ho, Y. C., Applied Optimal Control, Blaisdell Publishing Co., Waltham, Massachusetts, 1969.

[33] Pinson, J. C., "Inertial Guidance for Cruise Vehicles," in Guidance and Control of Aerospace Vehicles, edited by C. T. Leondes, McGraw-Hill Book Co., Inc., New York, 1963, Chapter 4.

[34] Jurenka, F. D. and Leondes, C. T., "Optimum Alignment of an Inertial Autonavigator," IEEE Trans. on Aerospace and Electronic Systems, Vol. AES-3, No. 6, November 1967, pp. 880-888.

[35] Dushman, A., "On Gyro Drift Models and Their Evolution," IRE Trans. on Aerospace and Navigational Electronics, Vol. ANE-9, No. 4, December 1962, pp. 230-234.

[36] Fagin, S. L., "A Unified Approach to the Error Analysis of Augmented Dynamically Exact Inertial Navigation Systems," IEEE Trans. on Aerospace and Navigational Electronics, Vol. ANE-11, No. 4, December 1964, pp. 234-248.

[37] Prichard, J. S., "The VOR/DME/TACAN System, Its Present State and Its Potential," IEEE Trans. on Aerospace and Navigational Electronics, Vol. ANE-12, No. 1, March 1965, pp. 6-10.

[38] Johansen, H., "A Survey of General Coverage Navaids for V/STOL Aircraft--A VOR/DME Error Model," NASA Contractor Report CR-1588, May 1970.

[39] Sorenson, H. W., "Kalman Filtering Techniques," in Advances in Control Systems, Vol. 3, edited by C. T. Leondes, Academic Press, New York, 1966, pp. 219-292.

[40] Kalman, R. E., "A New Approach to Linear Filtering and Prediction Problems," Trans. ASME, Series D, Journal of Basic Engineering, Vol. 82, March 1960, pp. 35-45.

[41] Kalman, R. E. and Bucy, R. S., "New Results in Linear Filtering and Prediction Theory," Trans. ASME, Series D, Journal of Basic Engineering, Vol. 83, March 1961, pp. 95-108.

[42] Heffes, H., "The Effect of Erroneous Models on the Kalman Filter Response," IEEE Trans. on Automatic Control, Vol. AC-11, No. 4, July 1966, pp. 541-543.

[43] Nishimura, T., "On the A Priori Information in Sequential Estimation Problems," IEEE Trans. on Automatic Control, Vol. AC-11, No. 2, April 1966, pp. 197-204.

[44] Nishimura, T., "Correction to and Extention of [43]," IEEE Trans. on Automatic Control (correspondence), Vol. AC-12, No. 1, February 1967, p. 123.

[45] Soong, T. T., "On A Priori Statistics in Minimum-Variance Estimation Problems," Trans. ASME, Series D, Journal of Basic Engineering, Vol. 87, March 1965, pp. 109-112.

[46] Nishimura, T., "Modeling Errors in Kalman Filters," in Theory and Application of Kalman Filtering, NATO Advisory Group for Aerospace Research and Development, AGARDograph 139, February 1970, pp. 87-103.

[47] Nishimura, T., "Error Bounds of Continuous Kalman Filters and the Application to Orbit Determination Problems," IEEE Trans. on Automatic Control, Vol. AC-12, No. 3, June 1967, pp. 268-275.

[48] Griffin, R. E. and Sage, A. P., "Large and Small Scale Sensitivity Analysis of Optimum Estimation Algorithms," IEEE Trans. on Automatic Control, Vol. AC-13, No. 4, August 1968, pp. 320-329.

[49] Aoki, M. and Huddle, J. R., "Estimation of the State Vector of a Linear Stochastic System with a Constrained Estimator," IEEE Trans. on Automatic Control, Vol. AC-12, No. 4, August 1967, pp. 432-433.

[50] Schmidt, S. F., "Application of State-Space Methods to Navigation Problems," in Advances in Control Systems, Vol. 3, edited by C. T. Leondes, Academic Press, New York, 1966, pp. 293-340.

[51] Stubberud, A. R. and Wismer, D. A., "Suboptimal Kalman Filter Techniques," in Theory and Application of Kalman Filtering, NATO Advisory Group for Aerospace Research and Development, AGARDograph 139, February 1970, pp. 105-117.

[52] Huddle, J. R. and Wismer, D. A., "Degradation of Linear Filter Performance Due to Modeling Error," IEEE Trans. on Automatic Control, Vol. AC-13, No. 4, August 1968, pp. 421-423.

[53] Silver, M. and Greenberg, M., "Area Navigation--A Quantitative Evaluation of the Effectiveness of Inertial System Aiding," Navigation, Vol. 18, No. 4, Winter 1971-72, pp. 360-368.

[54] Gelb, A. and Sutherland, A. A., Jr., "Software Advances in Aided Inertial Navigation Systems," Navigation, Vol. 17, No. 4, Winter 1970-71, pp. 358-369.